PALACKÝ UNIVERSITY IN OLOMOUC

Faculty of General Medicine and Dentistry

Institute of Molecular and Translational Medicine

Laboratory of Integrity of Genome

Application of Quantitative Image Analysis for Studies of Cellular Response to DNA damage

PhD thesis

Author:	**Mgr. Eva Veselá**
Study program:	LGE4 – Lékařská genetika
Supervisor:	**Mgr. Martin Mistrík, PhD.**

Termín odevzdání práce:	10.7.2017

I declare that this thesis was written solely by me and all the sources used in this thesis are cited and included in the reference part.

Olomouc, 10.7. 2017 ……..

I would like to thank my supervisor Mgr. Martin Mistrík, PhD for his leadership and my colleague RNDr. Tomáš Fürst, PhD for great collaboration. I would like to thank all my colleagues from the Laboratory of Integrity of Genome for their help and for being the best colleagues one can wish for.
I also want to thank all my friends and above all, my family for their love, support, patience and respect.

Bibliographical identification:

Author's first name and surname	M.Sc. Eva Veselá
Title	Application of quantitative image analysis for studies of cellular response to DNA damage
Type of thesis	Ph.D. thesis
Department	Laboratory of Integrity of Genome
Supervisor	Mgr. Martin Mistrík, PhD
The year of presentation	2017
Abstract	DNA damage response (DDR) is a complex signalling network important for maintenance of DNA stability. Disrupted DDR was proposed to contribute to mutagenesis, carcinogenesis, induction of apoptosis and senescence. Here, the dynamics of DDR proteins, MDC1, 53BP1 and FANCD2 are evaluated in live cells in response to localised DNA damage generated by laser micro-irradiation (LMI). A new approach of LMI performed on laser scanning microscope was tested and software for automated quantitative image analysis was developed. The method presented here possess several advantages compared to commonly used approaches to LMI: it is faster and the DNA damage is induced in a regular pattern of collinear stripes that enabled development of automated quantitative image analysis software routine. The method was tested to be usable also for other photo-manipulation technique called fluorescence recovery after photo-bleaching (FRAP), and for immunofluorescent detection of DDR markers. The method provides an easy and unbiased evaluation of sufficient numbers of cells for robust statistical analysis and facilitates the use of LSM techniques for high-content screening. In the second part of the thesis, image analysis was used to elucidate the role of XPC protein in cellular response to replication stress (RS). Several markers of DDR were evaluated in particular phases of the cell cycle. XPC was suggested to be involved in early stages of cellular response to RS. XPC may facilitate recruitment of particular DDR proteins and thus contribute to successful DDR signalling.
Keywords	DNA damage recognition, DNA damage repair, laser micro-irradiation, image analysis, microscopy, reporter cell lines, XPC, HCS, cancer
Number of pages	96
Number of appendices	6
Language	English

Bibliografická identifikace:

Jméno a příjmení autora	Mgr. Eva Veselá
Název práce	Aplikace kvantitativní mikroskopické analýzy pro studium buněčné odpovědi na DNA poškození
Typ práce	Disertační
Vedoucí práce	Laboratoř Integrity Genomu Mgr. Martin Mistrík, Ph.D.
Rok obhajoby práce	2017
Abstrakt	Soubor komplexních signálních drah zajišťující rozpoznání, signalizaci a opravu DNA poškození se souhrnně nazývá odpověď na DNA poškození. Tyto dráhy jsou nezbytné pro udržování stability genomu. Narušení těchto drah přispívá k mutagenezi, karcinogenezi, apoptóze a senescenci. V předkládané práci byla v živých buňkách měřena dynamika odpovědi na lokalizované DNA poškození tří proteinů: MDC1, 53BP1 a FANCD2. Lokalizované DNA poškození, tzv. laserová mikroiradiace (LMI), bylo indukováno pomocí laserového skenovacího mikroskopu. V práci je představen nový způsob iradiace vzorků, který má několik výhod oproti běžně používaným technikám LMI: DNA poškození je generováno rychleji a má pravidelnou strukturu souběžných pruhů, která umožňuje vyhodnocení pomocí automatizované obrazové analýzy. Metodu je možné využít také pro další foto-manipulační techniku FRAP a pro imunofluorescenční detekci markerů DNA poškození. Metoda umožňuje jednoduché a objektivní vyhodnocení dostatečného počtu vzorků pro robustní statistickou analýzu a představuje tak značné usnadnění využití laserové skenovací mikroskopie pro high-content screening. V druhé části této práce byla převážně pomocí kvantitativní obrazové analýzy studována role XPC proteinu v odpovědi na replikační stres. Bylo vybráno několik specifických markerů účastnících se odpovědi tento typ DNA poškození a jejich lokalizace do míst poškození byla vyhodnocena ve vybraných fázích buněčného cyklu. Výsledky ukazují, že XPC protein by mohl hrát roli v raných fázích odpovědi na DNA poškození. XPC pravděpodobně usnadňuje vazbu dalších proteinů, čímž přispívá ke správné a dostatečné aktivaci signálních drah aktivovaných DNA poškozením.
Klíčová slova	rozpoznání DNA poškození, oprava DNA poškození, lokalizované ozáření laserem, obrazová analýza, mikroskopie, reportérové buněčné linie, XPC, HCS, rakovina
Počet stran	96
Počet příloh	6
Jazyk	Anglický

TABLE OF CONTENTS

1 AIMS

- Summary and review the current knowledge about
    - DNA damage response focused mainly on DNA double strand breaks and replication stress
    - the technique of laser micro-irradiation
- Development and optimisation of novel approaches to microscopy-based data acquisition and subsequent image analysis in order to study DNA damage response
    - in live cells using reporter cell lines with fluorescently tagged DNA damage response proteins
    - in fixed cells using immunofluorescence detection of DNA damage response proteins
- Adaptation of the methods for high-content analysis in order to study factors interfering with DNA damage response

2 INTRODUCTION

DNA is a very prominent molecule predominantly occupying the cell nucleus. It is bearing the genetic information that holds the key to cellular life, beginning from the basic metabolic reaction up to the complex process of cellular division giving life to a new cell.

Damage to DNA molecule can be deleterious and the errors (mutations) may accumulate with severe consequences for the cell and the whole organism. Mutations can be conserved and as a result senescence, apoptosis or tumorigenesis may emerge. Therefore, it is necessary to understand properly the DNA damage recognition and signalling mechanisms.

Although many techniques and approaches have been already developed and many signalling pathways were described, our knowledge is far from being complete. In this thesis, I focused on one of the modern techniques called laser micro-irradiation. The technique was used for DNA damage induction in live cells. The so-far used approach was modified and improved to be more suitable for high-content screening. The presented approach is accompanied by a new custom developed image analysis software and altogether the new procedure is faster, and less work and time demanding. It enables analysis of significantly more cells than commonly used approaches, so it brings the possibility of robust statistical testing.

2.1 Sources and types of DNA damage

2.1.1 Endogenous

The majority of the DNA damage the cells have to cope with every day is generated endogenously. The most prominent sources are metabolic intermediates, mainly reactive oxygen species (ROS) cause oxidative damage to the bases and to the backbone of the DNA molecule (Cadet et al., 2003). Also, other cellular molecules can be affected by ROS and lead to the formation of reactive aldehydes that can form mutagenic DNA adducts (Chung et al., 1996). DNA is also prone to spontaneous depurination and depyrimidination which occurs due to the labile N-glycosidic bond between the pentose sugar and the nucleoside (Lindahl,

1974, Lindahl, 1993). Spontaneous deamination, hydrolysis and non-enzymatic methylation of DNA molecule can lead to base substitutions and eventually result in mutations (Helleday et al., 2014). The lesions described above count to tens of thousands lesions per day the cell has to cope with, all of them possessing the potential to modify the genetic information (Lindahl and Barnes, 2000, Helleday et al., 2014). It is, therefore, evident that cells have evolved very powerful machinery to eradicate the damage. The Nobel Prize in Chemistry in 2015 was awarded to three scientists, Tomas Lindahl, Aziz Sancar and Paul Modrich, for the elucidation of three repair pathways, namely base excision repair (BER), nucleotide excision repair (NER) and mismatch repair (MMR), respectively.

Moreover, some of the DNA sequences are more prone to experience DNA damage than the others. Heterochromatin structure, origin-poor regions, some types of repetitive sequences (Huh et al., 2016, Gelot et al., 2015, Krasilnikova and Mirkin, 2004), various secondary DNA structures, e.g., hairpins and high-flexibility islands, or non-B structures, all present obstacles that can impair processes ongoing on the DNA molecule and result in DNA damage formation (Gelot et al., 2015). All of them emerge physiologically or upon specific conditions, such as oncogenic stress and/or chemical treatment (Mirkin and Mirkin, 2007, Kim and Mirkin, 2013). Heterochromatin was observed to hamper double strand break (DSB) repair. DSB in euchromatin regions are repaired faster than in heterochromatin regions (Goodarzi et al., 2008).

2.1.2 Exogenous

2.1.2.1 Chemical sources

DNA damaging agents can interact with the DNA molecule directly or indirectly. The direct interactions involve crosslinking agents, alkylating adducts and intercalating compounds. The indirect interactions are more variable as there are many proteins with different functions closely connected to DNA.

Crosslinking agents generate irreversible covalent bonds between the nucleotides localised either on the opposing strands (interstrand crosslinks, ICL) or on the same DNA strand (intrastrand crosslinks). ICL prevents strand separation, therefore, blocking the replication and transcription (Huang and Li, 2013) leading to chromosomal deletions (called as a clastogenic effect) (Noll et al., 2006). ICL agents are bifunctional compounds, however, in low extent also monovalent alkylation base adducts are generated, e.g., by nitrogen mustards, sulphur mustards and psoralens (Huang and Li, 2013, Shahin et al., 2001). Alkyl adducts cause different spectra of DNA damage than ICL but are also widely used for cancer treatment, e.g., chlorambucil half-mustard, temozolomide and dacarbazine (Kondo et al., 2010). On the other hand, intrastrand crosslinks can be bypassed by several DNA polymerases, so they exhibit less toxicity than ICL (Huang and Li, 2013). Cis-platin and mitomycin C are the most widely used compounds causing intrastrand crosslinks (> 90%) above ICL (5 - 10%) (Damsma et al., 2007). Cells defective for ICL repair are very sensitive to crosslinking agents and are highly susceptible to carcinogenesis (Huang and Li, 2013).

Compounds may also interact directly with DNA by non-covalent binding to DNA minor groove, or by intercalation. DNA minor groove binders (MGBs) have several common structural features. Several aromatic rings interfering by a hydrogen bond with second C atom of adenine are giving the structure the freedom of movement and torsion (Mišković et al., 2013). Compounds bind preferably at AT-rich sequences and have a characteristic curved shape compatible with the minor groove, so the DNA structure is not violated (Palchaudhuri and Hergenrother, 2007). MGBs cause permanent cell arrest at S/G2 boundary (Yamori et al., 1999), blocking replication and transcription (Bielawski et al., 2001). However, their utilisation for therapy is limited due to lack of selectivity (Mišković et al., 2013). Widely studied MGBs are Hoechst compounds (discussed further as potent laser irradiation sensitizers) which were observed in gene expression analysis to downregulate several genes of transcription regulation. Based on this knowledge, combined treatment may be designed to

enhance the selectivity and efficacy of MGBs (Zhang et al., 2011). Intercalators are structurally diverse molecules, with a planar aromatic chromophore that can be inserted between the neighbouring base pairs in DNA. The interaction with DNA is based upon non-covalent binding (van der Waals and charge transfer forces, hydrogen and hydrophobic bonds) (Martínez and Chacón-García, 2005). Intercalators alter the DNA structure significantly, therefore, the DNA, and RNA synthesis is inhibited, leading to sister chromatid exchange (SCE) (Raj and Heddle, 1980) and micronuclei formation (Wilson et al., 1984). Some intercalators interact with topoisomerase II resulting in even more profound topological changes, e.g., doxorubicin (Bodley et al., 1989). Another group of compounds (predominantly antibiotics) called radiomimetics are causing free radical damage (e.g., bleomycin, neocarzinostatin) to sugar moieties in DNA resulting in DSB and abasic sites which are considered as hot spots for mutations during DNA replication (Povirk, 1996).

Compounds interfering indirectly with DNA molecule are diverse regarding the structure and mechanism of action. DNA molecules are extremely vulnerable during replication, so the most potent compounds causing DNA damage are mainly interfering with enzymes necessary for successful S phase progression.

Inhibitors of DNA polymerases (e.g., aphidicolin) cause disconnection of the replicon and generate long stretches of ssDNA between helicases and polymerases, making the DNA more vulnerable to breakage and errors (Cheng and Kuchta, 1993, Chang et al., 2006).

The topological stress of DNA generated by the molecule unwinding is released by topoisomerases, so the inhibition of topoisomerase I (camptothecin) (Hsiang et al., 1989, Koster et al., 2007) and topoisomerase II (etoposide) (Liu et al., 1983) is highly cytotoxic.

A big group of compounds called antimetabolites alter the synthesis of nucleic acids by several mechanisms. First, the synthesis of nucleotides is violated resulting in an imbalance of nucleotide triphosphates, e.g., hydroxyurea inhibits ribonucleotide reductase (RNR) (Hakansson et al., 2006), 5-fluorouracil leads to inhibition of thymidylate synthase

(Danenberg et al., 2016). Nucleotide analogues block the DNA polymerases as well as RNR, e.g., gemcitabine after conversion to the active compound (Mini et al., 2006).

Moreover, other chemical compounds may interfere with DNA indirectly by violating the function of numerous proteins dealing with DNA damage recognition, signalling and repair. The compounds may prevent the loading of the proteins to sites of damage, inhibit their catalytic function, prevent their dissociation from sites of damage, etc. The various are the functions of DNA damage response (DDR) proteins the same diverse are the effects of interfering compounds. In the following chapters selected DDR proteins' functions are described in detail. Some of them are very promising targets for so-called personalised/targeted medicine. This new approach is based on analysis of patients' tumour and according to observed mutations and dysregulations the treatment is selected (Weber and Ryan, 2015) (Moles et al., 2016).

2.1.2.2 Physical sources – UV irradiation

The most significant physical sources of DNA damage for humans are ionising and nonionizing radiation. The most abundant nonionizing source of DNA damage is the solar radiation, particularly the UV component. The type of DNA damage generated is dependent on its wavelength. UV radiation may be absorbed by DNA bases leading to photo-induced reactions generating the most common photoproducts cyclobutane pyrimidine dimers (CPDs) and (6-4) pyrimidine-pyrimidone photoproduct, ((6-4)PPs) (Ravanat et al., 2001). The latter can absorb 320 nm UV-A radiation and form Dewar valence isomers (DewPPs) (Perdiz et al., 2000). The CPDs and (6-4)PPs physically block the replication and transcription machineries (McKay et al., 2002) (Batista et al., 2006) (Ljungman and Lane, 2004) and therefore are the most important drivers of the apoptotic, cytotoxic, mutagenic and carcinogenic effects of UV (Brash, 1988). UV-A (315-400 nm) and visible light (>400 nm) are absorbed by DNA very weakly. However, UV-A was shown to induce CPDs, DewPPs and oxidative damage. CDPs

induced by UV-A were shown to be generated by a different mechanism than UV-B (Besaratinia et al., 2005). Typical damage caused by UV-B (290-320 nm) and UV-C (200-290 nm) are CPDs and (6-4)PPs, due to maximum DNA absorption at 260 nm (Ravanat et al., 2001). UV-A and visible light are widely used in photodynamic therapy (PDT). The combination of light, chemical substance (a photosensitiser) and molecular oxygen is employed to induce cell death. This is a selective method for local treatment of various diseases, e.g., psoriasis, dermatitis and recently also cancer. The selectivity is based on the accumulation of the photosensitiser in the target tissue and the efficient generation of singlet oxygen or other highly reactive species/radicals, that induce cell death (Josefsen and Boyle, 2008). PDT is in fact known for a long time; first reports come from ancient Egypt when it was used for vitiligo treatment. Its usage for cancer therapy is rather new but successful, e.g., skin, head, neck, or bladder cancer can be indicated for PDT (Ikeda et al., 2011, Yano et al., 2014, Akimoto, 2016).

Indirect damage is caused due to the presence of endogenous sensitizers. The sensitizer is a compound able to absorb the light energy of a particular wavelength that changes the distribution of photosensitizer's electrons creating an excited state (Ravanat et al., 2001). Mechanistically, DNA damage induction can be caused by either reaction of the excited sensitizer molecule with DNA, or by reactions with other secondary intermediates. For example, excited sensitizer molecule may react with membrane lipids, that give rise to malondialdehyde and 4-hydroxynonenal which can form mutagenic DNA adducts (Marnett, 1999). Also, other secondary intermediates may be formed, e.g., as decomposition products of the excited molecules (Epe, 2012).

Exogenous, also called as environmental sources of DNA damage challenge the genomic integrity in addition to endogenous sources. Even cells with unperturbed repair pathways may

become overwhelmed by the DNA damage induced to the molecule resulting in increased number of various errors introduced to DNA molecule.

2.2 DNA damage recognition and signalling

DNA lesions pose a significant threat to genomic stability therefore, cells have evolved the DNA damage response (DDR), a complex network of interconnected pathways to alleviate the risk. DDR proteins are indispensable for DNA integrity maintenance. Mutations in these genes are reported to cause cancer and other disorders (Shiloh, 2003, Bartek et al., 2007).

Lesions introduced to just one strand of DNA are readily repaired by NER, BER and MMR as mentioned previously.

2.2.1 DNA double-strand break recognition and signalling

The most challenging and deleterious lesions are DNA double-strand breaks (DSB) for there is a lack of template (intact complementary strand in close proximity) that would facilitate the repair. DSB are therefore potent inducers of chromosomal rearrangements that can result in the activation of oncogenes, loss of tumour suppressors, or proteins' function alterations which in turn fuel malignant transformation (Jackson and Bartek, 2009). At first, DDR orchestrates significant compartmentalization of the nucleus. Many proteins assemble in so-called ionising radiation-induced foci (IRIF) which form an affinity platform for a number of DDR proteins increasing their local concentration (Bekker-Jensen and Mailand, 2010). The functions of IRIF are hypothesized to: (1) help to shelter the broken ends and prevent illegitimate repair (Yin et al., 2009), (2) stimulate the activity of DDR proteins by their accumulation (Lisby and Rothstein, 2009), (3) provide the break with all the repair factors in close proximity so all possible enzymatic reactions may be employed (Bekker-Jensen and Mailand, 2010). The IRIF-forming proteins play significant roles in DNA damage recognition, signal transduction and damage repair, moreover are reported to be involved in

cellular processes, e.g., in apoptosis, cell cycle regulation, transcriptional regulation or chromatin modification (Bekker-Jensen and Mailand, 2010).

As summarised in Fig. 1, DSB are recognised and signalled by recruitment and modifications of many proteins. The most important and relevant components of DSB recognition, signalling and repair for this work are introduced in the following chapters. The selected, below introduced proteins were used either as a readout of DDR (MDC1, 53BP1, γH2AX, FANCD2) or inhibited in order to validate the new technique introduced here (MRN complex, ATM, DNA-PK, PARP1).

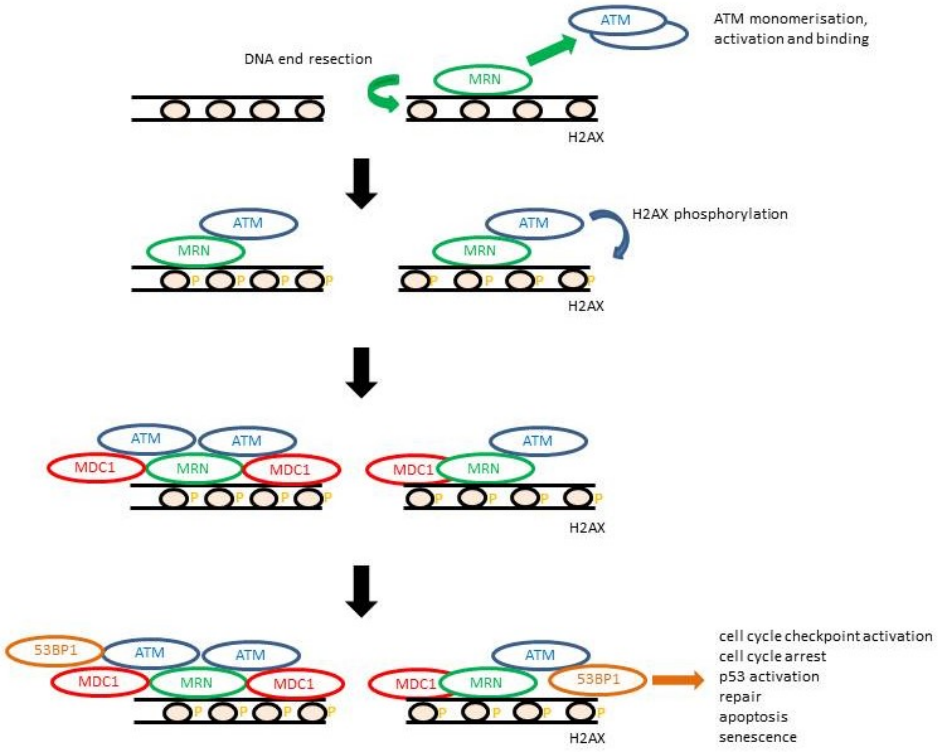

Figure 1. DNA double strand breaks recognition and signalling. DSBs are recognised by MRN complex, Mre11 exonuclease activity leads to DNA ends resection and facilitates the repair by HR. Mostly IRIF forming proteins are loaded and retained at the sites of damage: ATM, followed by MDC1 protein that serves as a docking platform for more ATM molecules and p53-binding protein (53BP1). As a result, repair proteins are recruited, DSB is repaired, or cell cycle arrest, apoptosis or senescence may be triggered.

2.2.1.1 MRN complex

Mre11/Rad50/Nbs1 complex (Meiotic recombination protein 1/Rad50/Nijmegen breakage syndrome 1 complex) works as a DSB sensor and as a bridging molecule between the flanking ends of DSB. MRN complex triggers the signalling of DNA damage and possesses nucleolytic function.

The Mre11 protein binds to DNA through its DNA-binding domain and also interacts with Rad50 and Nbs1 that do not interact with each other. Mre11 protein possesses endo- and exonuclease activities, both required for subsequent repair by HR. Mre11's 3‘- 5‘ endonuclease cleavage initiates resection, and this event is a licensing factor for future HR. Mre11 exonuclease functions downstream its endonuclease activity and in cooperation with 5‘-3’ EXO1/BLM facilitates homologous recombination repair pathway (HR) (Shibata et al., 2014). Rad50 possess ATPase activity which is probably responsible for the partial unwinding of the DNA ends and hairpins (Paull and Gellert, 1999). Conformational changes of the Rad50-ATPase domain after ATP is bound, are well suited to prepare DNA ends for nucleolytic cleavage by Mre11 (Hopfner et al., 2001). Rad50 also contains Zn-hook domain that fulfils the bridging function holding the flanking ends of DSBs. The Zn- hook domain is critical in the prevention of chromosomal damage (Lobachev et al., 2004). Rad50 stimulates binding of ATM kinase (Lee and Paull, 2005).

Nbs1 is responsible for Mre11 phosphorylation upon DNA damage (Dong et al., 1999) by activating ATM kinase (Lee and Paull, 2005).

MRN complex bound to DSBs promotes the formation of DNA damage signalling complexes, ATM monomerization and activation (Dupré et al., 2006). The overall model suggests a two-step mechanism, at first the MRN complex bound to DNA forms dimers increasing the local concentration of DNA ends to trigger ATM monomerization followed by ATM activation and autophosphorylation (Lavin, 2007, Dupré et al., 2006).

2.2.1.2 ATM

Ataxia telangiectasia mutated (ATM) belongs to a family of phosphatidylinositol 3 kinase-like protein kinases (PIKKs), a group of large enzymes involved in cellular response to various stresses. A common feature is a phosphatidylinositol 3 kinase (PI3K) domain, occupying approx. 10% of the protein, two C-terminal domains, FAT and FATC (FAT C-terminal) are also present in all PIKKs (Shiloh and Ziv, 2013). PIKKs phosphorylate a specific motif of serine or threonine followed by glutamic acid (SQ/TQ sites) (Kim et al., 1999).

The proteins that belong to this group are Mammalian Target of Rapamycin (mTOR), Suppressor of Mutagenesis in Genitalia 1 (SMG1), transformation/transcription domain-associated protein (TRRAP) and other three members are well-defined major players in responses to genotoxic stresses: Ataxia Telangiectasia Mutated (ATM), DNA-protein kinase (DNA-PKcs) and Ataxia telangiectasia Rad3-related (ATR).

ATM is a 350-kDa protein, and essential enzyme for maintenance of genome integrity, AT-deficient cells exhibit sensitivity to DSB inducing agents (Barlow et al., 1996). In its inactive form, it is a dimer which can be activated by phosphorylation on serine 1981 followed by dissociation to active monomers. ATM has been reported to be activated by several mechanisms, e.g., direct interaction with DSBs ends (You et al., 2007), or conformational change of DNA structure after DSB induction (Bakkenist and Kastan, 2003). Recently, ATM was reported to possess a concave surface that recognises a similar pattern on MRN complex (Lau et al., 2016). ATM binds by its C-terminal region on Nbs1 (Dupré et al., 2006). ATM was found to exhibit steady-state levels during the cell cycle and participate in all cell cycle checkpoints (Gately et al., 1998). ATM is rapidly relocalized to DNA damage sites after DSB induction and resides there for several hours (Andegeko et al., 2001). The initial activation and recruitment of ATM to chromatin is mediated by MRN complex and it is independent of Mediator of DNA Damage Checkpoint Protein 1 (MDC1) (Lou et al., 2006). The second step

of ATM recruitment is mediated by MDC1 protein and leads to significant enhancement of ATM accumulation on the chromatin (Lou et al., 2006). ATM phosphorylates many substrates to influence the cell cycle checkpoint response and modulate DNA repair, e.g., p53 (Canman et al., 1998), BRCA1 (Li et al., 2000), Nbs1 (Lim et al., 2000), etc.

2.2.1.3 γ-H2AX

H2AX is an isoform of histone H2A that possess 142 amino acid residues at the C-terminal sequence with the specific SQ motif (Mannironi et al., 1989). After DSB induction the H2AX is phosphorylated at serine 139 and is called γ-H2AX (Rogakou et al., 1998). The phosphorylation is detectable within 1 min, and the maximum is reached after 9 - 30 min (Rogakou et al., 1999). The H2AX variant may be phosphorylated up to 2 Mb of chromatin around the lesion. H2AX is a substrate of all Phosphatidylinositol-3-kinase-like protein kinases (PIKKs, described below) and serves as a docking platform for other proteins, e.g., MDC1 and 53BP1 (Stucki et al., 2005, Kleiner et al., 2015). Surprisingly, the initial recruitment of the factors to sites of damage is not abrogated upon deficient γH2AX (Celeste et al., 2003, Lou et al., 2006). H2AX was identified as a key component for ionising radiation-induced foci (IRIF) being indispensable for the redistribution of repair complexes to damaged chromatin, and retention of the proteins in the vicinity of DNA lesions (Paull et al., 2000, Bekker-Jensen and Mailand, 2010). Soon after its identification, γH2AX has been reported as a marker of DNA DSBs (Rogakou et al., 1998, Rogakou et al., 1999, Kuo and Yang, 2008). Moreover, in several studies, employing IR-induced DNA damage, the γH2AX was proposed to be present at every DSB as the number of γH2AX foci correlated with the estimated number of DSB (Rothkamm and Löbrich, 2003, Mariotti et al., 2013). However, this hypothesis was challenged by another study not using IR. Instead, the authors propose a hypothesis that DBS trigger γH2AX foci formation but not every γH2AX focus necessarily represents a DSB (Rybak et al., 2016).

In the last years, other cellular processes were also reported to employ γH2AX. During meiotic and mitotic division (Celeste, 2002, McManus and Hendzel, 2005) γH2AX was assigned with chromatin remodelling in the initiation of heterochromatin formation, or its maintenance (Turinetto and Giachino, 2015). Moreover, other processes are influenced by presence or absence of γH2AX, e.g., neural stem cells development (Andäng et al., 2008) and ageing (Rodier et al., 2009).

2.2.1.4 MDC1

Mediator of DNA damage checkpoint protein 1 (MDC1) is loaded to DNA soon after the DNA damage recognition as an enhancer of DNA damage signalling. MDC1 directly binds to γH2AX (phosphorylated independently of MDC1by ATM) by its breast cancer terminal (BRCT) domain (Stewart et al., 2003, Stucki et al., 2005). Then, it serves as a platform for ATM binding that phosphorylates other H2AX in proximity thus enabling loading of other MDC1 and ATM molecules. These three proteins work in a positive feedback loop that enhances the protein loading and chromatin modification up to megabase region around the DSB lesion thus forming IRIF. This amplification mediated by MDC1 seems to be indispensable upon physiological doses of radiation (Lou et al., 2006). MDC1 binding seems to be also indispensable for damage-induced cell cycle arrest at intra S-phase checkpoint and G2/M boundary, MDC1 controls the formation of damage-induced 53BP1 (p53-binding protein 1), BRCA1 and MRN foci (Stewart et al., 2003).

Also, other domains and structural motives of MDC1 participate in the DNA damage response. SDT repeats are bound by BRCT-domain of Topoisomerase (DNA) II Binding Protein 1 (TopBP1) (Leung et al., 2013) leading to sustaining and amplifying ATR activation. TopBP1 is also necessary for colocalization of 53BP1 at DSB sites (Cescutti et al., 2010). SDT repeat also interacts with Nbs1 protein (Lloyd et al., 2009).

2.2.1.5 53BP1

53BP1 protein is a DBS signalling mediator and it is very rapidly translocated to sites of damage. Enzymatic activity has not been detected within this large 250 kDa protein, but several sites for various DSB-responsive proteins were identified. BRCT repeats are responsible for interaction with p53 protein (Iwabuchi et al., 1998, Derbyshire, 2002) and chromatin-modulating factor EXPAND1 (Sy et al., 2010). Tandem Tudor domains were described to interact with methylated histone H4 (K20) (Botuyan et al., 2006). Terminal SQ/TQ sites were described as phosphorylation sites for ATM and ATR (Jowsey et al., 2007). But the phosphorylation of 53BP1 is not required for foci accumulation at the sites of damage (Ward et al., 2003). Upon IR, 53BP1 recruitment to sites of damage is predominantly ATM-dependent and upon UV ATR plays the main role (Jowsey et al., 2007).

53BP1 was identified as a signal enhancer. It is considered as a marker of DNA damage sites where the damage is being processed. Although 53BP1 is dispensable for DNA damage signalling, the non-homologous end-joining (NHEJ) repair pathway is severely affected by a 53BP1 deficiency (Ward et al., 2004).

53BP1 recruitment to sites of damage is MDC1 dependent as was demonstrated in MCD1-/- cells (Kleiner et al., 2015). In the absence of MDC1, 53BP1 recruitment to DNA damage sites depends on direct interaction with γH2AX (Kleiner et al., 2015). Upon low DNA damage, 53BP1 BRCT domain stimulates ATM activity and promotes checkpoint function (Mochan et al., 2004).

53BP1 plays an important role in the telomere maintenance (Martínez et al., 2012), facilitates long-range DNA end-joining during V(D)J recombination (also called class switch recombination, CSR) in lymphocytes during immunoglobulin synthesis (Difilippantonio et al., 2008). During CSR ATM and DNA-PKcs phosphorylate 53BP1 and regulate 53BP1 focus formation in a redundant manner (Callén et al., 2009).

Loss of 53BP1 or its failure to localise to damaged chromatin significantly reduces the phosphorylation of ATM targets such as p53, checkpoint kinase 2 (CHK2) and BRCA1 leading to defective G2–M checkpoint signalling and genomic instability (DiTullio et al., 2002, Fernandez-Capetillo et al., 2002, Ward et al., 2003). 53BP1 deficient fibroblasts do not exhibit spontaneous chromosomal breaks but are possibly defective in chromosome segregation as observed by a tendency to aneuploidy and/or tetraploidy in 53BP1-null cells (Ward et al., 2003).

2.2.1.6 DNA-PK

DNA-protein kinase (DNA-PK) is 250 kDa molecular sensor that promotes NHEJ repair pathway and V(D)J recombination. Decrease or deficiency in DNA-PK cellular levels leads to radiosensitivity, accumulation of cells in G2/M phase after irradiation and blocked progression of mitosis (Lee et al., 2011).

DNA-PK is comprised of small heterodimer subunit Ku70/80 which is responsible for binding the second subunit - DNA-PK catalytic subunit (DNA-PKcs) (Drouet et al., 2005). After initial binding, Ku 70/80 translocates inward about one helical turn upon the binding to allow DNA-PKcs interaction with the DNA ends (Kysela et al., 2003, Hammel et al., 2010) that leads to its activation (Roberts et al., 2010). Upon loading to DNA, DNA-PK associates with the DNA Ligase 4 and X-Ray Repair Cross Complementing 4 (LIG4-XRCC4 complex) (Drouet et al., 2005). DNA-PKcs dimerize with itself thus bringing the two opposing DNA ends together (DeFazio et al., 2002). This architecture also facilitates *trans*-autophosphorylation at the DSB followed by massive conformational changes that enable release of DNA-PK from DNA (Hammel et al., 2010, Sibanda et al., 2010). DNA-PK does not form IR-induced nuclear foci (Bekker-Jensen et al., 2006), efficient repair is therefore not dependent on molecules accumulation within the region surrounding the break.

DNA-PK is the most abundant H2AX-modifying kinase (Muñoz et al., 2013) and decreased DNA-PK protein levels lead to increased radiosensitivity (Gustafsson et al., 2014). However, the repair capacity of these cells seems to be unaffected as measured by the removal of 53BP1 or γ-H2AX foci (Gustafsson et al., 2014). When DNA-PK is absent from the cells the phenotype is very similar as with cells treated by the DNA-PKcs inhibitor NU7441, and DSB repair is severely compromised (Gustafsson et al., 2014, Mistrik et al., 2016).

DNA-PKcs seems to be an important player in drug-induced DNA damage repair and related to chemosensitivity (Li et al., 2015). Increased DNA-PK protein levels were detected in MG63 osteosarcoma cells upon cis-platin and etoposide treatment. Down-regulation of DNA-PKcs levels resulted in higher sensitivity towards the chemicals increasing the apoptosis and cell cycle arrest at G1 phase (Li et al., 2015). DNA-PK was also shown to contribute to changes in the tumour microenvironment promoting metastasis formation thus pointing at DNA-PK as a promising target for cancer therapy (Kotula et al., 2015).

2.2.1.7 PARP1

Poly (ADP-ribose) polymerase 1 (PARP1) was suggested to be one of the first DNA damage sensors (Haince et al., 2008). PARP1 interacts with many SSB repair proteins, e.g., X-ray repair cross-complementing protein (XRCC1), DNA ligase III, Proliferating cell nuclear antigen (PCNA) and Flap endonuclease 1 (FEN1), but was also reported to be localized to sites of DSBs and complex damage (Saquilabon Cruz et al., 2016). PARP1 parylates DNA which leads to chromatin relaxation (Kim et al., 2005b). Subsequently, autoparylation promotes PARP1 dissociation from the sites of damage. This extremely fast process was mechanistically explained by (Langelier et al., 2012): PARP1 binds to DNA through 2 zinc domains and one WGR domain in such conformation that helical core of other PARP1 domain called CAT is distorted. It is proposed that this distortion brings the CAT domain and AD domain to close proximity which leads to autoparylation on AD domain.

PARP1 is widely interacting with early activated DDR proteins, e.g., Mre11/Rad50/Nbs1 complex (described below) (Haince et al., 2008). Parylation facilitates spatial distribution of proteins at DSBs, moreover in PARP1-deficient cells reduced the number of DDR foci is observed (Haince et al., 2007). PARP1 also regulates the balance between HR and NHEJ repair pathways, in PARP1-deficient cells HR is observed to be reduced, and NHEJ pathways reported to be enhanced (Hochegger et al., 2006).

2.2.2 Replication stress

The DNA replication is responsible for the delivery of intact and unchanged genetic material to the next generation. Disturbances to replication, e.g., slowing down or stalling of replication forks (RF), or DNA synthesis are called replication stress (RS) (Burhans and Weinberger, 2007, Zeman and Cimprich, 2014). Errors occurring during DNA replication can have serious consequences. Mutations introduced during DNA replication provide the genetic basis for phenotypic variations. Rapid accumulation of mutations can disrupt either the cellular processes needed for viability, leading to cell death (Herr et al., 2011, Herr et al., 2014), or the elevated mutation rate has been proposed to be a key step in the progression of many cancers (Herr et al., 2011, Loeb, 2016). The components of the cellular response to replication stress that are the most relevant to this thesis are described in detail in the following chapter and the illustrative scheme of the process is visualised in Fig. 2.

2.2.2.1 ATR

ATR is a highly-conserved monomeric 300 kDa protein kinase activated in response to various DNA lesions associated with DNA replication and it is a crucial mediator of intra S phase checkpoint response (Zeman and Cimprich, 2014). ATR stabilises perturbed or stalled replication forks (Lopes et al., 2001) as well as unperturbed forks, therefore, enabling error-free replication (Flynn and Zou, 2011). ATR is activated in response to a variety of

genotoxins, e.g., UV and various chemicals (hydroxyurea, aphidicolin, psoralens) (Lupardus et al., 2002, Cimprich, 2007).

ATR binds to RPA coated ssDNA, either alone or in complex with ATR-interacting partner (ATRIP) with comparable affinities (Unsal-Kaçmaz and Sancar, 2004). Subsequently, Rad17 (Zou et al., 2002), Rad9-Hus1-Rad1 (Lee et al., 2007), Topoisomerase (DNA) II Binding Protein 1 (TopBP1) (Cotta-Ramusino et al., 2011, Haahr et al., 2016), claspin (Liu et al., 2006), Timeless (Tim) and Tim-interacting protein (TIPIN) (Unsal-Kaçmaz et al., 2007, Smith et al., 2009) protein complexes are loaded to activate ATR and promote RPA phosphorylation and facilitate checkpoint response. Recently, also other proteins were identified as ATR activators: Ewing tumour-associated antigen 1 (ETTA1) (Lee et al., 2016) and Downstream neighbour of SON (DONSON) (Reynolds et al., 2017).

2.2.2.2 RPA

Human replication protein A (RPA) is a heterotrimeric protein composed of RPA70, RPA32 and RPA14 subunits (named according to their molecular masses, also called RPA1, 2 and 3 respectively) (Iftode et al., 1999). RPA is a ssDNA-binding protein essential for ATR recruitment and for activation of DNA replication. Moreover, RPA is extremely important ATR target (Binz et al., 2004, Olson et al., 2006). RPA possess several phosphorylation sites, some were identified as common PIKKs targets (T21, T33, or S33) whereas others as targets of the cyclin-Cdk complexes (S23 and S29) or solely DNA-PK (S4, S8, S11, S12 and S13) (Block et al., 2004, Olson et al., 2006, Anantha et al., 2007, Niu et al., 1997, Dutta and Stillman, 1992, Zernik-Kobak et al., 1997).

The protein is at first specifically phosphorylated within the subunit RPA32 N-terminal on S33 by ATR (Binz et al., 2004, Unsal-Kaçmaz and Sancar, 2004) which stimulates phosphorylation by cyclin-Cdk and DNA-PK and results in hyperphosphorylated RPA (Anantha et al., 2007) with multiple cell cycle dependent functions. RPA phosphorylation

stimulates DNA repair in interphase cells, mutants with defective Cdk-dependent phosphorylation sites show aberrant DSBs repair (Anantha et al., 2007). Phosphorylation of S33 promotes DNA repair synthesis under RS conditions and increases ssDNA formation (Vassin et al., 2009). Specifically, phosphorylation sites T21 and S33 are necessary for recovery from replication stress (Vassin et al., 2009). Moreover, RPA hyperphosphorylation was shown to prevent RPA from association with replication centres *in vivo* and therefore help to repress DNA replication under DNA damage, or RS (Vassin et al., 2004).

2.2.2.3 FANCD2

The Fanconi anaemia complementation group D2 (FANCD2) is a 164 kDa protein of extreme importance for the Fanconi anaemia (FA) repair pathway.

FANCD2 participates in the repair of interstrand crosslinks (ICLs), and in the maintenance of genomic stability during DNA replication (Garcia-Higuera et al., 2001, Sims et al., 2007, Kottemann and Smogorzewska, 2013). It is also important for translesion synthesis (TLS), an important DNA damage tolerance pathway (Song et al., 2010) and DSB repair, namely HR (Nakanishi et al., 2005) while FANCD2 role in single-strand annealing is not clear as contradictory results have been reported (Nakanishi et al., 2005, Kais et al., 2016). The FA pathway proteins may also counteract some of the activities of the non-homologous end joining (NHEJ) pathway (Pace et al., 2010). FANCD2 forms nuclear foci during S phase and upon genotoxic stress (Garcia-Higuera et al., 2001).

FANCD2 undergoes monoubiquitinylation on Lys-56 that is crucial for FANCD2 foci formation (Garcia-Higuera et al., 2001). Ubiquitination requires the joint intervention of the other FA proteins (called core complex), including FA protein groups A, B, C, E, F, G and M, as well as FANCL protein (Garcia-Higuera et al., 2001). Several other proteins involved in cell cycle checkpoints and DNA repair, including RPA1, ATR, CHK1 and BRCA1 are also involved (Andreassen, 2004, Guervilly et al., 2008, Garcia-Higuera et al., 2001).

Deubiquitination is performed by Ubiquitin specific peptidase 1 when DNA damage is repaired (Nijman et al., 2005). FANCD2 can be also phosphorylated in response to various genotoxic stresses by ATM and/or ATR (Taniguchi et al., 2002, Ho et al., 2006).

FANCD2 plays a role in preventing breakage and loss of missegregation chromatin at the end of cell division, particularly after replication stress (Naim and Rosselli, 2009). Defects in FANCD2 protein or any other of the core proteins result in severe growth retardation, haematological abnormalities, up to 20% of patients develop cancer (Kutler et al., 2003).

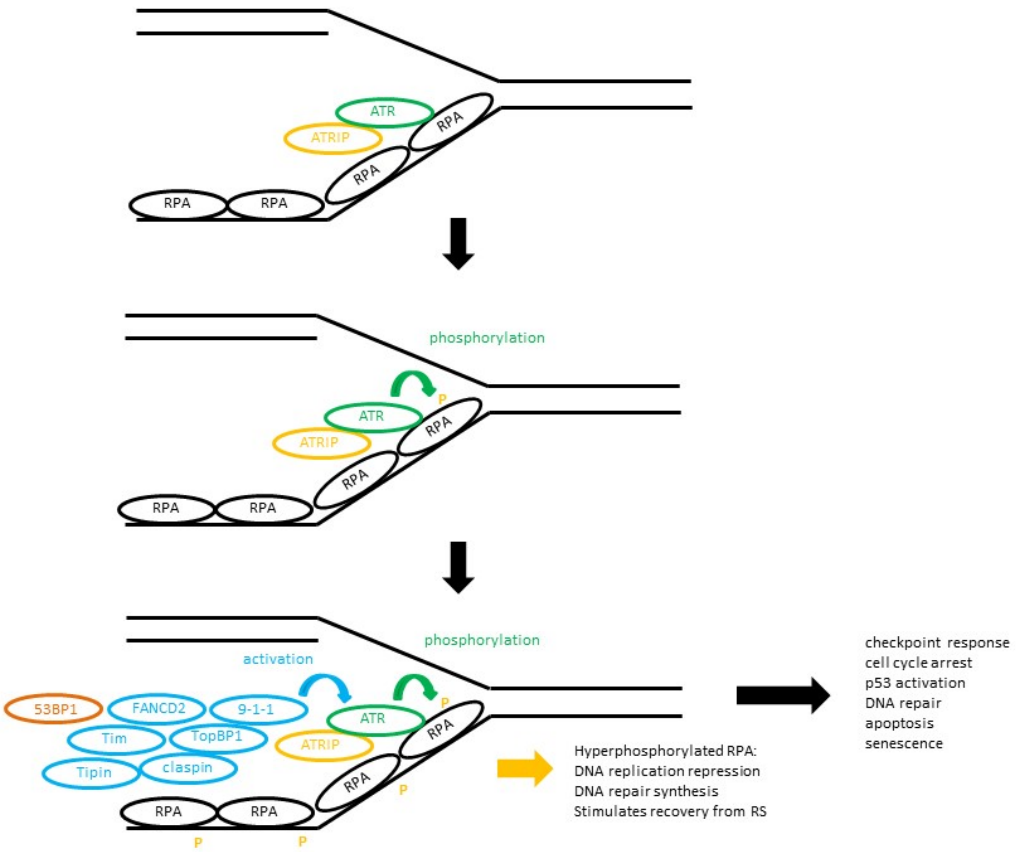

Figure 2. Replication stress response activation. Single-stranded DNA at stalled replication fork is coated by RPA protein that binds ATR protein alone or in complex with ATRIP. ATR phosphorylates RPA and this activation signal leads to recruitment of many other proteins, e.g. Rad1-Hus1-1, TopBP1, claspin, TIPIN and TIPIN-interacting protein that further activate ATR. ATR signalling is then responsible for recruitment of 53BP1, FANCD2 and triggers checkpoint response. As a result DNA repair synthesis is activated, DNA replication is repressed and cell cycle is arrested to gain cell more time for repair.

2.2.3 Checkpoint Kinases

Activation of DNA damage response by DNA damage sensor proteins leads not only to activation of repair pathways but at the same time to the cell cycle arrest hence more time for the repair is assured (Zhou and Elledge, 2000). CHK1 and CHK2 proteins are essential for cellular and organismal survival.

CHK1 is activated preferentially by ATR-response pathway (Paulsen and Cimprich, 2007) and it is necessary for cell cycle arrest upon DNA damage activation and when under-replicated DNA is present (Mackay and Ullman, 2015). The cell cycle arrest is executed by interaction with several proteins. CHK1 phosphorylates CDC25 which is a signal to CDC25-ubiquitin dependent degradation. Upon decrease of CDC25 protein levels, CDK-cyclin complexes are inhibited (by increased phosphorylation on their tyrosine residues) and cell cycle progression is blocked (Uto et al., 2004). CHK1 also phosphorylates histones, thus changing the epigenetic pattern and modulating the transcription of genes involved in the cell cycle progression (Shimada et al., 2008). Another CHK1 target is Retinoblastoma Protein A that directly interacts with E2F transcription factors that govern the cell cycle progression in all phases (Inoue et al., 2007), (Chen et al., 1996). Last but not least, p53 protein upon CHK1 phosphorylation promotes cell cycle arrest or initiates apoptosis.

CHK1 also interacts with several DDR proteins thus modulating the DNA repair. Upon CHK1-dependent phosphorylation, HR-related Rad51 protein is released from the complex with BRCA2 protein and binds extensively to chromatin and executes HR (Bahassi et al., 2008). CHK1 also phosphorylates FANCE protein which is a necessary prerequisite for FA complex and FANCD2 interaction (Wang et al., 2007), one of the critical pathways for the DNA crosslink repair. CHK1 is also indispensable for the maintenance of replication fork by interacting with PCNA (Yang et al., 2008)

The other protein kinase CHK2 has a similar function to CHK1 and also some of the targets are shared, e.g., CDC25, BRCA2, p53, it also modulates the activity of E2Fs (Stevens et al.,

2003). CHK2 promotes G2/M cell cycle arrest and phosphorylates tumour suppressor BRCA1, a key player in HR repair pathway (Moynahan et al., 1999). Among the CHK2 targets belong also MDM4 and PML that regulate apoptotic response in a p53-dependent manner (Migliorini et al., 2002, Mancini and Moretti, 2009, LeBron et al., 2006, Yang et al., 2002).

2.2.4 Common Fragile Sites

Specific parts of the genome called common fragile sites (CFS) are particularly prone to breakage and rearrangements (referred to as expression) upon RS (Sutherland, 1991). In the human genome approx. 80 CFS have been described, and some of them span up to several megabases (Zlotorynski et al., 2003). The most specific and reproducible CFS inductor is aphidicolin used in low concentrations (approx. 0.1 - 1 μM) (Durkin et al., 2008, Glover et al., 2005). There are also other factors generating CFS expression, e.g., hydroxyurea, camptothecin, hypoxia and folate deficiency, but none of them is so specific, nor efficient as aphidicolin (Bristow and Hill, 2008, MacGregor et al., 1990, Fujita et al., 2013, Janson et al., 2015). CFS expression varies among individuals, as well as tissue and cell type (Letessier et al., 2011, Le Tallec et al., 2013) but some of them, e.g., FRA3B and FRA16D, are found more often than the others (Denison et al., 2003).

Some of the structural features described in Chapter 2.1.1. can be found in CFS, e.g., frequent AT-rich islands, which enable them to fold into secondary structures as soon as the DNA double helix is unwound (Zlotorynski et al., 2003). This observation was not confirmed by direct observation *in vivo*, but it is assumed based on experiments in yeasts that such sequences may perturb DNA replication by presenting a hard-to-replicate structure for ongoing RF (Zhang and Freudenreich, 2007, Franchitto, 2013).

CFS expression is proposed to be also influenced by epigenetic patterns as observed within human FRA16C. Most of the replication origins within this CFS are activated under normal

growth conditions, which indicates that replication of this region is intrinsically perturbed (Ozeri-Galai et al., 2011).

Individual CFS clearly differ in their sequence and base composition among each other but it does not necessarily disprove the molecular basis of CFS fragility. The structural explanation for their fragility is considered as valid, as each CFS might be affected by different stress factors (Franchitto, 2013).

Other structurally unrelated factors leading to CFS expression has been also described. RF progression can be violated by low efficiency of origins located within CFS (Palakodeti et al., 2010). Expression of FRA3B, FRA6E and FRA16D were correlated with the presence of large initiation-poor regions (Letessier et al., 2011, Palumbo et al., 2010) pointing to the fact that the replication may not be completed before the end of S phase. Then, under-replicated regions enter G2 and may even remain undetected and enter mitosis. Several CFS have been overlapping the coding regions of large human genes, e.g. WW Domain Containing Oxidoreductase (WWOX) at FRA16D (Ludes-Meyers et al., 2003), or Fragile Histidine Triad (FHIT) at FRA3B (Zimonjic et al., 1997). It has been well established that transcription of such genes requires a long time to be completed. The probability that transcription and replication may occur at the same time is therefore enhanced. The collision between transcription machinery and RF may result in R-loop formation, considered as a rare byproduct of transcription and threat to genome stability (Helmrich et al., 2011, Aguilera and García-Muse, 2012). CFS stability is also challenged by defective proteins, so called CFS stability keepers, e.g., Ataxia Telangiectasia Rad3-related (ATR) kinase (Koundrioukoff et al., 2013), Werner Helicase (WRN) (Pirzio et al., 2008), or Breast Cancer 1 (BRCA1) protein (Arlt et al., 2004), and others.

Overall, it has been proposed that both structural and structure unrelated factors contribute to CFS expression in an additive manner (Franchitto, 2013). CFS are commonly associated with genomic rearrangements (Tsantoulis et al., 2008) often leading to altered gene products,

which may result in gain or loss of function of affected gene products. CFS were also studied in relation to precancerous and cancerous lesions (Bartkova et al., 2005). CFS are often found altered in tumours (Glover et al., 2005) and their causative role in cancer development has been suggested (Hellman et al., 2002).

It is evident that endogenous stresses arising from the DNA structure and cellular metabolism pose a significant threat to genome integrity and put significant demands on the efficiency of repair pathways.

2.3 Consequences of disturbed DNA damage response

Defective function of DDR either in the detection step, the signal transduction or signal enhancement, leads to improper activation of DNA repair and to disturbances of a wide range of cellular events. The impact of such circumstances is of a high biological significance as it results in the development of diverse human diseases or drug resistance. It also serves as a basis of multiple chemotherapeutic approaches, particularly in oncology.

Mutations introduced to the DDR genes further enhance DNA damage introduced in the cells and together with other deleterious events, e.g., disturbed replication or telomerase attrition (d'Adda di Fagagna et al., 2003) contribute to genomic instability (Hills and Diffley, 2014).

Genomic instability (GI) is defined as a process prone to genomic changes and alterations (Shen, 2011). GI can be described as a driving force of tumorigenesis promoting the acquisition of further DNA alterations, clonal evolution, and tumour heterogeneity. A great number of structural DNA abnormalities present in cancer genomes is largely attributed to GI. (Pikor et al., 2013).

Also, replication stress (RS) was proposed to contribute to GI and accelerate mutational phenotypes that allow selection for mutations (Murga et al., 2011). Chronic RS conditions, particularly in the absence of proper DNA damage repair pathway and/or non-functional checkpoint responses might result in the transfer of RS-related DNA alterations to daughter

cells. Chronic RS significantly contributes to induction and conservation of mutations, enhances GI, promotes senescence, apoptosis or fuels tumourigenesis (Gorgoulis et al., 2005, Zeman and Cimprich, 2014, Mladenov et al., 2016). Enhanced GI and RS have been associated with several hereditary syndromes exhibiting a quite broad range of symptoms: premature ageing, cancer predisposition, immunodeficiency, growth retardation, neurodegeneration and others. Aberrations in DNA damage recognition and repair enzymes are responsible for disorders like Seckel syndrome (deficiency in ATR kinase) (O'Driscoll et al., 2003, O'Driscoll and Jeggo, 2003), Ataxia telangiectasia (caused by the loss of ATM kinase) (McKinnon, 2004), Xeroderma pigmentosum (XP; various defects in XP protein family group) (DiGiovanna and Kraemer, 2012). Failure of replication fork progression and restart is connected with Fanconi anaemia (FA; mutations in FA pathway proteins) (Kim and D'Andrea, 2012, Joenje and Patel, 2001), Bloom and Werner syndrome (deficiency of Bloom and Werner helicase, respectively) (Lauper et al., 2013, Bernstein et al., 2010), or Rothmund-Thomson syndrome (defects in RECQ like helicase 1 protein) (Larizza et al., 2010, Lu et al., 2016).

Unsuccessful DNA damage repair leads to persistent activation of DDR, which promotes loss of proliferative capacity and results ins senescence or apoptosis (Bartkova et al., 2005). Senescence is a state of reduced proliferative activity and upon physiological conditions, it is triggered by shortened telomeres (Harley et al., 1990). Cells also trigger senescence after prolonged conditions of RS, e.g., altered DNA replication initiation (unscheduled firing and/or re-licensing of replication origins) by activated oncogenes (Bartkova et al., 2006, Di Micco et al., 2006). Such scenario has been reported for pre-cancerous lesions where senescence-induced persistent DDR is proposed to act as a natural barrier against tumour progression (Bartkova et al., 2006). Apoptosis is a precisely controlled process of immense importance in development and organismal homoeostasis. It is a regulated process executed by intrinsic cellular signalling and results as a response to environmental signals or internal

conditions. Elimination of pro-apoptotic pathways can be deleterious as it may contribute to development of some types of cancer (Wouters et al., 1999, Bartek et al., 2004, Jackson and Bartek, 2009, Polo and Jackson, 2011).

A precise understanding of how DNA lesions are generated, processed and repaired can lead to the selection of an effective disease treatment. For example, in HR-defective tumours, e.g. BRCA1/2 defective breast and ovarian cancer cells, were reported to be more susceptible to PARP1 inhibitors (Martin et al., 2008). As PARP1 inhibitor causes disturbances in single-strand breaks repair leading to more DSBs formation and more HR dependency. However, PARP1 inhibitors monotherapy was proven to be insufficient for complete tumour remission (Kaufman et al., 2015) but seem to be a promising agent for combination treatment. PARP1 was also observed to cause increased activation of ATR/CHK1 pathway and inhibition of both pathways was already tested in BRCA1-deficient tumour model with positive results (Kim et al., 2016). PARP1 inhibitors are also investigated to be used for the treatment of ovarian cancer with BRCA1/2 methylated promoters (Stordal et al., 2013). Another example can be the CHK1 inhibitor treatment in order to increase the replication stress. ATR inhibition was reported to lower the threshold and increase the tumour cell death of p53 mutant and wild type human cancer cell lines (Massey, 2016).

Elevated DDR can be considered to work as a natural anti-cancer barrier, especially in the precancerous lesion (Bartkova et al., 2005). However, prolonged elevated DDR or defective DDR may contribute to the selection pressure for clones that are then able to overcome the arrest and continue in proliferation despite mutations. It was also proposed that the defective pathways may be considered as the Achilles' heel of cancer cells and can be targeted by chemotherapeutics (Bartek et al., 2012). So, detailed knowledge of the processes being responsible for the disease development can provide the opportunities for cancer prevention and treatment.

2.4 Laser micro-irradiation

Laser micro-irradiation and the microbeam techniques are used for various purposes, mainly for cell lysis (Rau et al., 2006), microdissection and microsurgery (Botvinick et al., 2004) and DNA damage induction (Dinant et al., 2007). Laser interaction mechanisms with cellular components can be complex, involving photothermal, photochemical and photomechanical processes. The contributions of these processes to the laser–cell interactions depend on the laser power, laser wavelength, pulse duration, and laser beam diameter (Kong et al., 2009).

This chapter focuses on DNA damage induction by laser micro-irradiation (LMI). Mammalian cells damaged by localised UV radiation provide one of the best-known experimental systems for studies of the biological consequences of localised DNA damage. LMI has been in use for several decades (Cremer et al., 1974, Cremer and Cremer, 1986), however, it took until late 1990's when the technique became widely available.

The biggest advantage of LMI is the possibility of precise definition and control of the irradiated area (called the region of interest, ROI). Localised DNA damage caused by a laser beam enables to follow the temporal and spatial interactions between DNA damage and damage-binding proteins. The protein of interest can be visualised by IF technique, or by live cell imaging (Drexler and Ruiz-Gómez, 2015). The micro-irradiation enables detailed cytological analysis of DNA damage protein accumulation and post-translational modifications and easily distinguish the damage pattern from spontaneous and bystander effects (Seiler et al., 2011), Fig. 3a,b.

One of the first groups employing the LMI technique was Bonner's group (Rogakou et al., 1998, Rogakou et al., 1999). During the first ten years, a wide variety of laser systems and various types of dose estimation were used. Unfortunately, irradiation conditions were often only poorly specified making it difficult to compare the delivered energies and interpret the results (Kong et al., 2009, Reynolds et al., 2013). Although the laser output is user defined, unknown part of the energy is lost during the transfer to the sample. The types of DNA

damage generated are not entirely characterised and are dependent on multiple factors, e.g., laser wavelength, laser type (pulse, or continuous), laser beam size, treatment with a sensitizer, etc. (Splinter et al., 2010). High laser energies may lead to unspecific chromatin alterations (Drexler and Ruiz-Gómez, 2015). However, as the technique is used more often, the establishment of dose measurement or some type of unbiased reference for samples comparison will be necessary soon (Kong et al., 2009, Reynolds et al., 2013). The most relevant seems to be the measurement of the biological effect with a selected marker as reported by (Bekker-Jensen et al., 2006). However, this approach is demanding, time-consuming and therefore not widely used approach.

As demonstrated recently, the cellular response differs significantly upon the low and high dose of the energy delivered (Saquilabon Cruz et al., 2016). Using the near-infrared laser (NIR) at high power, TRF2 and PARP1 proteins were shown to load to sites of DNA damage, and the pan-nuclear γH2AX signal was detected. However, when lower NIR laser power was used none of the above-mentioned proteins was observed to recruit to sites of damage, instead 53BP1 was present, and γH2AX formed localised foci at the damaged sites. For an accurate description of DDR, precisely defined irradiation conditions are extremely important as well as for comparing the results.

There are multiple lasers currently in use for LMI technique, almost all of them can be used for direct DNA damage induction, e.g., NIR (Gomez-Godinez et al., 2007), or 266 nm lasers (Dinant et al., 2007). More severe, dense and complex damage caused by, e.g., NIR lasers enables to detect also the proteins that do not form IRIF. This is a great advantage because cytological detection of these proteins is difficult following conventional DNA damaging methods. For example, NHEJ repair protein Ku was cytologically first detected using the micro-irradiation technique (Kim et al., 2005a).

The most popular are UV-A lasers spanning the range 337 - 405 nm which are often used in combination with sensitizers, mostly nucleotide analogues (Bekker-Jensen et al., 2006) and/or

Hoechst dyes (Walter et al., 2003) that absorb the energy and pass it on the DNA (Rogakou et al., 1999). The most commonly used sensitising compounds are 5'-bromo-2-deoxyuridine (BrdU) and Hoechst33358 but also other nucleotide analogues, or other types of Hoechst dye were reported (Tashiro et al., 2000, Dinant et al., 2007). According to the literature many different concentrations of BrdU spanning the range of 1 - 10 μM are used (Stixová et al., 2014, Dinant et al., 2013, Bekker-Jensen et al., 2006). Generally, a higher concentration of BrdU and prolonged incubation times increase the amount of incorporation and lead to enhanced response upon UV-A irradiation (Limoli and Ward, 1993, Fujii et al., 2013). BrdU is incorporated into DNA during S phase instead of thymidine nucleotide (Bick and Davidson, 1976). The rate of ongoing replication is a limiting factor for the amount of incorporated BrdU and thus the level of sensitisation. Employment of the replication-independent sensitizer is therefore inevitable for experiments with non-cycling cells, e.g. senescent cells. Hoechst dyes, non-specifically binding to the minor groove of DNA (Searle and Embrey, 1990) are used for this purpose. Hoechst dyes are often used in concentration range 0.5-10 μg/ml and incubation time up to 20 min (Limoli and Ward, 1993, Rogakou et al., 1999, Paull et al., 2000, Abdou et al., 2015).

Sensitizers, in general, make the whole nucleus vulnerable to any UV-A light that might be scattered from the laser beam (Rogakou 1999), or absorbed from other sources. In addition, BrdU shows antiproliferative effects altering the cell cycle progression. In hamster melanoma cells it was observed that 18 μM BrdU was mutagenic and caused rapid exhaustion of dCTP pool, with a maximum at 6 – 12 h. The ratio BrdUTP/dCTP was shown to be the critical factor of mutagenesis (Ashman and Davidson, 1981). BrdU is also suppressing the DNA damage repair (Iliakis and Kurtzman, 1991). The incubation time is very important as cells entering the second replication in the BrdU presence will also incorporate the BrdU to the second strand of DNA resulting in higher damage upon exposure to laser irradiation (Fujii et al., 2013). Hoechst dye was reported to be cytotoxic at concentrations above 20 μM and

incubation times as short as 30min – 1h. Hoechst also affects DNA synthesis rate and significant cell cycle perturbations were reported when 5-10 μM of Hoechst for applied for 30 min (Durand and Olive, 1982). The plating efficiency is reduced by 4-5 fold in unirradiated cells and 25-45 fold in irradiated cells after treatment with 5-10 uM Hoechst for 1-2 h (Siemann and Keng, 1986). Moreover, several days long time-lapse imaging may cause apoptosis in Hoechst-stained cells (Purschke et al., 2010).

There are several studies showing that sensitization is not mandatory for UV-A DNA damage induction if enough laser power is used. The studies reveal varying degrees of DSB, SSB, UV, and base damage generated by UV-A with and without BrdU (Stixová et al., 2014, Splinter et al., 2010, Mistrik et al., 2016).

The LMI approach was proven invaluable in a series of laser microbeam experiments, which led to the identification of numerous proteins accumulating at the damage sites.

There is also another approach for LMI based on micropore filter irradiation and it was introduced by (Katsumi et al., 2001), Fig. 3c. Micropore filter absorbs the irradiation, so only cells or portions of the cells lying in the area of pores are damaged. It is an elegant, cheap and fast approach for DNA damage induction only in part of the nucleus while the rest stays intact. However, this approach is unsuitable for the dynamic studies as quite long irradiation times are required. Also, it is impossible to perform multiple irradiations in one cell, or precise irradiation only to the specified region, e.g., heterochromatin region within the nucleus.

The lasers may be used also for several techniques involving photo-manipulation of the fluorescent tag. The process of tag destruction is called bleaching and enables to follow the tagged component mobility. The technique fluorescence recovery after photobleaching (FRAP) is in use for several decades (Axelrod et al., 1976). During the bleaching, ROS are formed which may lead to significant phototoxicity (Yamagata et al., 2012). The other techniques, fluorescence loss in photobleaching (FLIP), inverse FRAP (iFRAP), and

fluorescence localisation after photobleaching (FLAP) are not so widely used owing also to the specific purpose the methods.

Commonly used approaches to photo-manipulations require the manual definition of a region of interest (ROI). After the photo-effect is induced, manual repositioning of ROI for precise measurements over time must be performed due to cellular movement. Such approach is laborious and time demanding in terms of laser irradiation, image acquisition and evaluation. In this thesis, a new method overcoming many drawbacks of commonly used approaches was developed.

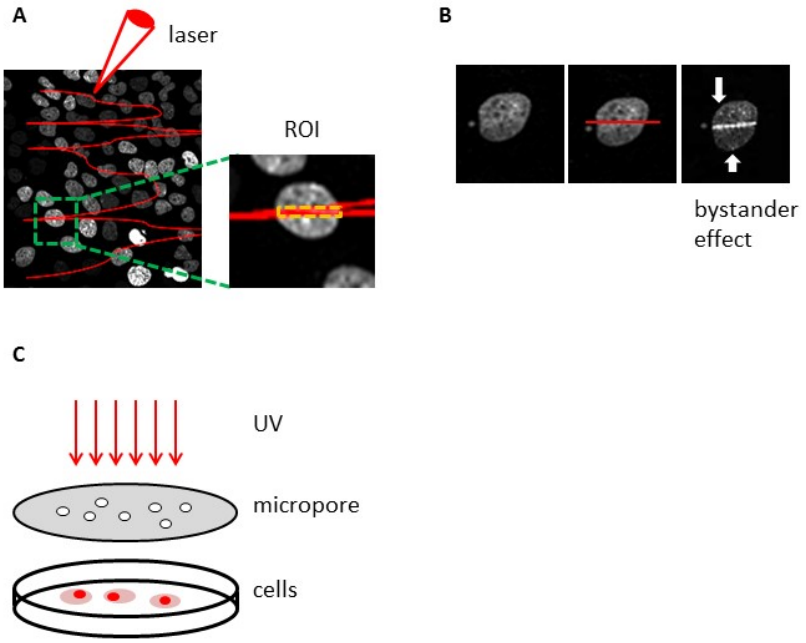

Figure 3 Illustration of laser micro-irradiation techniques. (a) Laser path (red line) defined manually is followed by the laser. In selected nucleus region of interest (ROI) is subsequently defined manually (dashed yellow line). **(b)** DNA damage was induced in the region of laser path (red line). MDC1-GFP protein accumulation is observed in the region. Weak bystander effect can be observed as small foci marked by white arrows. **(c)** Schematic view of micropore irradiation, adapted from http://www.cosmobiousa.com.

3 MATERIAL AND METHODS

Cell lines, cell culture conditions

All cell lines were cultivated in DMEM with stabilised glutamine and sodium pyruvate (Biosera), supplemented with 10 % foetal bovine serum (Gibco, Life Sci.) and penicillin-streptomycin (Sigma). Cells were kept under standard cultivation conditions in humidified incubator at 37°C, 5% CO_2. In the study the following cell lines were used: U-2-OS (ECACC), MRC-5 (ATCC), mouse McCoy fibroblasts (R-D Biotech), reporter cell lines: U-2-OS-MDC1-GFP, U-2-OS-53BP1-GFP, PD20F-FANCD2-GFP, U-2-OS-BRCA1-GFP were obtained from Danish Cancer Society. All reporter cell lines were seeded 1 cell per well (96 well plates, BD Influx, BD Biosciences) to obtain individual clones of specific fluorescence intensity. The clones were subsequently selected according to the GFP-signal subcellular distribution. The clones exhibiting the GFP-tagged nuclear protein in the cytoplasm were excluded. Selected clones were tested according to the efficiency of translocation of the GFP-tagged protein to sites of DNA damage generated by micro-irradiation. U-2-OS-H2B-GFP cell line was established, cloned and characterised by Ivo Frydrych (LEM, IMTM, Olomouc).

Cell seeding and treatment with sensitizers

Cells were seeded in 6 well plate (215.10^3 cell per well), 18 h later BrdU (Sigma) was added in indicated concentrations. After 6 h cells were seeded in 96 well plate with glass bottom (Corning) and kept in an incubator in the presence of BrdU for additional 18 h. Immediately before micro-irradiation, or as indicated, the cultivation medium was changed to HEPES-buffered medium (Invitrogen), supplemented with 10 % fetal bovine serum (FBS). In all experiments, the cells were sensitised by 1 μM BrdU for 24h in total unless stated otherwise.

In the case of Hoechst33342 (Invitrogen) sensitisation cells were processed the same as for BrdU sensitisation. 1 h before micro-irradiation cultivation medium was changed to HEPES-buffered medium (Gibco) with indicated concentrations of Hoechst33342 for 25 min; then the medium was replaced with HEPES-buffered medium without sensitizer. Micro-irradiation

was performed 30 min later to ensure proper diffusion of Hoechst33342 in the nuclei.

Compounds treatment

Compounds were added to cells 2 h before micro-irradiation unless stated otherwise. HEPES-buffered medium (Gibco) was used for compound dilution, and the cells were incubated in the presence of compounds during the whole experiment.

siRNA treatment

Following siRNAs were used: siGenome RISC FREE and siXPC SMART pool (both Dharmacon). Cells were seeded in 6 well plate (200.10^3 cells per well). The next day after 30 min incubation in penicillin/streptomycin-free medium, siRNA with Lipofectamine RNAiMAX (Invitrogen) diluted in OptiMEM (Gibco) was added for 6 h. Then transfection solution was replaced with standard cultivation medium. The experiments started 48 h after transfection.

Cell line establishment

U-2-OS-PARP1 chromobody stable cell line was established by transfection of commercial PARP1 chromobody plasmid construct (Chromotek) with Lipofectamine 2000 (Invitrogen) according to manufacturer's instructions. The stable cell line was generated by Geneticin418 (Sigma), and clones were generated as described above. Only clones exhibiting enhanced PARP1-chromobody nucleolus signal and significantly higher signal from the nucleus than from cytoplasm were selected for the experiments.

Microscope settings for UV-irradiation

Microscope Zeiss LSM780 equipped with incubator and ZEN 2011 software were used. For UV-irradiation 355 nm laser was used at maximum power (65 mW, 100 % output). The irradiation conditions were as follows: resolution 32 x 32 (or 64 x 64, 128 x 128) pixels, the lowest possible scanning speed (pixel dwell time for 32 x 32 resolution was 709.27 μs, bidirectional scan, zoom 0.6. The number of iterations is indicated in the figure legends. UV-irradiation at resolution 32 × 32 was chosen as it is causing approx. 1 – 2 stripes per cell

nucleus with 40 x objective. Autofocus was performed with 488 nm laser before irradiation, or manually if wild-type (wt) cells were used. All experiments were performed in a pre-heated incubator (37°C). Wells were sealed with tape to prevent evaporation of the medium and the plates were put in the incubator at least 30 min before the experiment to ensure proper temperature equilibration.

Microscope settings for bleaching

All settings were the same as for UV-irradiation, except for the laser wavelength. 488 nm at 100 % output was used to destroy the GFP tag.

Microscope settings for image acquisition

For live-cell experiments, the images were acquired with 488 nm laser (approx. laser output 2 %). Images were acquired in 16-bit depth, zoom 0.6, five z-stack planes (1 μm apart). Autofocus was based on reflected light of 561 nm laser also known as backscatter image. A thin contact layer between cells and the glass cultivation surface is reflected, and GFP-bleaching is minimised.

For image acquisition of IF samples 355 nm, 488 nm, 561 nm and 647 nm lasers at low laser power were used (experiment dependent). Automatic autofocus was performed before image acquisition based on Hoechst-stained nuclei. 5 z-stack planes (1 μm apart) were acquired per each channel. Images were taken at resolution 1024 x 1024, 16-bit depth, zoom 0.6.

Image analysis of striation pattern

Images were taken in 5 z-stack planes; maximum intensity projection was employed to create one image. IF images were analysed with the same software routine as the images obtained in the live-cell experiments. Slight modifications were employed: tracking module was deactivated, and the recognition of the nuclei was based on the Hoechst33342 signal.

Immunofluorescence staining

Cells were fixed in 10 % formalin (Sigma) for 15 min and permeabilized with 0.5 % Triton-X (SigmaAldrich) in PBS for 5 min. Samples were blocked with 1 % BSA in PBS for 20 min;

primary antibodies were added and incubated at 4°C overnight, secondary antibodies were incubated 1 h at RT. DNA was stained with 5 μg/ml Hoechst33342 (Invitrogen) in PBS.

Used antibodies: phospho-H2AX (Ser139) JBW301 (Millipore, 500x), 53BP1 (Santa Cruz, 500x), cyclin A (Leica, 50x), phospho-histoneH3 (Ser10) (Santa cruz, 500x), AlexaFluor488 and AlexaFluor568 (Invitrogen, 1000x).

Image acquisition and analysis of classical immunofluorescence samples

IF samples stained for cyclin A and 53BP1 were acquired with ScanR Acquisition software and analysed in ScanR Analysis software. Cells were recognised based on DNA staining (Hoechst33342), Signal integrated density (SID) of cyclin A was counted, and the threshold was set to distinguish between positive (S and G2 cells) and negative (G1) cells. Only in cyclin A negative cells the number of 53BP1 foci was counted and plotted. The method is based on the article (Lukas et al., 2011). Authors demonstrate that unrepaired damage induced in S and G2 phase is transferred through mitosis and shielded by 53BP1 in G1 cells.

Image acquisition and analysis of mitotic cells

IF samples for analysis of mitotic cells were stained with γH2AX and phospho-H3 (Ser10) antibodies. Samples were acquired with Zeiss Cell Observer (spinning disc microscope) at semi-automatic regime by the custom made routine developed in MatLab by Dr Tomáš Fürst. The samples were automatically scanned upon 10 x resolution and approx. 150 mitotic cells were selected based on phospho-H3 positive staining. Then, selected cells were acquired in detail upon 63x resolution. γH2AX foci were recognised, counted and plotted in box-plot charts. The analysis was done by a custom-made routine developed by Dr Tomáš Fürst. The method is based on principles described in articles by (Rogakou et al., 1998, Juan et al., 1998, Mistrik et al., 2009). Altogether these articles suggest that detection of γH2AX sensitively reflects the amount of damage present in the cells. Replication stress was generated by treatment with 0.4 μM aphidicolin which was reported to cause massive CFS expression (Durkin et al., 2008, Glover et al., 2005) in mitosis. γH2AX was elevated upon APH

treatment in mitotic cells suggesting that the observed damage is present preferentially at CFS.

Western blotting

Lysates were prepared by diluting the cells directly in 2x LSB, 1400 rpm shaking upon 95°C. Electrophoresis was performed on pre-cast gradient gels (Biorad), 20 mA per gel, 75 min of separation. Western blotting was performed upon semi-dry conditions, 150 mA per membrane for 1.5 h. Membranes were blocked in 5 % milk for 1 h, shaking 100 rpm. Primary antibodies were incubated overnight at 4°C; secondary horseradish-conjugated antibodies were incubated for 1 h at RT. Antibodies were visualised by Super Signal West Chemiluminescence Substrate (ThermoScientific), mixed pico:femto 3:1 luminescence was visualised by ChemiDoc MP Documentation system (Biorad). Used antibodies: CHK1 (Santa Cruz, 500x), phosphorylated CHK1(Ser345) (Santa Cruz, 500x), XPC (Novus Biologicals, 1000x), GAPDH (GeneTex, 4000x), secondary antibodies: antimouse (GE-Healthcare, 1000x), antirabbit (GE-Healthcare, 1000x).

EdU assay

Cells were treated for 20 min with 10 μM EdU diluted in cultivation medium. Fixation was performed as described in the section immunofluorescence. EdU was detected by CLICKiT EdU Imaging Kit (Thermofisher) according to manufacturer protocol, AlexaFluor488azide (Invitrogen, 1000x) was used. The antibody detection was performed as described in the section immunofluorescence. DNA was stained with 5 μg/ml Hoechst33342 in PBS for 30 min.

Cell cycle analysis

For cell cycle analysis, cells were fixed with 10 % formalin (Sigma) and stained with Hoechst33342 5 μg/ml in PBS (Invitrogen) for 10 min. Images were taken by OlympusBX71 inverted microscope, and ScanR Acquisition and cell cycle were analysed in Analysis

software (Olympus).

Striation pattern visualisation

The standard glass slide was covered by a homogeneous layer of a permanent marker paint (Permanent 8566, ink colour 04, Centropen), air dried, mounted by water, covered by a cover glass (0.17 mm) and sealed by a nail polish. The paint was irradiated by 355 nm laser, 100% output, 32x32 pixels resolution, 1 iteration, pixel dwell time 709.27 μ s, bi-directional scan. The image was acquired using 561 nm laser and emission spectrum 570–710 nm.

4 RESULTS

4.1 Optimisation of the new laser micro-irradiation approach and its validation for DNA damage response studies

A new micro-irradiation approach based on specific software settings was developed. The process enables simultaneous irradiation of a huge amount of cells, i.e. irradiation of the whole acquisition area by a regular pattern. The technique is accompanied by a newly developed image analysis routine thus facilitating evaluation of the DDR in a quantitative manner resembling high-content screening (HCS).

4.1.1 Standard laser scanning microscope (LSM) can be set to generate predefined regular pattern covering the entire acquisition area

Standard laser micro-irradiation approach for DNA damage induction is performed by manual laser path definition. The high-power laser then follows the path and DNA damage is induced. The process is time-consuming for both, sample irradiation and subsequent analysis. A novel automated approach for LMI described here takes the advantage of unusual software settings. In case the acquisition software of LSM system is set to a low resolution and slow scanning speed, in combination with a high-power laser, specific striation pattern is generated. Basically, the entire acquisition area is scanned with a small resolution, e.g., only 32 pixels in each dimension (x and y) and as a result, the pattern of 32 horizontal lines is generated. Visualisation of the resulting striation pattern on a layer of fluorescent paint is shown in Fig. 4a. The scanning speed (determined by a pixel dwell time) and the number of repetitions of the scanning cycle (iterations) determine the dose of light energy delivered. If the used laser has DNA damaging properties, the pattern can be visualised by detection of DDR protein (Fig. 4b, c).

The described settings enable to perform the fastest photo-effect generation achievable because the defined laser path is fully in line with laser movement (as for standard image

acquisition). Other LSM systems than Zeiss LSM780 were successfully tested to generate the striation pattern, particularly SP5 Leica (tested in cooperation with Hana Hanzlikova, Ph.D., IMG, ACS, Prague, summarised in Mistrik et al., 2016) and ImageXpress Ultra Confocal High-Content Analysis System, Molecular devices (Josef Jaros, Ph.D., MU Brno, personal communication).

The described approach was also tested with several objectives. The property of each objective varies thus significantly affecting the efficiency to cause DNA damage (Fig. 4d). Moreover, the amount of micro-irradiated cells is dependent on the objectives' resolution and on the size of the cells.

a **b**

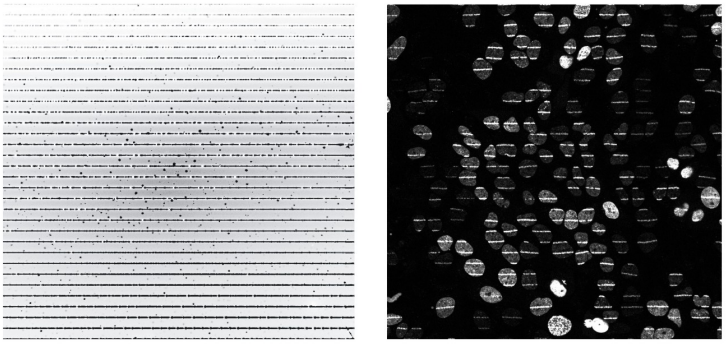

c

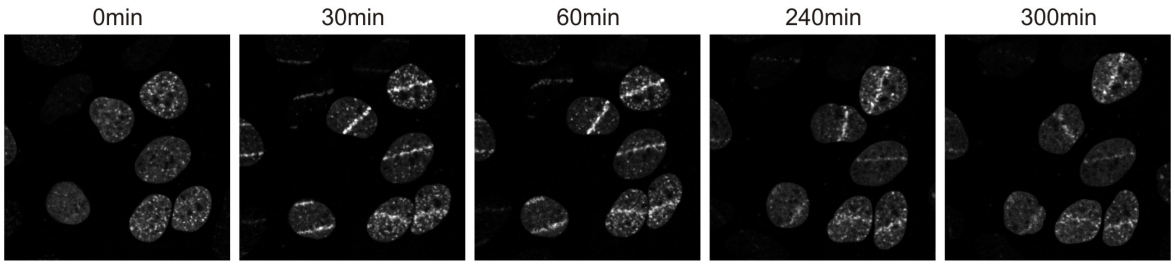

d

magnification	immersion	stripes formation	objective type
20x	none	yes	Zeiss, Pln-Apo, 0.8, DICII
20x	water	no	Zeiss, Pln-Apo, 1W, DICIII
20x	water	no	Zeiss, N-ACP, 0.5W
40x	oil	yes	Zeiss, EC Pln 1.30 DICII
40x	water	yes	Zeiss, C-Apo, 1.2 DICIII
63x	oil	yes	Zeiss, Alpha Pln Apo 63x/1.40
100x	oil	yes	Zeiss, Pln Apo100x/1.46

Figure 4. Method introduction. **(a)** Visualisation of the striation pattern on a layer of fluorescent paint**. (b)** Striation pattern induced by a 355 nm laser (32 lines/field) in BrdU sensitised cells. DNA damage is visualised by recruitment of ectopically expressed MDC1-GFP protein. **(c)** Evolution of the striation pattern over time. DNA damage induction was the same as in **(b)**. **(d)** List of tested objectives on Zeiss LSM780 system with respect to their ability to form stripes in BrdU sensitised cells using a 355 nm laser. U-2-OS-MDC1-GFP cell line was used for all images.

4.1.2 The induced striation pattern allows automated quantitative image analysis and robust statistical testing

The pattern generated by the presented method is regular, well-defined and enables automated software-based analysis. However, it cannot be easily analysed in any commercially, nor open-source image analysis program. Therefore, new evaluation method was developed in MatLab software in cooperation with Dr Tomáš Fürst (Faculty of Science, UP, Olomouc). The scripts have been made freely available and can be downloaded from Nature Protocols Exchange website (http://www.nature.com/protocolexchange/protocols/4597), and are enclosed as an appendix 6. The software reduces the workload needed for image analysis, and a number of analysed cells can achieve hundreds of cells instead of dozens of cells (a typical amount for manual approaches) per sample. Such large datasets bring the advantage of robust statistical analysis.

The first part of the software routine is segmentation of images, i.e., detection of nuclei. Nuclei can be recognised for example based on the expression of the nuclear fluorescently tagged protein. Reporter cell lines used in this study exhibited variable expression of the tagged protein even within a clonal population. Upon such conditions, standard thresholding methods do not allow segmentation of all nuclei within the image. Therefore, a different approach was employed. The nuclei are found by a “sliding frame” method combined with an adaptive threshold technique. By this approach, the segmentation was significantly improved

even in a very heterogeneous population. Nuclear staining by e.g. Hoechst dye that may easily overcome this problem was avoided for several reasons. First, the cells should be prevented from any additional interfering agents. Second, the acquisition of additional images would slow down the whole process.

After image segmentation, the DNA damage response is evaluated in each individual nucleus. The DNA damage is induced in a defined pattern of parallel stripes, and DDR protein with the fluorescent tag is translocated to the sites of DNA damage thus visualising the pattern (Fig. 4b). The position of the stripes is found based on their diameter and the distance between stripes (gauge), Fig. 5a. Signal integrated density (SID) and area of stripes and of the whole nucleus is calculated. Based on these measurements a new value called the 'measure of striation' (MS) was defined in this project for evaluation of DDR dynamics. MS is counted as a relative value, according to equations 1 and 2. This value is independent of the total amount of signal within the nucleus. As a result, the response among cells with different expression of the fluorescent protein can be compared.

$$MS = \frac{J_{meas} - J_{expt}}{J_{expt}}$$

Equation (1): J_{meas} (measured) stands for the actual signal integrated density of stripes' region, and J_{expt} (expected) stands for the expected value of the signal integrated density of the stripes' region, if the nucleus was perfectly homogeneous and no stripes were present.

J_{expt} is computed according to equation (2):

$$J_{expt} = \frac{Area\ inside\ the\ stripes}{Total\ area\ of\ the\ nucleus}\ SID\ of\ the\ nucleus$$

Equation (2): SID stands for signal integrated density.

For further details about the routine principles and used algorithms, please refer to the Method section: ‘Quantitative analysis of the striation patterns’ in (Mistrik et al., 2016).

By plotting MS values over time, DDR curve is generated which follows the dynamics of the tagged protein during DDR. For statistical analysis, three parameters were defined to describe the DDR curve (Fig. 5b). The amplitude of the response (Amp) measures the maximum amount of the protein recruited to the stripes. It is calculated as the maximum of MS over all observed time points. The time to peak response (Tpeak) measures the speed of the protein recruitment. It is calculated as the time (in minutes) when the MS reaches its maximum. The relaxation speed (Relax) measures the dynamics of protein release from the sites of damage, reflecting the repair process after the peak response. It is calculated as the slope of the line fitted to the function $MS(t)$ for $t > Tpeak$ (MS stands for the measure of striation, and t for the time). For the cases when MS increases over all timepoints, the Relax parameter was measured by the slope of the line fitted to $MS(t)$ for $t > 30\ min$). The parameters are calculated for each nucleus within a sample and differences among samples are tested for statistical significance by means of the Kruskal-Wallis test on the significance level 0.05. As demonstrated in Fig. 5c,d the MS is a reasonable parameter reflecting the DDR.

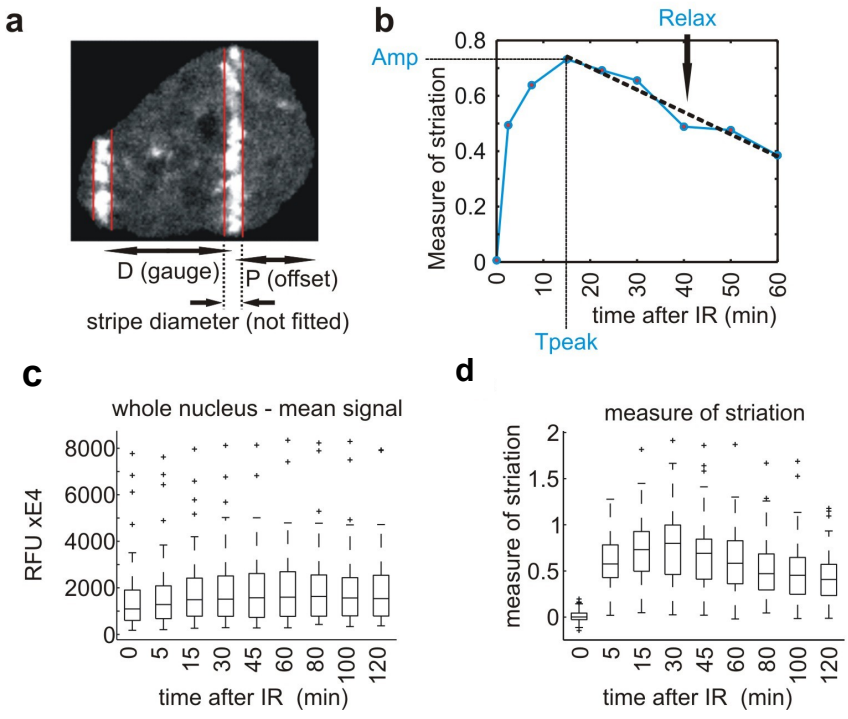

Figure 5. Optimisation of the quantification of the striation pattern. (**a**) Automatic stripe recognition in the nucleus is based on known values (gauge, the diameter of the stripe and offset) (**b**) Typical evolution of striation pattern after DNA damage caused by a 355 nm laser irradiation. The curve is plotted as medians of MS values at indicated time points. Amp (amplitude, maximum MS), Tpeak (time to reach maximum MS), Relax (slope of the line fitted to MS values after Tpeak) are used to describe the curve. (**c**), (**d**) Comparison of different types of signal quantification for an MDC1-GFP protein which translocates into the sites of damage. Signal was plotted either as mean signal per nucleus (**c**) or measure of striation (MS) (**d**). BrdU pre-sensitized U-2-OS-MDC1-GFP cells and 355 nm laser irradiation (32 lines/field) were used unless stated otherwise.

4.1.3 The method enables versatile settings for the induction of DNA damage

The LSM780 software settings enable several parameters to be manipulated thus influencing the resulting striation pattern including: the number of iterations (i.e., repeated runs of the laser through the same location), the number of stripes, laser power output and speed of irradiation (defined as pixel dwell time). It is important to optimise the settings for each reporter cell line to avoid saturation and at the same time achieve a satisfactory difference between irradiated and non-irradiated controls.

Cellular response to a different number of stripes can be observed in Fig. 6a,b. As more stripes are induced, more sites of damage are present and less protein is available to translocate to each site because the protein pool is limited. As a result, the amplitude reaches lower MS values if more lines are introduced (Fig. 6a). For further experiments, 32 lines per image were selected because (1) all nuclei within the acquisition area are hit by at least one stripe, (2) each nucleus is hit by 1-3 stripes thus giving the most pronounced response to induced damage, (3) the number of stripes per cell corresponds to number of stripes induced by widely used manual approaches.

As the number of iterations increases, then a higher amount of DNA damage is induced and

more protein is translocated to the sites of damage. There is always a threshold for each protein in terms of the maximum molecules that can be loaded to sites of damage, either the protein pool is exhausted (all available protein is translocated), or no more protein can sterically be present on the site. Both possibilities can be observed as no increase in amplitude even if more damage is induced (saturation is reached).

However, a higher amount of DNA damage in such cases is reflected by the slopes of the MS curves as demonstrated in Fig. 7c: the Amp values for 5 μM and 10 μM BrdU-treated samples are the same. However, the samples differ in the Relax parameter. The slope of DDR curve is flatter for the 10 μM BrdU sample indicating more initial DNA damage induced and therefore longer time needed for repair. For further experiments, the number of iterations inducing Amp just below saturation was selected for each reporter cell line.

The amount of induced DNA damage can be manipulated also by the energy delivered from the laser source. Energy can be controlled by the laser power output value.

The energy delivered to the sample also depends on the speed of the laser beam movement defined as pixel dwell time. The slower movement of the laser (i.e. longer pixel dwell time), the more DNA damage is induced. It is important to bear in mind that the longer pixel dwell time cannot be substituted by more iterations with a shorter pixel dwell time. As demonstrated by an example in Fig. 6c. It is evident that it is more efficient to increase the pixel dwell time rather than laser iterations.

Several reporter cell lines were successfully tested for stripes formation, Fig. 6d. The reporter systems used in this study were generated by plasmid transfection. The response of the reporter cell lines used in this study was compared with previously published data (Bekker-Jensen et al., 2005, Mortusewicz et al., 2007). All cell lines were found suitable for the DDR studies in high-content screening approach upon tested conditions

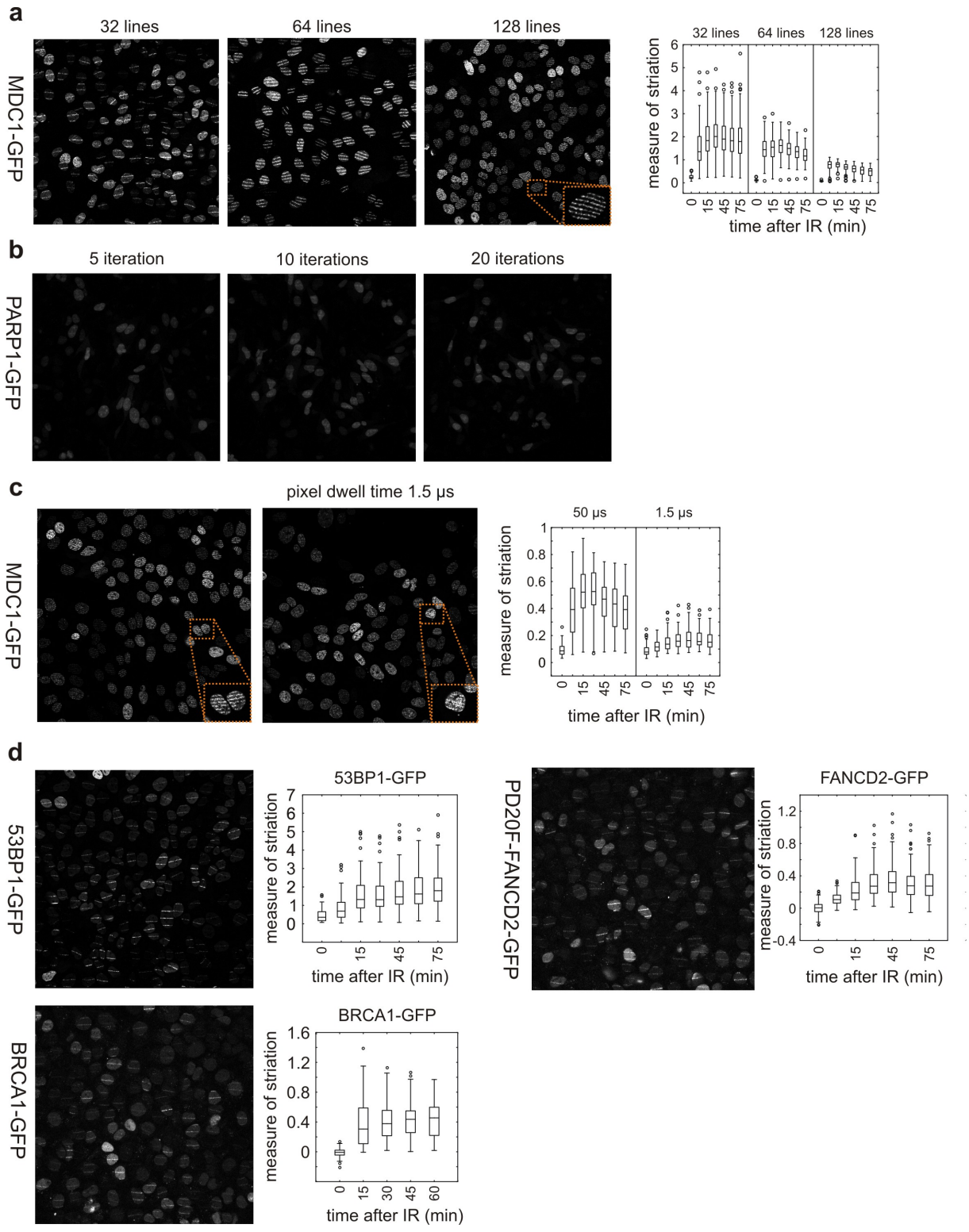

Figure 6. Optimisation of a number of stripes per field and number of iterations. (a) The striation pattern induced by a 355 nm laser in U-2-OS-MDC1-GFP cell line after BrdU sensitisation. DNA damage is visualised by recruitment of ectopically expressed MDC1-GFP protein; 1 iteration. Images were taken 30 min after micro-irradiation. (**b**) The striation pattern induced by a 355 nm laser

in BrdU sensitised U-2-OS-PARP1 chromobody stable cell lines (10 μM, 24 h). **(c)** The U-2-OS-MDC1-GFP cell line was sensitised with BrdU and irradiated for 6 seconds in total with the same laser power, but with a different pixel dwell time (either 50 μs, or 1.5 μs per pixel). **(d)** The indicated cell lines were tested for stripes formation, the cells were sensitised with BrdU, irradiated and images were taken 30 min after irradiation, U-2-OS-53BP1-GFP was irradiated with 2 iterations, PD20F-FANCD2-GFP with 5 iterations, U-2-OS-BRCA1-GFP 10 iterations.

4.1.4 Optimisation of the sensitization strategy

UV-A sensitizers are commonly used for more efficient DNA damage induction by LMI. The sensitization strategy is, therefore, another important step to be optimised. In the beginning, the laser output was set to 100 % power, 32 lines and the number of iterations was tested (Fig. 7a) without sensitizer. One iteration induced almost undetectable DNA damage in U-2-OS-MDC1-GFP cell line without sensitisation and therefore was selected for further experiments.
There are two compounds extensively used in combination with laser micro-irradiation: 5'-bromodeoxyuridine (BrdU) and Hoechst (Hoe) dye. BrdU, a nucleotide analogue must be incorporated into DNA during replication, so the incubation time as long as one population doubling was chosen. For U-2-OS cell line the incubation time was set to 24 h (Solly et al., 2004).
At first, the effect on cell cycle progression was evaluated. BrdU incorporation influences the S phase progression at concentrations above 1 μM (Fig. 7b). Then, DNA damage induced by various BrdU doses was quantified. As can be observed in Fig. 7c increasing concentration of BrdU leads to higher amplitudes and flatter relax curves, indicating that more DNA damage is present. Also, the saturation (no increase in amplitude) is visible for MDC1 reporter cell line at concentrations above 1 μM of BrdU.

Based on this pilot study, for further experiments 0.5 μM BrdU was chosen for following reasons: (1) the impact on cell cycle progression is minimal (Fig. 7b), (2) the stripe signal is

strong enough for detection, (3) the stripe signal is below saturation providing a possibility for studies with sensitizing factors, (4) the MS dynamics is in concordance with published DDR model for γH2AX (Stucki et al., 2005) and (5) the repair dynamics of the selected proteins can be followed in the 120 min time period. Significant release of the protein from sites of DNA damage within the observed time period suggests that the induced DNA damage can be properly handled by the cells. Importantly, the chosen 0.5 μM BrdU concentration proved to be optimal on both tested LSM systems (for 405 nm laser results, please refer to Supplement 3 in (Mistrik et al., 2016)).

BrdU may not be always suitable for sensitisation as the replication of DNA is needed for its incorporation. The physiological state of the cells (e.g. senescence, contact inhibition) or the treatment (e.g., compounds, siRNA treatment) may influence the cell cycle, or S phase progression so the amount of incorporated BrdU is different among samples undergoing different treatment and the obtained data cannot be compared. As an example, the differences in the amount of incorporated BrdU after the siRNA knockdown of various proteins of BRCA1-A complex are illustrated in Fig. 7f.

This drawback of BrdU can be overcome by the use of other sensitizers, e.g., Hoechst33342 or Hoechst33358. Both compounds can be used as replication-independent sensitizers. Incubation in the range of minutes is sufficient as Hoechst is a membrane permeable DNA dye. In this study, longer incubation times and lower concentrations were used as reported previously (Limoli and Ward, 1993). The method is supposed to be used for HCS in the future, so it was assumed that longer incubation times (25 minutes) and lower concentrations should provide more reproducible results and allow more time for handling the samples. Several Hoechst dye concentrations were tested and compared to the DNA damage response in BrdU-treated samples (Fig. 7c, d, e). The concentration of 1 ng/ml of Hoechst33342 was shown to induce comparable DNA damage response as 1 μM BrdU after 24 h incubation in U-2-OS-MDC1-GFP cell line, Fig 7e. It is important to select the approach for the

sensitisation strategy that best suits to the expriment design in terms of incubation time and concentration used. It is also important to investigate if the treatment affects DNA replication or cell cycle distribution.

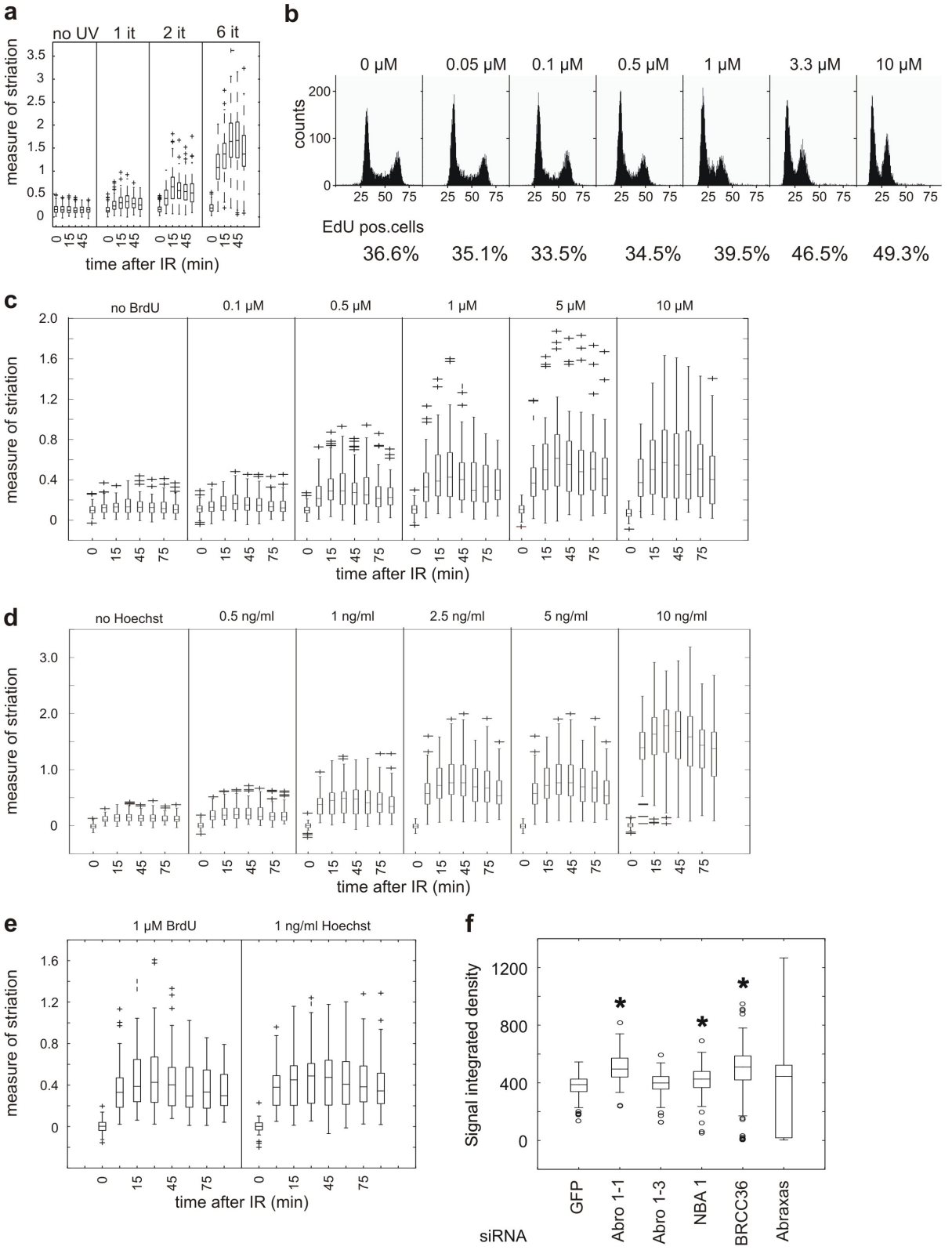

Figure 7. Sensitisation strategy. (a) MS reflects various irradiation doses of a 355 nm laser in non-sensitized cells (32 lines/field). Irradiation dose was manipulated by the number of iterations at 100% laser power. (**b**) Effect of selected concentrations of BrdU after 24 h incubation on cell cycle progression. (**c**) MS after constant laser power applied to cells pre-incubated for 24h with indicated concentrations of BrdU, a 355 nm laser (32 lines/field, 1 iteration). (**d**) Effect of selected concentrations of Hoechst33342 incubated with cells for 25 min, followed by 30 min incubation in the Hoechst33342-free medium. (**e**) Correlation of damage caused by the same laser dose between BrdU and Hoechst sensitised cells, p-values (Amp=0.79, Tpeak=0.43, Relax=0.29), Kruskal-Wallis test. (**f**) 48h of siRNA treatment influences the incorporation of BrdU, * $p<0.05$. For all experiments, U-2-OS-MDC1-GFP cell line was used.

4.1.5 The method is usable for quantification of DNA damage response proteins after IF detection

The method can be also used for fixed samples followed by detection of proteins by IF (Fig 8a). Because IF is an end-point assay, for every observed timepoint separate field must be irradiated, fixed and stained to observe the process dynamics. The assay provides several advantages compared to live cell imaging approach used here: detection of endogenous levels of proteins in non-transformed cells, detection of post-translational modifications and simultaneous detection of more proteins and possibility of co-localisation studies. As an example, approx. 150 murine cells were irradiated, fixed and simultaneously stained for γH2AX and 53BP1 (Fig. 8a).

The principles of software evaluation for IF samples are the same as for live-cell imaging, except for the tracking module that must be inactivated. Evaluation of MS for post-translational modifications provides a bigger difference between control and irradiated sample than commonly used signal integrated density (SID) evaluation (Fig. 8b). SID is calculated as

a sum of intensities if each pixel within a defined area. As nuclear proteins are evaluated, the area used for calculations is the nucleus defined by the signal from DNA intercalating dye.

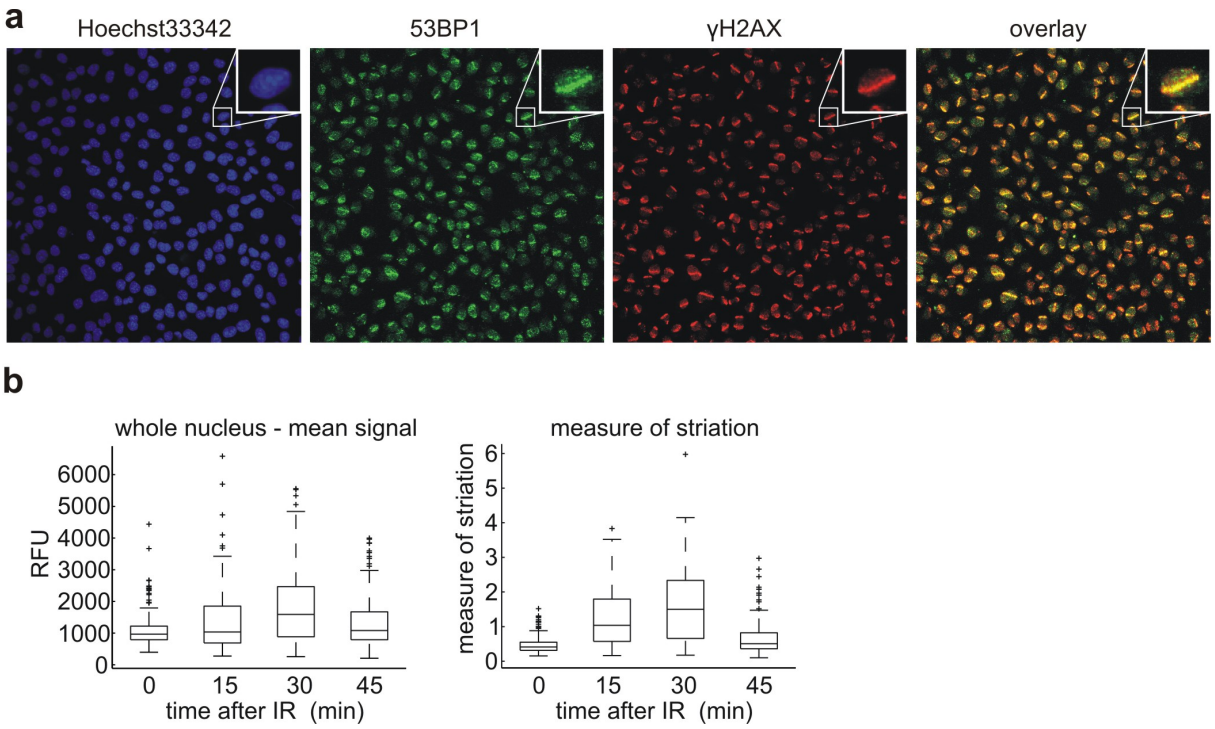

Figure 8. Evaluation of IF samples. (**a**) IF detection of endogenous 53BP1 and γH2AX at damaged sites. Mouse McCoy fibroblasts were irradiated by a 355 nm laser (32 lines/field, 5 iterations) and fixed 30 min after irradiation (**b**) Comparison of different types of signal quantification of γH2AX. Cells were BrdU pre-sensitized, irradiated by a 355 nm laser (32 lines/field, 5 iterations) and fixed at the indicated time points. Signal was plotted either as mean signal per nucleus (left panel) or MS (right panel).

4.1.6 Method validation, effect of DDR inhibitors

The method was validated in a setup resembling HCS approach. A panel of selected previously characterised inhibitors of important enzymes in the DNA damage recognition and repair pathways was selected. Compounds were incubated with the cells at 10 μM concentration for 2 h before micro-irradiation until the end of the experiment. At indicated timepoints, the MS was measured, parameters characterising the DDR curve were counted

and statistically tested. Representative curves are shown in the graphs in Fig. 9b. The response of cells influenced by the compound is compared to mock-treated cells (i.e., the cells influenced by the compound solvent).

The response of three selected proteins MDC1-GFP and 53BP1-GFP in U-2-OS cells and FANCD2-GFP in PD20F cells was observed. Results for parameters Amp, Tpeak and Relax are summarised in Fig. 9a. MDC1 recruitment was affected by all compounds with the exception of caffeine. Results for MDC1 protein recruitment were expected as MDC1 is one of the first DNA damage recognition proteins (Stucki et al., 2005). 53BP1 was not influenced by mirin and caffeine. FANCD2 protein recruitment was not influenced by more than half of the inhibitors (inhibitors of CHK1, DNA-PK, Aurora A, mTOR and Mre11) as FANCD2 is an important player in a specific repair pathways (Garcia-Higuera et al., 2001, Sims et al., 2007, Song et al., 2010). The presented set-up of the method proved to be applicable for high-content screening approach for evaluation of compounds interfering with DDR.

a

cell line		U-2-OS-MDC1-GFP				U-2-OS-53BP1-GFP				PD20F-FANCD2-GFP			
Target	Compound	Amp	Tpeak	Relax30	Relax	Amp	Tpeak	Relax30	Relax	Amp	Tpeak	Relax30	Relax
ATR	VE-821												
CHK1	LY2603618												
pan	caffeine												
DNA-PK	NU7026												
PARP	olaparib												
ATM	KU55933												
Aurora A	MLN8237												
mTOR	CC115												
Mre11	mirin												

b

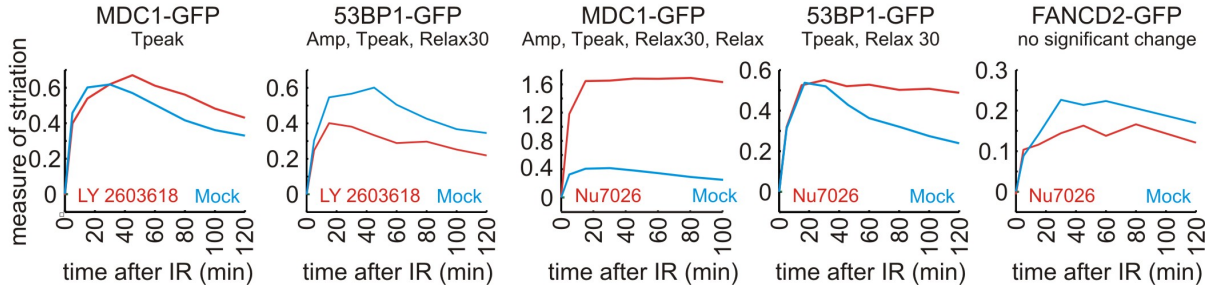

Figure 9. Method validation – DNA damage analysis. (**a**) Summary table for three reporter cell lines addressing parameters of DDR curve, Amp (amplitude, the maximum of MS over all time points), Tpeak (time to reach maximum MS), Relax (slope of the line fitted to DDR curve after Tpeak), Relax30 (slope of the line fitted to DDR curve after 30 min). The effects are color-coded: red – parameter upregulated, blue – downregulated, grey – no significant effect, Kruskal-Wallis test, $p < 0.05$. (**b**) Representative graphs of MS median values for selected compounds show different reporter-dependent response (the parameters with significant change are listed in the graph titles), Kruskal-Wallis test, $p < 0.05$.

4.2 Optimisation of the new laser micro-irradiation approach and its validation for FRAP studies

The above introduced novel approach for laser microirradiation is versatile and can be used for other photomanipulation techniques. The method was successfully applied for fluorescence recovery after photobleaching (FRAP) approach, including the software evaluation principles. The histone H2B mobility at sites of DNA damage was evaluated.

4.2.1 The method is usable for FRAP technique

The method was proven to be generic as it was tested to be fully compatible with FRAP technique. The fluorescent tag is bleached i.e., destroyed by a laser of a particular wavelength and signal reappearance in the stripes is measured and reflects the protein mobility. In Fig. 10a, the negative striation pattern is illustrated.

The principles of analysis and evaluation of generated stripes are the same as for DNA damage response. Therefore, the MS values are negative as the fluorescent signal is destroyed in the stripes (Fig. 10b). The parameter Tpeak is not evaluated for FRAP because the maximum is reached immediately after the bleaching. The relax slope reflects the dynamics of the protein reappearance within the bleached sites (Fig. 10b).

The bleaching procedure can be manipulated in the same manner as DNA damage induction approach in terms of a number of stripes, the number of iterations (Fig. 10c,d), laser power and pixel dwell.

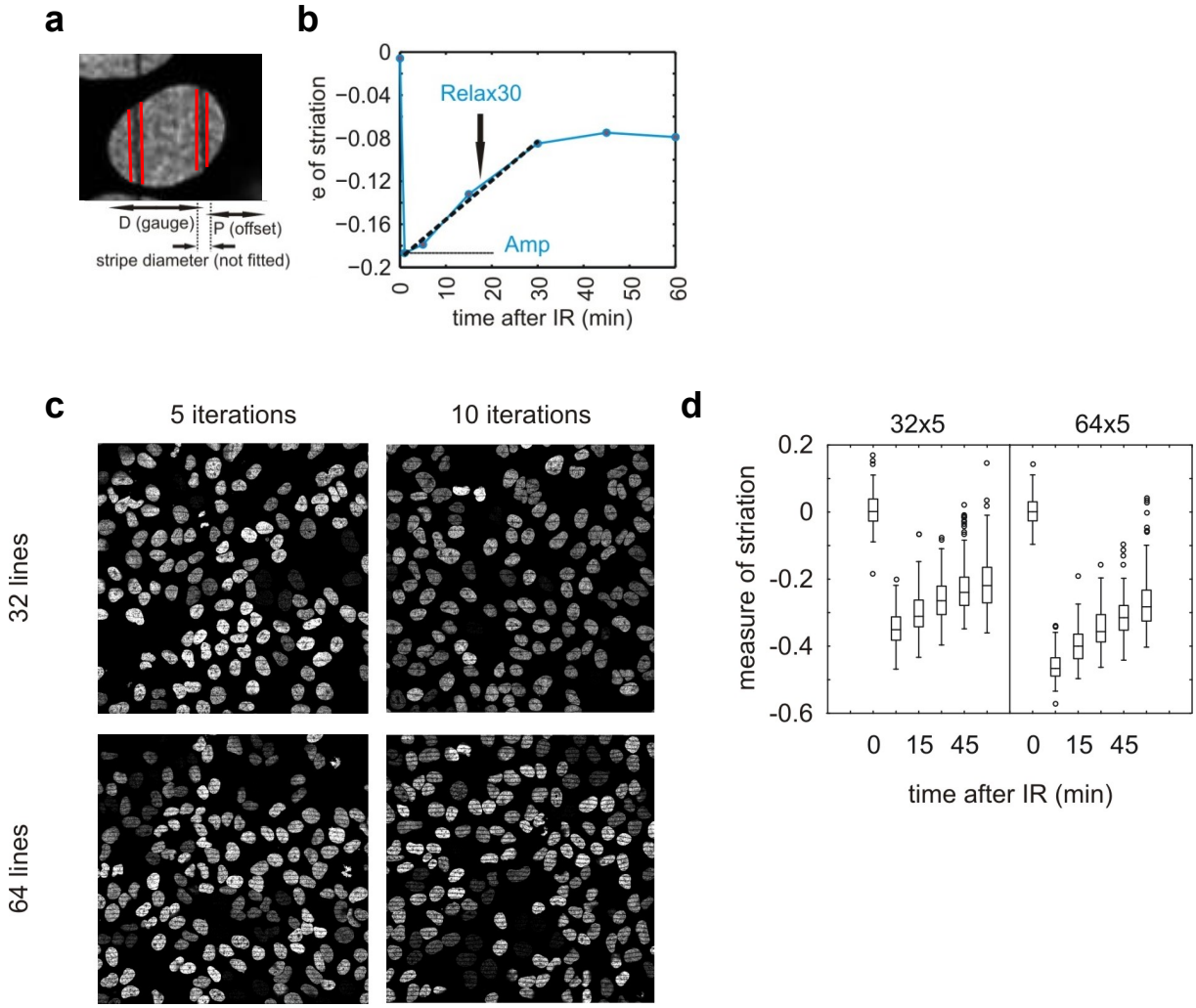

Figure 10. Method application - FRAP technique. (**a**) The negative striation pattern is recognised and quantified based on the same parameters as the positive striation pattern. (**b**) Typical evolution of bleached pattern caused by a 488 nm laser irradiation (32 lines/field, 1 iteration) in U-2-OS–H2B-GFP cells. The curve is plotted as medians of MS values at indicated time points. Amp and Relax are used to describe the curve. (**c**) Striation pattern induced by a 488 nm laser in U-2-OS-H2B-GFP cells, amount of bleached GFP proteins can be manipulated by a number of stripes or a number of iterations. Images were taken immediately after bleaching. **(d)** U-2-OS-H2B-GFP cell line bleached by 5 iterations of either 32 lines/field or 64 lines/field and followed at indicated timepoints.

4.2.2 UV-A induced DNA damage influences the mobility of H2B histone at the sites of damage

The FRAP approach was tested to prove the versatility and usability of the method. Previous reports suggested that the mobility of histones is faster within UV-C damaged chromatin as a result of ongoing repair processes involving histone turnover within the damaged sites (Dinant et al., 2013). Since UV-C induces different type of lesions than UV-A in BrdU sensitized cells, the phenomenon was investigated. U-2-OS H2B-GFP reporter cells were sensitised by 0.5 μM BrdU for 24h. In one subset of cells, the GFP tag was bleached with 488 nm laser. The delivered energy was previously tested not to cause DNA damage in U-2-OS-MDC1-GFP reporter cell line. In the second subset of cells, the GFP tag was bleached to the same level with 355 nm laser. Due to BrdU sensitisation DNA damage was introduced during bleaching with 355 nm laser. MS was evaluated in both samples and as can be observed from the graph in Fig. 11a,b the turnover of H2B histone after DNA damage induction is faster than in control cells. This observation is in concordance with previously published data (Dinant et al., 2013) suggesting that the faster histone turnover at the sites of damaged chromatin may be independent on the type of lesion induced.

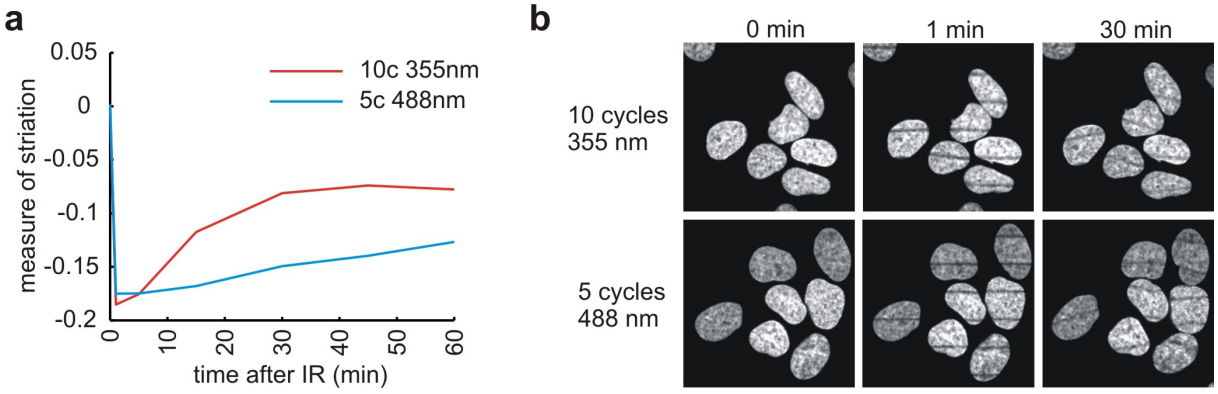

Figure 11. Method validation - FRAP analysis. (**a**) Illustrative graph of MS median values for H2B-GFP recovery after bleaching (FRAP). Bleaching was performed either with a 355 nm or 488 nm

laser (32 lines/field) to the same level, Kruskal-Wallis test (difference in Amp is non-significant, p = 0.87), Relax30 shows significant change (p < 1.E-4). (**b**) Illustrative images of U-2-OS-H2B-GFP cells bleached by a 355 nm or 488 nm laser and evolution of the striation pattern over time.

4.3 Optimisation of the striation approach for in situ UV-A photorelease of caged APH molecule

Caged molecules are photosensitive inactive compounds which can be turned into biologically active molecules by photolysis. *In situ* photolysis of caged molecules (either inhibitors or activators of enzymes) can be used for precise spatiotemporal observation of biological processes. *In situ* DNA replication polymerases inhibition may provide a precise novel approach for DDR studies at stalled replication forks. This approach would be of high impact for the cancer biology field as stalled replication is nowadays widely studied in relation to malignant transformation and cancer treatment (Zellweger et al., 2015, Zhang et al., 2016).

Aphidicolin, an inhibitor of several DNA polymerases was modified by PPG compound (APH-PPG) (Mgr. Soňa Křupková, PhD and RNDr. Jakub Stýskala, PhD, Palacky University, Olomouc) and the efficient UV photolysis of APH-PPG bond was tested (Mgr. Soňa Křupková, PhD, Palacky University, Olomouc).

At first, the inactivation of the APH by PPG was tested. Cells were treated with 10 μM APH, or APH-PPG for 2 h, for the last 30 min 10 μM EdU was added to monitor the ongoing replication. Upon described conditions, APH stalled replication forks as only 3.4 % of cells were positive for EdU staining (corresponds to the 2 % background values - cells not treated with EdU but treated with EdU detection solutions). Without APH, 47 % of the cells were stained positive for EdU incorporation, with APH-PPG molecule 37 % of the population was stained positive for EdU incorporation (Fig. 12a). The incorporation of EdU was slightly decreased upon APH-PPG treatment compared to untreated cells but the inactivation was

considered sufficient for further experiments. The ability of APH-PPG solution to partially stall replication forks can be caused by the spontaneous dissociation of the complex, or by the fact that not every molecule in the solution was caged during the organic synthesis.

Then, the LSM was used for APH-PPG photolysis (355 nm laser) in living cells and local inhibition of DNA polymerases was measured. LSM was used for micro-irradiation of the whole acquisition field with 355 nm laser to photorelease the APH-PPG molecule *in situ*. It was desirable to avoid DNA damage induction as it may interfere with DNA replication (Minca and Kowalski, 2011). Therefore, several laser doses were tested in terms of DNA damage induction measured by γH2AX signal quantification. Following conditions were selected for further experiments: 15 % laser power, 2048 x 2048 resolution and 2 iterations (it is the highest laser dose that can be delivered to the cells and does not cause DNA damage), Fig. 12b. Dissociation of APH and the PPG was measured by EdU incorporation assay. It was assumed that if APH is released by UV-A irradiation, EdU incorporation would be decreased. Cells were incubated with 10 μM APH, or APH-PPG for 1 h, then whole field micro-irradiation with 355 nm laser was performed (2048 x 2048, 2 iterations, speed 6, 15 % laser output), cells were incubated 30 min at 37°C and then 10 μM EdU was added for 30 min. Only cells positive for cyclin A (cell cycle regulator protein, expressed in all cycle phases except G1 (Pagano et al., 1992)) were evaluated for EdU incorporation. No difference was observed between control sample and sample treated with 10 μM APH-PPG (Fig. 12c). This result may indicate that the energy delivered to the cells during micro-irradiation was not sufficient to cause the photorelease of APH. Another explanation may be that the number of molecules released by the micro-irradiation settings was not sufficient to efficiently stall the replication forks, or the stalled replication forks can be quickly repaired, and replication continues. Although the assay would provide a very elegant tool for replication fork progression studies, in the current set-up it is not effective. The PPG photosensitive bond requires for its dissociation such amount of energy that DNA damage is generated. Also, a

different photolabile group that requires either lower energy for its dissociation or DNA non-damaging laser wavelength may be used.

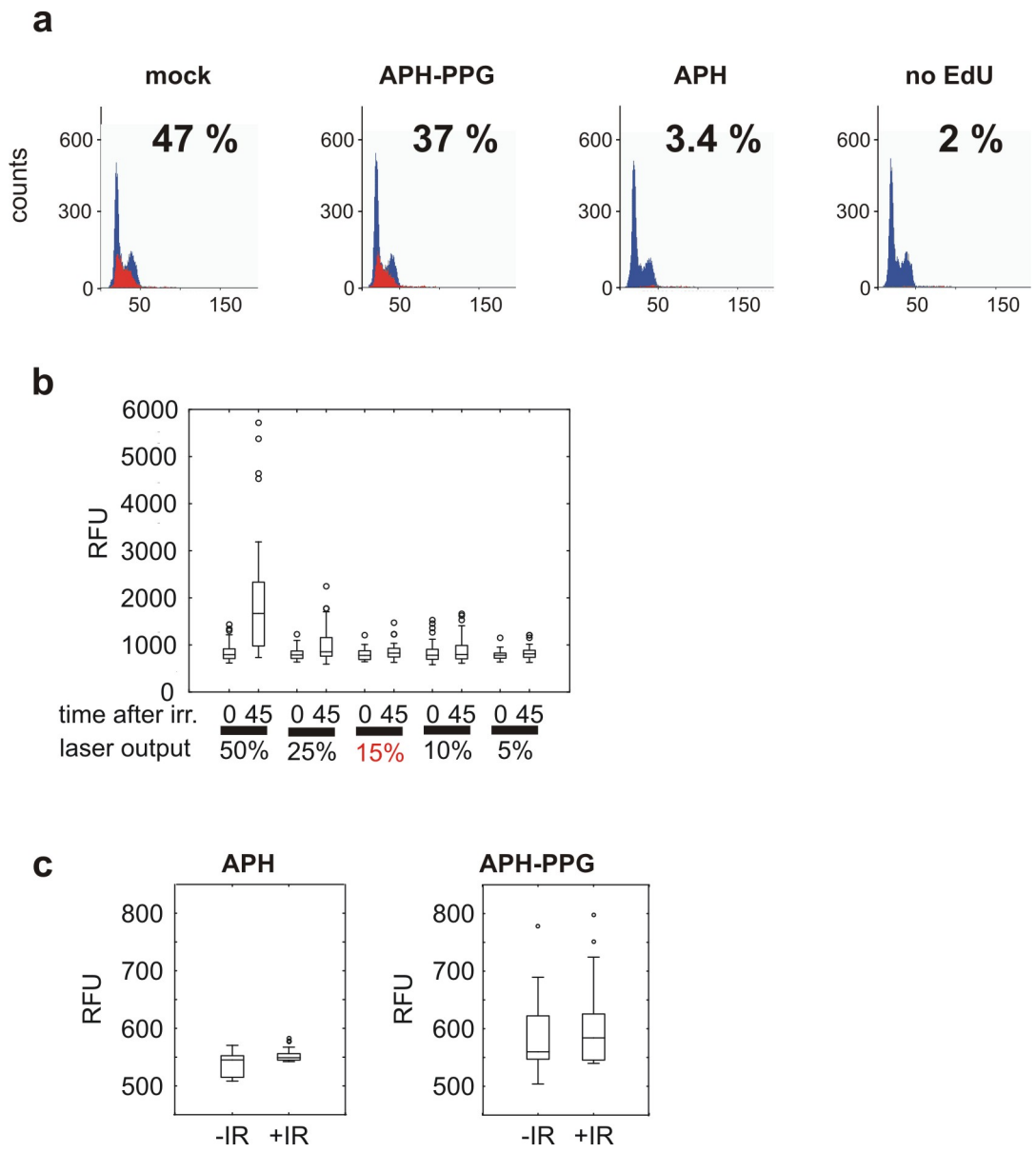

Figure 12. Optimisation of the LSM for monitoring of *in situ* photolysis of APH

(**a**) Cell cycle profiles after incubation with 10 μM APH, or APH-PPG for 1 h, S phase progression is measured by the positivity of EdU staining (30 min incubation), % of EdU positive cells is indicated. (**b**) DNA damage measured by γH2AX signal, irradiation settings were 2048 x 2048, 2 iterations; pixel dwell 50 μs, % of the laser output is indicated. (**c**) EdU signal from cyclin A positive cells after APH and APH-PPG treatment and irradiation (the same settings as in (**b**) and 15% of laser power).

4.4 XPC role after APH-induced replications stress revealed by image analysis

Image analysis was used for evaluation of cellular response to replication stress caused by 0.4 μM APH treatment in the background of XPC protein (Xeroderma Pigmentosum Complementation Group C) deficiency. At first, in cooperation with Dr Tomáš Fürst (Faculty of Science, Palacky University, Olomouc) a new routine was developed for automated acquisition and analysis of mitotic cells (described in detail in Chapter 3 – Material and Methods).

The first experiment was designed to reveal if the silencing of XPC protein combined with replication stress caused by APH is revealed as damage in mitotic cells. As a marker of DNA damage, γH2AX was chosen. Surprisingly, XPC silencing caused a decrease in a number of γH2AX foci upon APH treatment in mitotic cells (Fig. 13a) suggesting either the lower amount of DNA damage or attenuated signalling of DNA damage. To find out which scenario occurs, cells in G1 phase of the cell cycle were analysed as described by (Lukas et al., 2011). (Lukas et al., 2011) claim that cells experiencing replication stress may enter mitosis with unrepaired DNA damage and then exhibit higher number of 53BP1 foci in subsequent G1 phase. 53BP1 protein is suggested to shield the DNA damage and facilitate the repair. In our experiment, in G1phase cells (cells negative for cyclin A) 53BP1 foci were analysed and a significant increase in 53BP1 foci numbers was observed after XPC knockdown, (Fig. 13b). These observations suggest that XPC deficiency decreases the efficiency of recognition and repair of the RS-caused lesions which are subsequently transferred to mitosis and then to the next generation in U-2-OS cells.

To further evaluate the impact of XPC on RS-induced stress, the ATR-CHK1 pathway (the main RS response pathway) was examined. ATR protein bound to chromatin was evaluated as well as its binding partner RPA (a marker of ssDNA) and ATRIP proteins, Fig. 13c. XPC deficiency caused a mild increase of RPA protein but decreased the amount of chromatin-

bound ATR and ATRIP which is in concordance with decreased phosphorylation of CHK1 (Ser345), Fig. 13d. Such results may indicate that XPC deficiency results in attenuated signalling of ATR-CHK1 pathway. The effect was more pronounced at 12 h of APH treatment thus further confirming the XPC role in early stages of RS induced stress.

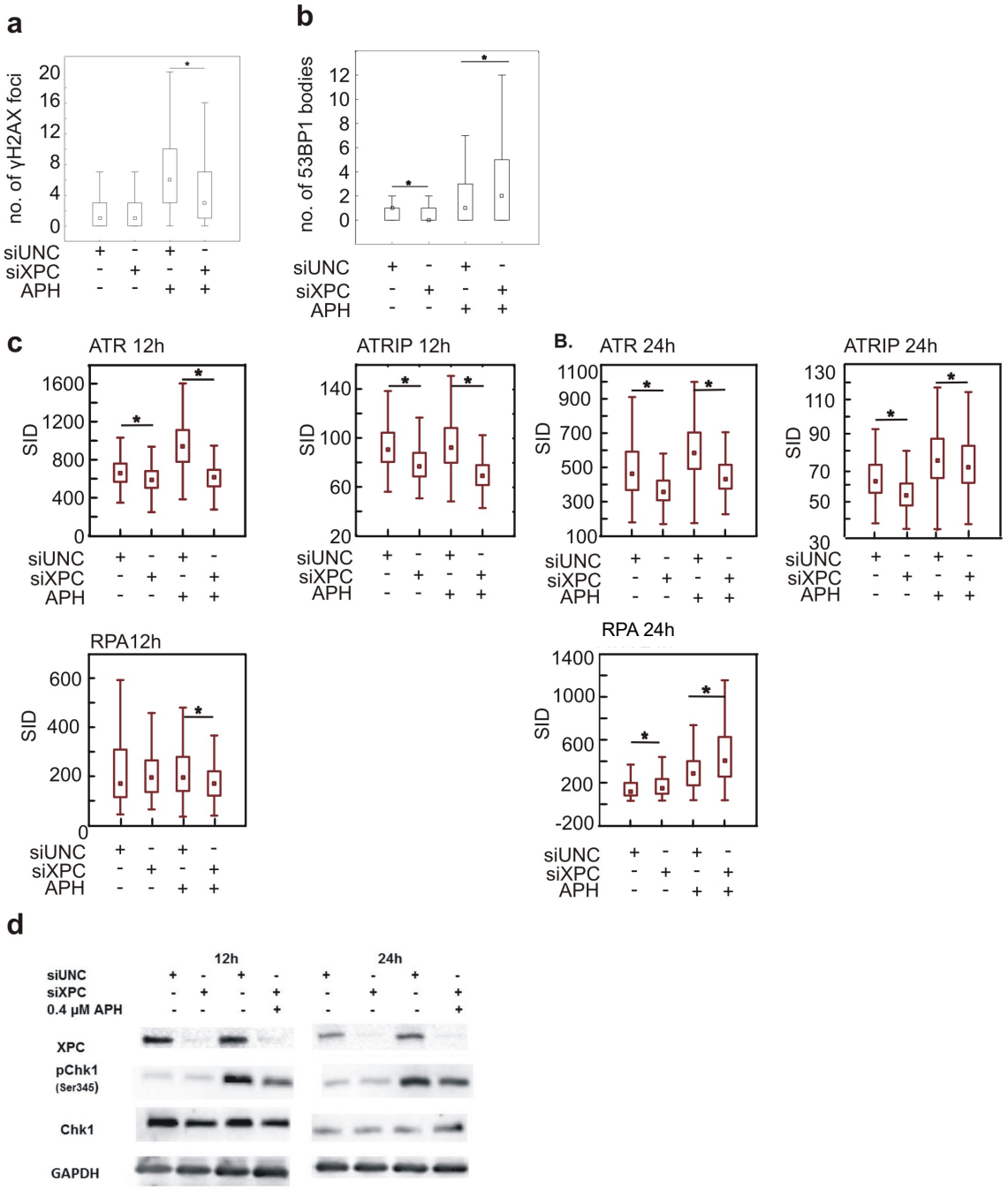

Figure 13. XPC role in CFS expression under replication stress. (**a**) Quantification of γH2AX foci in mitotic cells, U-2-OS cell line was silenced with XPC and treated with 0.4 μM APH for 24 h, mitotic cells were identified as pH3 positive. (**b**) Quantification of 53BP1 foci in G1 cells, U-

2-OS cell line was silenced with XPC for 72 h and treated with 0.4 μM APH for 24 h, cells negative for cyclin A were analyzed. (**c**) Quantification of chromatin-bound ATR, ATRIP and RPA proteins, after 12 h and 24 h of 0.4 μM APH treatment. (**d**) Detection of phosphorylated CHK1 (Ser345) after 12 h and 24 h of 0.4 μM APH treatment.

5 DISCUSSION

In this thesis, a new method for generation and analysis of localised laser-induced photomanipulations is introduced. Laser micro-irradiation combined with live cell imaging offer the opportunity to study precise spatiotemporal observations not achievable with assays using fixed samples. The novel approach to laser micro-irradiation described in this thesis overcomes several drawbacks of current manual approaches, it is accompanied by a software for automated image analysis and therefore significantly facilitates the use of LSM for high-content screening applications.

The method enables simultaneous irradiation and acquisition of up to hundreds of cells followed by automated analysis. The method was designed and optimised for DNA damage analysis, but it is applicable also to FRAP experiments. In comparison to currently used manual approaches (Bekker-Jensen et al., 2006, Adamson et al., 2012, Galanty et al., 2012, Adam et al., 2013, Dinant et al., 2013, Larsen et al., 2014, Wang et al., 2014, Gong et al., 2015) the automated irradiation approach enables irradiation of higher number of cells in a shorter time. The new approach also minimises the probability of biased results. The current manual approach is based on the manual selection of the nuclei. This can bias the results as only subset of nuclei in the population (e.g., only nuclei exhibiting a certain amount of fluorescently tagged protein) are likely to be selected for analysis. The new approach enables whole acquisition field irradiation and evaluation thus eliminating the bias caused by manual selection of individual cells. Also, higher numbers of cells are evaluated. The new approach enables analysis of up to hundreds of cells, while with the manual approach usually approx. up to few tens of cells are evaluated (Larsen et al., 2014, Gong et al., 2015, Wang et al., 2014, Weston et al., 2012, Yin et al., 2012). The new approach also enables automation of the image analysis so the results cannot be biased by manual evaluation (e.g. incorrect definition of ROI). Last but not least, the method settings are highly variable so can be adjusted to fit best the assay design, or observed protein. The method can be optimised in terms of the laser

output, used laser wavelength, the number of iterations, the number of stripes per field (or cell), scanning speed and pre-treatment with a sensitizer. Despite the fact that settings these parameters is crucial also for the manual approach, settings are often just adapted from previous studies (Kim et al., 2005a, Gomez-Godinez et al., 2007, Meerang et al., 2011, Adamson et al., 2012, Wang et al., 2014, Larsen et al., 2014, Gong et al., 2015). As each reporter cell line may respond differently, it is very important to optimise the parameters for each cell line to address well the issue to be investigated.

The micro-irradiation pattern generated by the novel approach is regular and enables automated software analysis. However, none of the open-source or commercial software available was found suitable, so new analysis software was developed. It enables evaluation of live and fixed samples in the semi-automatic regime and currently is ready to be modified for proper high-content screening. Also a value was defined for quantification of the DDR proteins recruited to and released from the sites of damage. The new value is called ‘measure of striation’ and was defined to be independent of the total amount of fluorescent protein present in the cell. Three parameters were defined to describe the dynamics of DDR and were used for statistical testing. Amplitude (Amp) describes the amount of protein recruited to sites of damage as is indicative of the extent of DNA damage induced. Time to reach amplitude (Tpeak) reflects the speed of DDR and slope after maximum (Relax) reflects the protein release from sites of damage. The image analysis software is now available as an open-source MatLab code and can be further used and modified.

The described approach possesses also several disadvantages and drawbacks that have to be borne in mind when establishing the assay. At first, the dose delivered to the sample and each cell cannot be precisely measured. The only possibility how to estimate the dose is to stain for a suitable DNA damage reporter, e.g., γH2AX, or RPA and compare with the response to a damage caused by a known dose of UV, IR, or chemical compound (Bekker-Jensen et al., 2006). As more and more studies emerge, it is becoming more important to have a common

readout for the dose delivered as many contradictory results are observed (Kong et al., 2009). The cellular response is, indeed, dose-dependent as demonstrated by (Saquilabon Cruz et al., 2016). Another disadvantage of this method comes from the manner of image acquisition. Scanning the image point-by-point allows very precise irradiation but takes much longer than other image acquisition methods (wide-field imaging, spinning disc microscopy). To overcome this drawback, zoom for smaller acquisition field can be applied at the expense of the lower amount of cells analysed. In case no zoom is used, the time for field acquisition can reach up to seconds or dozen seconds which may not be suitable for some assays, e.g., rapid kinetics measurements such as PARP1 recruitment to sites of DNA damage, or FRAP assays with fast protein turnover.

The proposed method proved the ability to detect compounds interfering with DNA damage response. A panel of 10 compounds with known function was evaluated in several parameters reflecting the DNA damage recognition and repair. The compounds were chosen for the test panel in order to inhibit early stages of DDR as well as some of these that act at later stages. Inhibitors of PARP1, Mre 11 and all PIKKs were tested, from the later acting proteins, CHK1 was inhibited by a specific inhibitor LY2603618. Also mTOR and Aurora A inhibitors generally known to play role in other cellular processes e.g. cell growth and proliferation (Fingar et al., 2004) and mitosis (Fu et al., 2007) resp., were included in the assay as reported to influence the DDR as well (Bandhakavi et al., 2010, Rai et al., 2008). Three reporter cell lines bearing MDC1, 53BP1 and FANCD2 proteins coupled to GFP tag were used as a readout for the DNA damage response. In the majority of the cases, significantly upregulated parameters were observed. Upregulated Amp indicates more protein loaded to sites of damage. Upregulated Tpeak indicates longer time needed for the protein to reach the maximum amount loaded to sites of damage. Relax upregulation suggests slower release of the protein from the sites of damage therefore probably lower repair rates.

MDC1 protein recruitment was affected by all chemicals tested which is in accordance with the MDC1 protein function. MDC1 gets recruited to sites of DNA damage in the very early stages of DDR by direct binding of γH2AX (Stewart et al., 2003, Stucki et al., 2005). Moreover, MDC1 serves as a docking platform for other proteins and enhances activation of ATM kinase by positive feedback loop therefore indirectly influencing DNA damage repair and cellular checkpoint response (Stucki et al., 2005, Goldberg et al., 2003, Jungmichel et al., 2012).

The 53BP1 reporter was affected by a lower number of the selected chemicals, which is in concordance with its role as a signal transducer loaded later to DNA lesions than MDC1 protein (Stewart et al., 2003). PIKKs also do not exhibit same effects as with MDC1 reporter. As described previously, 53BP1 is activated by all PIKKs depending on the type of lesion induced and cell type observed (Jowsey et al., 2007, Mochan et al., 2003, DiTullio et al., 2002, Callén et al., 2009, Difilippantonio et al., 2008).

FANCD2 reporter was affected by only a subset of chemicals, as FANCD2 pathway is very specific and it is recruited to only some types of DNA lesions. The most profound effect was observed upon inhibition of ATR that belongs to the direct pathway leading to FANCD2 activation.

The presented method including the software solution is easily adaptable for other photo-manipulation techniques and was successfully tested for fluorescence recovery after photobleaching technique (FRAP). The time requirements are more limiting for FRAP technique than for DNA damage induction. FRAP technique is very often used to study processes that are in the range of seconds (Hildick et al., 2012, Shih and Yamada, 2011) or even milliseconds (Subramanian and Meyer, 1997, Periasamy and Verkman, 1998). This means that upon above described condition only proteins with rather slow mobility can be studied or the method must be adjusted at the expense of the lower amount of cells analysed.

Kinetics of histone turnover was measured in cells without DNA damage or at the sites where UV-A DNA damage was induced. Increased turnover of histones at sites of damage was observed, which is in concordance with previously published data by (Dinant et al., 2013) for UVC-C DNA damage suggesting that faster histone turnover is a common feature after DNA damage induction.

The method described here enables fast irradiation followed by an automatic image analysis of hundreds of cells in parallel which introduces a possibility of robust statistical testing. Altogether, the method significantly improves the use of LSM in high-content screening and enables precise spatio-temporal resolution of DDR. The method brings a significant versatility as it was successfully applied to FRAP analysis in a very similar manner as for DDR analysis.

The above described technique was modified and used in order to investigate the phenomenon of replication stress (RS). RS is defined as a slow-down of DNA synthesis and perturbations to DNA synthesis process. RS induces genomic instability therefore potentiates mutagenesis and oncogenic transformation. The mechanisms of genome integrity maintenance during S phase are therefore of great importance and contribute to cellular defence against cancer (Bartkova et al., 2005). RS is promoted also by unscheduled DNA synthesis, e.g. premature cell cycle entry due to activated oncogenes, defective DDR and DNA damage checkpoints. Generally, higher levels of RS and RS-related adverse effect on GI were observed in cancer cells, therefore the process of RS is becoming a new promising target to cancer therapy (Zhang et al., 2016). Precise knowledge of all the factors playing role in this phenomenon would be highly beneficial for novel cancer therapy approaches. Therefore, another experiment using LMI was designed to locally perturb DNA replication *in situ*. An attempt to establish a new approach for generation of stalled replication forks only in part of the nucleus was carried out. At first, APH molecule was inactivated by binding a ‘cage molecule’ that blocks the APH active site. The photolabile bond between the protective molecule and the

APH molecule can be disrupted by UV-A irradiation and active compound is released. The sufficient inactivation of APH by the cage compound was tested. As 355 nm laser was used for bond disruption, laser dose not causing DNA damage was determined. Otherwise the induced DNA damage may interfere with the ongoing replication. However, under laser settings when DNA damage was not induced, APH activation was undetectable as measured by the amount of incorporated EdU. This could have been caused by low laser energy delivered resulting in no APH activation. Or, only low amount of APH molecules was released and the DNA polymerase inhibition was below the threshold detection of the EdU assay. Or, activation of APH molecules only in part of the nucleus can be compensated for by other unaffected DNA polymerases in close proximity. The described set-up was tested unsuitable for replication fork stalling and it was suggested that different type of photolabile bond should be used. Either the bond should be more labile (destabilized by a lower laser irradiation dose), or should absorb in different range of the spectrum that is not causing cellular and DNA damage.

Replication stress was also investigated in the last part of this thesis and was approached by different technique than LSM. The role of XPC protein in response to replication stress caused by APH was studied mainly by IF and automated image analysis. A hypothesis was suggested that XPC binds to stalled replication forks and initiate incision of the DNA structures emerging upon APH treatment. APH is a potent inductor of CFS (Glover et al., 1984) and it was reported that APH-induced CFS contain sequences with high potential to create secondary structures that can result in DNA breaks and/or perturb various processes like transcription or telomere maintenance (Dillon et al., 2013). The XPC-initiated incision of such problematic secondary structures may contribute to DDR activation and lead to γH2AX signalling in mitosis. In the case of XPC deficiency the described process would not be performed properly, and the number of γH2AX foci in mitosis would be decreased. This can

result in accumulation of errors threatening the genome stability, preferentially at CFS which are prone to breakage upon replication stress conditions.

At first, γH2AX foci were scored in mitotic cells after APH-induced replication stress. The decrease in the number of foci was indeed observed upon XPC protein deficiency indicating that either DNA damage signalling is attenuated or less amount of DNA damage is present.

In order to find out which scenario occurs, a method described in (Lukas et al., 2011) was employed. As described in (Lukas et al., 2011) DNA damage that emerges in the S phase can be transferred to following G1 cells and is revealed by increased number of 53BP1 bodies.

In case XPC deficiency causes attenuated DDR as presumed, lesions would not be repaired and would be transferred to subsequent G1 and increased number of 53BP1 bodies would be observed. Indeed, analysis of DNA damage in G1 cells measured by 53BP1 revealed increase in 53BP1 bodies.

Analysis of other RS-related proteins ATR and ATRIP loaded to chromatin revealed lower amount of both proteins in cells lacking XPC protein thus supporting the XPC signalling role in the process. The amount of RPA protein, indicative of ssDNA (Zou and Elledge, 2003) was enhanced in XPC depleted cells after 24h of APH, and checkpoint signalling measured by phosphorylated CHK1 (Ser345) as well. Therefore, it was predicted that XPC deficiency leads to a lower efficacy of RS-related DNA lesions recognition and signalling, preventing proper repair and allowing cells to bypass the checkpoint signalling and enter mitosis. The lesions that are not recognised and signalled might be sites of unreplicated DNA that are transformed to breaks during mitosis and revealed by 53BP1 protein in G1 cells. These findings were published in the article (Beresova et al., 2016) that address untargeted identification of proteins that play role in CFS stability by proteomic approach. XPC was identified in this screening and its role was further studied. It was proposed that XPC contributes to recognition and processing of replication forks stalled within hard-to-replicate DNA areas such as CFS.

6 LIST OF APPENDICES

Appendix 1 **Curriculum vitae**

Appendix 2 **Cells and Stripes: A novel quantitative photo-manipulation technique**

Mistrik M*, Vesela E*, Furst T, Hanzlikova H, Frydrych I, Gursky J, Majera D, Bartek J
Scientific Reports, 2016 Jan 18;6:19567. doi: 10.1038/srep19567, IF 4.25
* shared first authorship

Appendix 3 **Common Chemical Inductors of Replication Stress: Focus on Cell-Based Studies**.
Vesela E, Chroma K, Turi Z, Mistrik M
Biomolecules, 2017 Feb 21;7(1). pii: E19. doi: 10.3390/biom7010019.
Peer-reviewed journal

Appendix 4 **Role of DNA repair factor XPC in response to replication stress, revealed by DNA fragile site affinity chromatography and quantitative proteomics.**

Beresova L, Vesela E, Chamrád I, Voller J, Yamada M, Furst T, Lenobel R, Chroma K, Gursky J, Krizova K, Mistrik M, Bartek J.

J Proteome Res., 30.10.2016, Doi: 10.1021/acs.jproteome.6b00622

Appendix 5 **List of publications**

Appendix 6 **Software for evaluation of stripes formation in live cells** (only on CD)

7 ABBREVIATIONS

DDR
GI
RF
DSB
IR
UV
ROS
MRN
ATM
PARP1
WRN
XP
NER
BER
MMR
APH
53BP1
PPG
NIR
Hoe
H2AX
BrdU
IF
HCS
HTS
mTOR
EdU
UNC
CFS
ICL
MGB
SCE
CPD
(6-4)PP
WWOX
SQ/TQ
TRRAP
FAT
PI3K
PIKK
FRA3B
FRA16D
FRA6E
FHIT
WRN
R-loop
V(D)J
LIG4
XRCC
DewPPs
PDT
AD
IRIF
PCNA

FEN1
WGR
CAT
EXO/BLM
NBS1
STING
RNR
MDC1
BRCA 1
RPA
CHK1
ssDNA
ATR
Tim
TIPIN
ETTA1
TRF2
DONSON
CDK
RS
ATRIP
TLS
CDC25
E2F
MDM4
PML
PCNA
FANC
HR
NHEJ
ROI
LSM
LMI
GFP
MS
Amp
Tpeak
Relax
FRAP
iFRAP
FLIP
FLAP
SID
DDR
CHK2
BRCT
BRCA1
TopBP1
EXPAND1
DNA-PK
mTOR
p53
SMG1

8 REFERENCES

Abdou, I., Poirier, G.G., Hendzel, M.J., and Weinfeld, M. (2015). DNA ligase III acts as a DNA strand break sensor in the cellular orchestration of DNA strand break repair. Nucleic Acids Research *43*, 875–892.

Adam, S., Polo, S.E., and Almouzni, G. (2013). Transcription recovery after DNA damage requires chromatin priming by the H3.3 histone chaperone HIRA. Cell *155*, 94–106.

Adamson, B., Smogorzewska, A., Sigoillot, F.D., King, R.W., and Elledge, S.J. (2012). A genome-wide homologous recombination screen identifies the RNA-binding protein RBMX as a component of the DNA-damage response. Nat. Cell Biol. *14*, 318–328.

Aguilera, A., and García-Muse, T. (2012). R Loops: From Transcription Byproducts to Threats to Genome Stability. Molecular Cell *46*, 115–124.

Akimoto, J. (2016). Photodynamic Therapy for Malignant Brain Tumors. Neurol. Med. Chir. (Tokyo) *56*, 151–157.

Anantha, R.W., Vassin, V.M., and Borowiec, J.A. (2007). Sequential and synergistic modification of human RPA stimulates chromosomal DNA repair. J. Biol. Chem. *282*, 35910–35923.

Andäng, M., Hjerling-Leffler, J., Moliner, A., Lundgren, T.K., Castelo-Branco, G., Nanou, E., Pozas, E., Bryja, V., Halliez, S., Nishimaru, H., et al. (2008). Histone H2AX-dependent GABA(A) receptor regulation of stem cell proliferation. Nature *451*, 460–464.

Andegeko, Y., Moyal, L., Mittelman, L., Tsarfaty, I., Shiloh, Y., and Rotman, G. (2001). Nuclear retention of ATM at sites of DNA double strand breaks. J. Biol. Chem. *276*, 38224–38230.

Andreassen, P.R. (2004). ATR couples FANCD2 monoubiquitination to the DNA-damage response. Genes & Development *18*, 1958–1963.

Arlt, M.F., Xu, B., Durkin, S.G., Casper, A.M., Kastan, M.B., and Glover, T.W. (2004). BRCA1 Is Required for Common-Fragile-Site Stability via Its G2/M Checkpoint Function. Mol Cell Biol *24*, 6701–6709.

Ashman, C.R., and Davidson, R.L. (1981). Bromodeoxyuridine mutagenesis in mammalian cells is related to deoxyribonucleotide pool imbalance. Mol. Cell. Biol. *1*, 254–260.

Axelrod, D., Koppel, D.E., Schlessinger, J., Elson, E., and Webb, W.W. (1976). Mobility measurement by analysis of fluorescence photobleaching recovery kinetics. Biophys. J. *16*, 1055–1069.

Bahassi, E.M., Ovesen, J.L., Riesenberg, A.L., Bernstein, W.Z., Hasty, P.E., and Stambrook, P.J. (2008). The checkpoint kinases Chk1 and Chk2 regulate the functional associations between hBRCA2 and Rad51 in response to DNA damage. Oncogene *27*, 3977–3985.

Bakkenist, C.J., and Kastan, M.B. (2003). DNA damage activates ATM through intermolecular autophosphorylation and dimer dissociation. Nature *421*, 499–506.

Bandhakavi, S., Kim, Y.-M., Ro, S.-H., Xie, H., Onsongo, G., Jun, C.-B., Kim, D.-H., and Griffin, T.J. (2010). Quantitative nuclear proteomics identifies mTOR regulation of DNA damage response. Mol. Cell Proteomics *9*, 403–414.

Barlow, C., Hirotsune, S., Paylor, R., Liyanage, M., Eckhaus, M., Collins, F., Shiloh, Y., Crawley, J.N., Ried, T., Tagle, D., et al. (1996). Atm-deficient mice: a paradigm of ataxia telangiectasia. Cell *86*, 159–171.

Bartek, J., Lukas, C., and Lukas, J. (2004). Checking on DNA damage in S phase. Nat. Rev. Mol. Cell Biol. *5*, 792–804.

Bartek, J., Bartkova, J., and Lukas, J. (2007). DNA damage signalling guards against activated oncogenes and tumour progression. Oncogene *26*, 7773–7779.

Bartek, J., Mistrik, M., and Bartkova, J. (2012). Thresholds of replication stress signaling in cancer development and treatment. Nat. Struct. Mol. Biol. *19*, 5–7.

Bartkova, J., Horejsí, Z., Koed, K., Krämer, A., Tort, F., Zieger, K., Guldberg, P., Sehested, M., Nesland, J.M., Lukas, C., et al. (2005). DNA damage response as a candidate anti-cancer barrier in early human tumorigenesis. Nature *434*, 864–870.

Bartkova, J., Rezaei, N., Liontos, M., Karakaidos, P., Kletsas, D., Issaeva, N., Vassiliou, L.-V.F., Kolettas, E., Niforou, K., Zoumpourlis, V.C., et al. (2006). Oncogene-induced senescence is part of the tumorigenesis barrier imposed by DNA damage checkpoints. Nature *444*, 633–637.

Batista, L.F.Z., Chiganças, V., Brumatti, G., Amarante-Mendes, G.P., and Menck, C.F.M. (2006). Involvement of DNA replication in ultraviolet-induced apoptosis of mammalian cells. Apoptosis *11*, 1139–1148.

Bekker-Jensen, S., and Mailand, N. (2010). Assembly and function of DNA double-strand break repair foci in mammalian cells. DNA Repair (Amst.) *9*, 1219–1228.

Bekker-Jensen, S., Lukas, C., Melander, F., Bartek, J., and Lukas, J. (2005). Dynamic assembly and sustained retention of 53BP1 at the sites of DNA damage are controlled by Mdc1/NFBD1. The Journal of Cell Biology *170*, 201–211.

Bekker-Jensen, S., Lukas, C., Kitagawa, R., Melander, F., Kastan, M.B., Bartek, J., and Lukas, J. (2006). Spatial organization of the mammalian genome surveillance machinery in response to DNA strand breaks. The Journal of Cell Biology *173*, 195–206.

Beresova, L., Vesela, E., Chamrad, I., Voller, J., Yamada, M., Furst, T., Lenobel, R., Chroma, K., Gursky, J., Krizova, K., et al. (2016). Role of DNA Repair Factor Xeroderma Pigmentosum Protein Group C in Response to Replication Stress As Revealed by DNA Fragile Site Affinity Chromatography and Quantitative Proteomics. J. Proteome Res. *15*, 4505–4517.

Bernstein, K.A., Gangloff, S., and Rothstein, R. (2010). The RecQ DNA helicases in DNA repair. Annu. Rev. Genet. *44*, 393–417.

Besaratinia, A., Synold, T.W., Chen, H.-H., Chang, C., Xi, B., Riggs, A.D., and Pfeifer, G.P. (2005). DNA lesions induced by UV A1 and B radiation in human cells: comparative analyses in the overall genome and in the p53 tumor suppressor gene. Proc. Natl. Acad. Sci. U.S.A. *102*, 10058–10063.

Bick, M.D., and Davidson, R.L. (1976). Nucleotide analysis of DNA and RNA in cells with thymidine totally replaced by bromodeoxyuridine. Somatic Cell Genet. *2*, 63–76.

Bielawski, K., Wołczyński, S., and Bielawska, A. (2001). DNA-binding properties and cytotoxicity of extended aromatic bisamidines in breast cancer MCF-7 cells. Pol J Pharmacol *53*, 143–147.

Binz, S.K., Sheehan, A.M., and Wold, M.S. (2004). Replication protein A phosphorylation and the cellular response to DNA damage. DNA Repair (Amst.) *3*, 1015–1024.

Block, W.D., Yu, Y., and Lees-Miller, S.P. (2004). Phosphatidyl inositol 3-kinase-like serine/threonine protein kinases (PIKKs) are required for DNA damage-induced phosphorylation of the 32 kDa subunit of replication protein A at threonine 21. Nucleic Acids Res. *32*, 997–1005.

Bodley, A., Liu, L.F., Israel, M., Seshadri, R., Koseki, Y., Giuliani, F.C., Kirschenbaum, S., Silber, R., and Potmesil, M. (1989). DNA topoisomerase II-mediated interaction of doxorubicin and daunorubicin congeners with DNA. Cancer Res. *49*, 5969–5978.

Botuyan, M.V., Lee, J., Ward, I.M., Kim, J.-E., Thompson, J.R., Chen, J., and Mer, G. (2006). Structural Basis for the Methylation State-Specific Recognition of Histone H4-K20 by 53BP1 and Crb2 in DNA Repair. Cell *127*, 1361–1373.

Botvinick, E.L., Venugopalan, V., Shah, J.V., Liaw, L.H., and Berns, M.W. (2004). Controlled Ablation of Microtubules Using a Picosecond Laser. Biophysical Journal *87*, 4203–4212.

Brash, D.E. (1988). UV mutagenic photoproducts in Escherichia coli and human cells: a molecular genetics perspective on human skin cancer. Photochem. Photobiol. *48*, 59–66.

Bristow, R.G., and Hill, R.P. (2008). Hypoxia and metabolism. Hypoxia, DNA repair and genetic instability. Nat. Rev. Cancer *8*, 180–192.

Burhans, W.C., and Weinberger, M. (2007). DNA replication stress, genome instability and aging. Nucleic Acids Research *35*, 7545–7556.

Cadet, J., Douki, T., Gasparutto, D., and Ravanat, J.-L. (2003). Oxidative damage to DNA: formation, measurement and biochemical features. Mutat. Res. *531*, 5–23.

Callén, E., Jankovic, M., Wong, N., Zha, S., Chen, H.-T., Difilippantonio, S., Di Virgilio, M., Heidkamp, G., Alt, F.W., Nussenzweig, A., et al. (2009). Essential Role for DNA-PKcs in DNA Double-Strand Break Repair and Apoptosis in ATM-Deficient Lymphocytes. Molecular Cell *34*, 285–297.

Canman, C.E., Lim, D.S., Cimprich, K.A., Taya, Y., Tamai, K., Sakaguchi, K., Appella, E., Kastan, M.B., and Siliciano, J.D. (1998). Activation of the ATM kinase by ionizing radiation and phosphorylation of p53. Science *281*, 1677–1679.

Celeste, A. (2002). Genomic Instability in Mice Lacking Histone H2AX. Science *296*, 922–927.

Celeste, A., Fernandez-Capetillo, O., Kruhlak, M.J., Pilch, D.R., Staudt, D.W., Lee, A., Bonner, R.F., Bonner, W.M., and Nussenzweig, A. (2003). Histone H2AX phosphorylation is dispensable for the initial recognition of DNA breaks. Nat. Cell Biol. *5*, 675–679.

Cescutti, R., Negrini, S., Kohzaki, M., and Halazonetis, T.D. (2010). TopBP1 functions with 53BP1 in the G1 DNA damage checkpoint. EMBO J. *29*, 3723–3732.

Chang, D.J., Lupardus, P.J., and Cimprich, K.A. (2006). Monoubiquitination of Proliferating Cell Nuclear Antigen Induced by Stalled Replication Requires Uncoupling of DNA Polymerase and Mini-chromosome Maintenance Helicase Activities. Journal of Biological Chemistry *281*, 32081–32088.

Chen, P.L., Riley, D.J., Chen-Kiang, S., and Lee, W.H. (1996). Retinoblastoma protein directly interacts with and activates the transcription factor NF-IL6. Proc. Natl. Acad. Sci. U.S.A. *93*, 465–469.

Cheng, C.H., and Kuchta, R.D. (1993). DNA polymerase epsilon: aphidicolin inhibition and the relationship between polymerase and exonuclease activity. Biochemistry *32*, 8568–8574.

Chung, F.L., Chen, H.J., and Nath, R.G. (1996). Lipid peroxidation as a potential endogenous source for the formation of exocyclic DNA adducts. Carcinogenesis *17*, 2105–2111.

Cimprich, K.A. (2007). Probing ATR activation with model DNA templates. Cell Cycle *6*, 2348–2354.

Cotta-Ramusino, C., McDonald, E.R., Hurov, K., Sowa, M.E., Harper, J.W., and Elledge, S.J. (2011). A DNA damage response screen identifies RHINO, a 9-1-1 and TopBP1 interacting protein required for ATR signaling. Science *332*, 1313–1317.

Cremer, C., and Cremer, T. (1986). Induction of chromosome shattering by ultraviolet light and caffeine: the influence of different distributions of photolesions. Mutat. Res. *163*, 33–40.

Cremer, C., Zorn, C., and Cremer, T. (1974). An ultraviolet laser microbeam for 257 nm. Microsc Acta *75*, 331–337.

Damsma, G.E., Alt, A., Brueckner, F., Carell, T., and Cramer, P. (2007). Mechanism of transcriptional stalling at cisplatin-damaged DNA. Nature Structural & Molecular Biology *14*, 1127–1133.

Danenberg, P.V., Gustavsson, B., Johnston, P., Lindberg, P., Moser, R., Odin, E., Peters, G.J., and Petrelli, N. (2016). Folates as adjuvants to anticancer agents: Chemical rationale and mechanism of action. Critical Reviews in Oncology/Hematology *106*, 118–131.

DeFazio, L.G., Stansel, R.M., Griffith, J.D., and Chu, G. (2002). Synapsis of DNA ends by DNA-dependent protein kinase. EMBO J. *21*, 3192–3200.

Denison, S.R., Simper, R.K., and Greenbaum, I.F. (2003). How common are common fragile sites in humans: interindividual variation in the distribution of aphidicolin-induced fragile sites. Cytogenet. Genome Res. *101*, 8–16.

Derbyshire, D.J. (2002). Crystal structure of human 53BP1 BRCT domains bound to p53 tumour suppressor. The EMBO Journal *21*, 3863–3872.

Di Micco, R., Fumagalli, M., Cicalese, A., Piccinin, S., Gasparini, P., Luise, C., Schurra, C., Garre', M., Giovanni Nuciforo, P., Bensimon, A., et al. (2006). Oncogene-induced senescence is a DNA damage response triggered by DNA hyper-replication. Nature *444*, 638–642.

Difilippantonio, S., Gapud, E., Wong, N., Huang, C.-Y., Mahowald, G., Chen, H.T., Kruhlak, M.J., Callen, E., Livak, F., Nussenzweig, M.C., et al. (2008). 53BP1 facilitates long-range DNA end-joining during V(D)J recombination. Nature *456*, 529–533.

DiGiovanna, J.J., and Kraemer, K.H. (2012). Shining a light on xeroderma pigmentosum. J. Invest. Dermatol. *132*, 785–796.

Dillon, L.W., Pierce, L.C.T., Ng, M.C.Y., and Wang, Y.-H. (2013). Role of DNA secondary structures in fragile site breakage along human chromosome 10. Hum Mol Genet *22*, 1443–1456.

Dinant, C., de Jager, M., Essers, J., van Cappellen, W.A., Kanaar, R., Houtsmuller, A.B., and Vermeulen, W. (2007). Activation of multiple DNA repair pathways by sub-nuclear damage induction methods. Journal of Cell Science *120*, 2731–2740.

Dinant, C., Ampatziadis-Michailidis, G., Lans, H., Tresini, M., Lagarou, A., Grosbart, M., Theil, A.F., van Cappellen, W.A., Kimura, H., Bartek, J., et al. (2013). Enhanced chromatin dynamics by FACT promotes transcriptional restart after UV-induced DNA damage. Mol. Cell *51*, 469–479.

DiTullio, R.A., Mochan, T.A., Venere, M., Bartkova, J., Sehested, M., Bartek, J., and Halazonetis, T.D. (2002). 53BP1 functions in an ATM-dependent checkpoint pathway that is constitutively activated in human cancer. Nat. Cell Biol. *4*, 998–1002.

Dong, Z., Zhong, Q., and Chen, P.L. (1999). The Nijmegen breakage syndrome protein is essential for Mre11 phosphorylation upon DNA damage. J. Biol. Chem. *274*, 19513–19516.

Drexler, G.A., and Ruiz-Gómez, M.J. (2015). Microirradiation techniques in radiobiological research. J. Biosci. *40*, 629–643.

Drouet, J., Delteil, C., Lefrançois, J., Concannon, P., Salles, B., and Calsou, P. (2005). DNA-dependent protein kinase and XRCC4-DNA ligase IV mobilization in the cell in response to DNA double strand breaks. J. Biol. Chem. *280*, 7060–7069.

Dupré, A., Boyer-Chatenet, L., and Gautier, J. (2006). Two-step activation of ATM by DNA and the Mre11-Rad50-Nbs1 complex. Nat. Struct. Mol. Biol. *13*, 451–457.

Durand, R.E., and Olive, P.L. (1982). Cytotoxicity, Mutagenicity and DNA damage by Hoechst 33342. J. Histochem. Cytochem. *30*, 111–116.

Durkin, S.G., Ragland, R.L., Arlt, M.F., Mulle, J.G., Warren, S.T., and Glover, T.W. (2008). Replication stress induces tumor-like microdeletions in FHIT/FRA3B. Proceedings of the National Academy of Sciences *105*, 246–251.

Dutta, A., and Stillman, B. (1992). cdc2 family kinases phosphorylate a human cell DNA replication factor, RPA, and activate DNA replication. EMBO J. *11*, 2189–2199.

Epe, B. (2012). DNA damage spectra induced by photosensitization. Photochem. Photobiol. Sci. *11*, 98–106.

d'Adda di Fagagna, F., Reaper, P.M., Clay-Farrace, L., Fiegler, H., Carr, P., Von Zglinicki, T., Saretzki, G., Carter, N.P., and Jackson, S.P. (2003). A DNA damage checkpoint response in telomere-initiated senescence. Nature *426*, 194–198.

Fernandez-Capetillo, O., Chen, H.-T., Celeste, A., Ward, I., Romanienko, P.J., Morales, J.C., Naka, K., Xia, Z., Camerini-Otero, R.D., Motoyama, N., et al. (2002). DNA damage-induced G2-M checkpoint activation by histone H2AX and 53BP1. Nat. Cell Biol. *4*, 993–997.

Fingar, D.C., Richardson, C.J., Tee, A.R., Cheatham, L., Tsou, C., and Blenis, J. (2004). mTOR controls cell cycle progression through its cell growth effectors S6K1 and 4E-BP1/eukaryotic translation initiation factor 4E. Mol. Cell. Biol. *24*, 200–216.

Flynn, R.L., and Zou, L. (2011). ATR: a Master Conductor of Cellular Responses to DNA Replication Stress. Trends Biochem Sci *36*, 133–140.

Franchitto, A. (2013). Genome Instability at Common Fragile Sites: Searching for the Cause of Their Instability. Biomed Res Int *2013*.

Fu, J., Bian, M., Jiang, Q., and Zhang, C. (2007). Roles of Aurora Kinases in Mitosis and Tumorigenesis. Mol Cancer Res *5*, 1–10.

Fujii, Y., Genet, M.D., Roybal, E.J., Kubota, N., Okayasu, R., Miyagawa, K., Fujimori, A., and Kato, T.A. (2013). Comparison of the bromodeoxyuridine-mediated sensitization effects between low-LET and high-LET ionizing radiation on DNA double-strand breaks. Oncol. Rep. *29*, 2133–2139.

Fujita, M., Sasanuma, H., Yamamoto, K.N., Harada, H., Kurosawa, A., Adachi, N., Omura, M., Hiraoka, M., Takeda, S., and Hirota, K. (2013). Interference in DNA replication can cause mitotic chromosomal breakage unassociated with double-strand breaks. PLoS ONE *8*, e60043.

Galanty, Y., Belotserkovskaya, R., Coates, J., and Jackson, S.P. (2012). RNF4, a SUMO-targeted ubiquitin E3 ligase, promotes DNA double-strand break repair. Genes Dev. *26*, 1179–1195.

Garcia-Higuera, I., Taniguchi, T., Ganesan, S., Meyn, M.S., Timmers, C., Hejna, J., Grompe, M., and D'Andrea, A.D. (2001). Interaction of the Fanconi anemia proteins and BRCA1 in a common pathway. Mol. Cell *7*, 249–262.

Gately, D.P., Hittle, J.C., Chan, G.K., and Yen, T.J. (1998). Characterization of ATM expression, localization, and associated DNA-dependent protein kinase activity. Mol. Biol. Cell *9*, 2361–2374.

Gelot, C., Magdalou, I., and Lopez, B. (2015). Replication Stress in Mammalian Cells and Its Consequences for Mitosis. Genes *6*, 267–298.

Glover, T.W., Berger, C., Coyle, J., and Echo, B. (1984). DNA polymerase alpha inhibition by aphidicolin induces gaps and breaks at common fragile sites in human chromosomes. Hum. Genet. *67*, 136–142.

Glover, T.W., Arlt, M.F., Casper, A.M., and Durkin, S.G. (2005). Mechanisms of common fragile site instability. Hum. Mol. Genet. *14 Spec No. 2*, R197-205.

Goldberg, M., Stucki, M., Falck, J., D'Amours, D., Rahman, D., Pappin, D., Bartek, J., and Jackson, S.P. (2003). MDC1 is required for the intra-S-phase DNA damage checkpoint. Nature *421*, 952–956.

Gomez-Godinez, V., Wakida, N.M., Dvornikov, A.S., Yokomori, K., and Berns, M.W. (2007). Recruitment of DNA damage recognition and repair pathway proteins following near-IR femtosecond laser irradiation of cells. J Biomed Opt *12*, 020505.

Gong, F., Chiu, L.-Y., Cox, B., Aymard, F., Clouaire, T., Leung, J.W., Cammarata, M., Perez, M., Agarwal, P., Brodbelt, J.S., et al. (2015). Screen identifies bromodomain protein ZMYND8 in chromatin recognition of transcription-associated DNA damage that promotes homologous recombination. Genes Dev. *29*, 197–211.

Goodarzi, A.A., Noon, A.T., Deckbar, D., Ziv, Y., Shiloh, Y., Löbrich, M., and Jeggo, P.A. (2008). ATM signaling facilitates repair of DNA double-strand breaks associated with heterochromatin. Mol. Cell *31*, 167–177.

Gorgoulis, V.G., Vassiliou, L.-V.F., Karakaidos, P., Zacharatos, P., Kotsinas, A., Liloglou, T., Venere, M., DiTullio, R.A., Kastrinakis, N.G., Levy, B., et al. (2005). Activation of the DNA damage checkpoint and genomic instability in human precancerous lesions. Nature *434*, 907–913.

Guervilly, J.-H., Macé-Aimé, G., and Rosselli, F. (2008). Loss of CHK1 function impedes DNA damage-induced FANCD2 monoubiquitination but normalizes the abnormal G2 arrest in Fanconi anemia. Hum. Mol. Genet. *17*, 679–689.

Gustafsson, A.-S., Abramenkovs, A., and Stenerlöw, B. (2014). Suppression of DNA-dependent protein kinase sensitize cells to radiation without affecting DSB repair. Mutat. Res. *769*, 1–10.

Haahr, P., Hoffmann, S., Tollenaere, M.A.X., Ho, T., Toledo, L.I., Mann, M., Bekker-Jensen, S., Räschle, M., and Mailand, N. (2016). Activation of the ATR kinase by the RPA-binding protein ETAA1. Nat. Cell Biol. *18*, 1196–1207.

Haince, J.-F., Kozlov, S., Dawson, V.L., Dawson, T.M., Hendzel, M.J., Lavin, M.F., and Poirier, G.G. (2007). Ataxia telangiectasia mutated (ATM) signaling network is modulated by a novel poly(ADP-ribose)-dependent pathway in the early response to DNA-damaging agents. J. Biol. Chem. *282*, 16441–16453.

Haince, J.-F., McDonald, D., Rodrigue, A., Déry, U., Masson, J.-Y., Hendzel, M.J., and Poirier, G.G. (2008). PARP1-dependent kinetics of recruitment of MRE11 and NBS1 proteins to multiple DNA damage sites. J. Biol. Chem. *283*, 1197–1208.

Hakansson, P., Hofer, A., and Thelander, L. (2006). Regulation of Mammalian Ribonucleotide Reduction and dNTP Pools after DNA Damage and in Resting Cells. Journal of Biological Chemistry *281*, 7834–7841.

Hammel, M., Yu, Y., Mahaney, B.L., Cai, B., Ye, R., Phipps, B.M., Rambo, R.P., Hura, G.L., Pelikan, M., So, S., et al. (2010). Ku and DNA-dependent protein kinase dynamic conformations and assembly regulate DNA binding and the initial non-homologous end joining complex. J. Biol. Chem. *285*, 1414–1423.

Harley, C.B., Futcher, A.B., and Greider, C.W. (1990). Telomeres shorten during ageing of human fibroblasts. Nature *345*, 458–460.

Helleday, T., Eshtad, S., and Nik-Zainal, S. (2014). Mechanisms underlying mutational signatures in human cancers. Nat. Rev. Genet. *15*, 585–598.

Hellman, A., Zlotorynski, E., Scherer, S.W., Cheung, J., Vincent, J.B., Smith, D.I., Trakhtenbrot, L., and Kerem, B. (2002). A role for common fragile site induction in amplification of human oncogenes. Cancer Cell *1*, 89–97.

Helmrich, A., Ballarino, M., and Tora, L. (2011). Collisions between Replication and Transcription Complexes Cause Common Fragile Site Instability at the Longest Human Genes. Molecular Cell *44*, 966–977.

Herr, A.J., Ogawa, M., Lawrence, N.A., Williams, L.N., Eggington, J.M., Singh, M., Smith, R.A., and Preston, B.D. (2011). Mutator suppression and escape from replication error-induced extinction in yeast. PLoS Genet. *7*, e1002282.

Herr, A.J., Kennedy, S.R., Knowels, G.M., Schultz, E.M., and Preston, B.D. (2014). DNA replication error-induced extinction of diploid yeast. Genetics *196*, 677–691.

Hildick, K.L., González-González, I.M., Jaskolski, F., and Henley, J.M. (2012). Lateral diffusion and exocytosis of membrane proteins in cultured neurons assessed using fluorescence recovery and fluorescence-loss photobleaching. J Vis Exp.

Hills, S.A., and Diffley, J.F.X. (2014). DNA replication and oncogene-induced replicative stress. Curr. Biol. *24*, R435-444.

Ho, G.P.H., Margossian, S., Taniguchi, T., and D'Andrea, A.D. (2006). Phosphorylation of FANCD2 on Two Novel Sites Is Required for Mitomycin C Resistance. Molecular and Cellular Biology *26*, 7005–7015.

Hochegger, H., Dejsuphong, D., Fukushima, T., Morrison, C., Sonoda, E., Schreiber, V., Zhao, G.Y., Saberi, A., Masutani, M., Adachi, N., et al. (2006). Parp-1 protects homologous recombination from interference by Ku and Ligase IV in vertebrate cells. EMBO J. *25*, 1305–1314.

Hopfner, K.-P., Karcher, A., Craig, L., Woo, T.T., Carney, J.P., and Tainer, J.A. (2001). Structural Biochemistry and Interaction Architecture of the DNA Double-Strand Break Repair Mre11 Nuclease and Rad50-ATPase. Cell *105*, 473–485.

Hsiang, Y.H., Lihou, M.G., and Liu, L.F. (1989). Arrest of replication forks by drug-stabilized topoisomerase I-DNA cleavable complexes as a mechanism of cell killing by camptothecin. Cancer Res. *49*, 5077–5082.

Huang, Y., and Li, L. (2013). DNA crosslinking damage and cancer - a tale of friend and foe. Transl Cancer Res *2*, 144–154.

Huh, M.S., Ivanochko, D., Hashem, L.E., Curtin, M., Delorme, M., Goodall, E., Yan, K., and Picketts, D.J. (2016). Stalled replication forks within heterochromatin require ATRX for protection. Cell Death Dis *7*, e2220.

Iftode, C., Daniely, Y., and Borowiec, J.A. (1999). Replication protein A (RPA): the eukaryotic SSB. Crit. Rev. Biochem. Mol. Biol. *34*, 141–180.

Ikeda, N., Usuda, J., Kato, H., Ishizumi, T., Ichinose, S., Otani, K., Honda, H., Furukawa, K., Okunaka, T., and Tsutsui, H. (2011). New aspects of photodynamic therapy for central type early stage lung cancer. Lasers Surg Med *43*, 749–754.

Iliakis, G., and Kurtzman, S. (1991). Mechanism of Radiosensitization by Halogenated Pyrimidines: Bromodeoxyuridine and β-Arabinofuranosyladenine Affect Similar Subsets of Radiation-Induced Potentially Lethal Lesions in Plateau-Phase Chinese Hamster Ovary Cells. Radiation Research *127*, 45.

Inoue, Y., Kitagawa, M., and Taya, Y. (2007). Phosphorylation of pRB at Ser612 by Chk1/2 leads to a complex between pRB and E2F-1 after DNA damage. The EMBO Journal *26*, 2083–2093.

Iwabuchi, K., Li, B., Massa, H.F., Trask, B.J., Date, T., and Fields, S. (1998). Stimulation of p53-mediated transcriptional activation by the p53-binding proteins, 53BP1 and 53BP2. J. Biol. Chem. *273*, 26061–26068.

Jackson, S.P., and Bartek, J. (2009). The DNA-damage response in human biology and disease. Nature *461*, 1071–1078.

Janson, C., Nyhan, K., and Murnane, J.P. (2015). Replication Stress and Telomere Dysfunction Are Present in Cultured Human Embryonic Stem Cells. Cytogenet. Genome Res. *146*, 251–260.

Joenje, H., and Patel, K.J. (2001). The emerging genetic and molecular basis of Fanconi anaemia. Nat. Rev. Genet. *2*, 446–457.

Josefsen, L.B., and Boyle, R.W. (2008). Photodynamic Therapy and the Development of Metal-Based Photosensitisers. Metal-Based Drugs *2008*, 1–23.

Jowsey, P., Morrice, N.A., Hastie, C.J., McLauchlan, H., Toth, R., and Rouse, J. (2007). Characterisation of the sites of DNA damage-induced 53BP1 phosphorylation catalysed by ATM and ATR. DNA Repair *6*, 1536–1544.

Juan, G., Traganos, F., James, W.M., Ray, J.M., Roberge, M., Sauve, D.M., Anderson, H., and Darzynkiewicz, Z. (1998). Histone H3 phosphorylation and expression of cyclins A and B1 measured in individual cells during their progression through G2 and mitosis. Cytometry *32*, 71–77.

Jungmichel, S., Clapperton, J.A., Lloyd, J., Hari, F.J., Spycher, C., Pavic, L., Li, J., Haire, L.F., Bonalli, M., Larsen, D.H., et al. (2012). The molecular basis of ATM-dependent dimerization of the Mdc1 DNA damage checkpoint mediator. Nucleic Acids Res. *40*, 3913–3928.

Kais, Z., Rondinelli, B., Holmes, A., O'Leary, C., Kozono, D., D'Andrea, A.D., and Ceccaldi, R. (2016). FANCD2 Maintains Fork Stability in BRCA1/2-Deficient Tumors and Promotes Alternative End-Joining DNA Repair. Cell Reports *15*, 2488–2499.

Katsumi, S., Kobayashi, N., Imoto, K., Nakagawa, A., Yamashina, Y., Muramatsu, T., Shirai, T., Miyagawa, S., Sugiura, S., Hanaoka, F., et al. (2001). In situ visualization of ultraviolet-light-induced DNA damage repair in locally irradiated human fibroblasts. J. Invest. Dermatol. *117*, 1156–1161.

Kaufman, B., Shapira-Frommer, R., Schmutzler, R.K., Audeh, M.W., Friedlander, M., Balmaña, J., Mitchell, G., Fried, G., Stemmer, S.M., Hubert, A., et al. (2015). Olaparib monotherapy in patients with advanced cancer and a germline BRCA1/2 mutation. J. Clin. Oncol. *33*, 244–250.

Kim, H., and D'Andrea, A.D. (2012). Regulation of DNA cross-link repair by the Fanconi anemia/BRCA pathway. Genes Dev. *26*, 1393–1408.

Kim, J.C., and Mirkin, S.M. (2013). The Balancing Act of DNA Repeat Expansions. Curr Opin Genet Dev *23*, 280–288.

Kim, H., George, E., Ragland, R.L., Rafail, S., Zhang, R., Krepler, C., Morgan, M., Herlyn, M., Brown, E.J., and Simpkins, F. (2016). Targeting the ATR/CHK1 axis with PARP inhibition results in tumor regression in BRCA mutant ovarian cancer models. Clin. Cancer Res.

Kim, J.-S., Krasieva, T.B., Kurumizaka, H., Chen, D.J., Taylor, A.M.R., and Yokomori, K. (2005a). Independent and sequential recruitment of NHEJ and HR factors to DNA damage sites in mammalian cells. J. Cell Biol. *170*, 341–347.

Kim, M.Y., Zhang, T., and Kraus, W.L. (2005b). Poly(ADP-ribosyl)ation by PARP-1: "PAR-laying" NAD+ into a nuclear signal. Genes Dev. *19*, 1951–1967.

Kim, S.-T., Lim, D.-S., Canman, C.E., and Kastan, M.B. (1999). Substrate Specificities and Identification of Putative Substrates of ATM Kinase Family Members. J. Biol. Chem. *274*, 37538–37543.

Kleiner, R.E., Verma, P., Molloy, K.R., Chait, B.T., and Kapoor, T.M. (2015). Chemical proteomics reveals a γH2AX-53BP1 interaction in the DNA damage response. Nat. Chem. Biol. *11*, 807–814.

Kondo, N., Takahashi, A., Ono, K., and Ohnishi, T. (2010). DNA damage induced by alkylating agents and repair pathways. J Nucleic Acids *2010*, 543531.

Kong, X., Mohanty, S.K., Stephens, J., Heale, J.T., Gomez-Godinez, V., Shi, L.Z., Kim, J.-S., Yokomori, K., and Berns, M.W. (2009). Comparative analysis of different laser systems to study cellular responses to DNA damage in mammalian cells. Nucleic Acids Res. *37*, e68.

Koster, D.A., Palle, K., Bot, E.S.M., Bjornsti, M.-A., and Dekker, N.H. (2007). Antitumour drugs impede DNA uncoiling by topoisomerase I. Nature *448*, 213–217.

Kottemann, M.C., and Smogorzewska, A. (2013). Fanconi anemia and the repair of Watson and Crick crosslinks. Nature *493*, 356–363.

Kotula, E., Berthault, N., Agrario, C., Lienafa, M.-C., Simon, A., Dingli, F., Loew, D., Sibut, V., Saule, S., and Dutreix, M. (2015). DNA-PKcs plays role in cancer metastasis through regulation of secreted proteins involved in migration and invasion. Cell Cycle *14*, 1961–1972.

Koundrioukoff, S., Carignon, S., Técher, H., Letessier, A., Brison, O., and Debatisse, M. (2013). Stepwise activation of the ATR signaling pathway upon increasing replication stress impacts fragile site integrity. PLoS Genet. *9*, e1003643.

Krasilnikova, M.M., and Mirkin, S.M. (2004). Replication stalling at Friedreich's ataxia (GAA)n repeats in vivo. Mol. Cell. Biol. *24*, 2286–2295.

Kuo, L.J., and Yang, L.-X. (2008). Gamma-H2AX - a novel biomarker for DNA double-strand breaks. In Vivo *22*, 305–309.

Kutler, D.I., Singh, B., Satagopan, J., Batish, S.D., Berwick, M., Giampietro, P.F., Hanenberg, H., and Auerbach, A.D. (2003). A 20-year perspective on the International Fanconi Anemia Registry (IFAR). Blood *101*, 1249–1256.

Kysela, B., Doherty, A.J., Chovanec, M., Stiff, T., Ameer-Beg, S.M., Vojnovic, B., Girard, P.-M., and Jeggo, P.A. (2003). Ku stimulation of DNA ligase IV-dependent ligation requires inward movement along the DNA molecule. J. Biol. Chem. *278*, 22466–22474.

Langelier, M.-F., Planck, J.L., Roy, S., and Pascal, J.M. (2012). Structural basis for DNA damage-dependent poly(ADP-ribosyl)ation by human PARP-1. Science *336*, 728–732.

Larizza, L., Roversi, G., and Volpi, L. (2010). Rothmund-Thomson syndrome. Orphanet J Rare Dis *5*, 2.

Larsen, D.H., Hari, F., Clapperton, J.A., Gwerder, M., Gutsche, K., Altmeyer, M., Jungmichel, S., Toledo, L.I., Fink, D., Rask, M.-B., et al. (2014). The NBS1-Treacle complex controls ribosomal RNA transcription in response to DNA damage. Nat. Cell Biol. *16*, 792–803.

Lau, W.C.Y., Li, Y., Liu, Z., Gao, Y., Zhang, Q., and Huen, M.S.Y. (2016). Structure of the human dimeric ATM kinase. Cell Cycle *15*, 1117–1124.

Lauper, J.M., Krause, A., Vaughan, T.L., and Monnat, R.J. (2013). Spectrum and Risk of Neoplasia in Werner Syndrome: A Systematic Review. PLoS One *8*.

Lavin, M.F. (2007). ATM and the Mre11 complex combine to recognize and signal DNA double-strand breaks. Oncogene *26*, 7749–7758.

LeBron, C., Chen, L., Gilkes, D.M., and Chen, J. (2006). Regulation of MDMX nuclear import and degradation by Chk2 and 14-3-3. EMBO J. *25*, 1196–1206.

Lee, J.-H., and Paull, T.T. (2005). ATM activation by DNA double-strand breaks through the Mre11-Rad50-Nbs1 complex. Science *308*, 551–554.

Lee, J., Kumagai, A., and Dunphy, W.G. (2007). The Rad9-Hus1-Rad1 checkpoint clamp regulates interaction of TopBP1 with ATR. J. Biol. Chem. *282*, 28036–28044.

Lee, K.-J., Lin, Y.-F., Chou, H.-Y., Yajima, H., Fattah, K.R., Lee, S.-C., and Chen, B.P.C. (2011). Involvement of DNA-dependent protein kinase in normal cell cycle progression through mitosis. J. Biol. Chem. *286*, 12796–12802.

Lee, Y.-C., Zhou, Q., Chen, J., and Yuan, J. (2016). RPA-Binding Protein ETAA1 Is an ATR Activator Involved in DNA Replication Stress Response. Curr. Biol. *26*, 3257–3268.

Le Tallec, B., Millot, G.A., Blin, M.E., Brison, O., Dutrillaux, B., and Debatisse, M. (2013). Common Fragile Site Profiling in Epithelial and Erythroid Cells Reveals that Most Recurrent Cancer Deletions Lie in Fragile Sites Hosting Large Genes. Cell Reports *4*, 420–428.

Letessier, A., Millot, G.A., Koundrioukoff, S., Lachagès, A.-M., Vogt, N., Hansen, R.S., Malfoy, B., Brison, O., and Debatisse, M. (2011). Cell-type-specific replication initiation programs set fragility of the FRA3B fragile site. Nature *470*, 120–123.

Leung, C.C.Y., Sun, L., Gong, Z., Burkat, M., Edwards, R., Assmus, M., Chen, J., and Glover, J.N.M. (2013). Structural insights into recognition of MDC1 by TopBP1 in DNA replication checkpoint control. Structure *21*, 1450–1459.

Li, S., Ting, N.S., Zheng, L., Chen, P.L., Ziv, Y., Shiloh, Y., Lee, E.Y., and Lee, W.H. (2000). Functional link of BRCA1 and ataxia telangiectasia gene product in DNA damage response. Nature *406*, 210–215.

Li, X., Tian, J., Bo, Q., Li, K., Wang, H., Liu, T., and Li, J. (2015). Targeting DNA-PKcs increased anticancer drug sensitivity by suppressing DNA damage repair in osteosarcoma cell line MG63. Tumour Biol. *36*, 9365–9372.

Lim, D.S., Kim, S.T., Xu, B., Maser, R.S., Lin, J., Petrini, J.H., and Kastan, M.B. (2000). ATM phosphorylates p95/nbs1 in an S-phase checkpoint pathway. Nature *404*, 613–617.

Limoli, C.L., and Ward, J.F. (1993). A new method for introducing double-strand breaks into cellular DNA. Radiat. Res. *134*, 160–169.

Lindahl, T. (1974). An N-glycosidase from Escherichia coli that releases free uracil from DNA containing deaminated cytosine residues. Proc. Natl. Acad. Sci. U.S.A. *71*, 3649–3653.

Lindahl, T. (1993). Instability and decay of the primary structure of DNA. Nature *362*, 709–715.

Lindahl, T., and Barnes, D.E. (2000). Repair of Endogenous DNA Damage. Cold Spring Harb Symp Quant Biol *65*, 127–134.

Lisby, M., and Rothstein, R. (2009). Choreography of recombination proteins during the DNA damage response. DNA Repair *8*, 1068–1076.

Liu, L.F., Rowe, T.C., Yang, L., Tewey, K.M., and Chen, G.L. (1983). Cleavage of DNA by mammalian DNA topoisomerase II. J. Biol. Chem. *258*, 15365–15370.

Liu, S., Bekker-Jensen, S., Mailand, N., Lukas, C., Bartek, J., and Lukas, J. (2006). Claspin operates downstream of TopBP1 to direct ATR signaling towards Chk1 activation. Mol. Cell. Biol. *26*, 6056–6064.

Ljungman, M., and Lane, D.P. (2004). Transcription - guarding the genome by sensing DNA damage. Nat. Rev. Cancer *4*, 727–737.

Lloyd, J., Chapman, J.R., Clapperton, J.A., Haire, L.F., Hartsuiker, E., Li, J., Carr, A.M., Jackson, S.P., and Smerdon, S.J. (2009). A supramodular FHA/BRCT-repeat architecture mediates Nbs1 adaptor function in response to DNA damage. Cell *139*, 100–111.

Lobachev, K., Vitriol, E., Stemple, J., Resnick, M.A., and Bloom, K. (2004). Chromosome Fragmentation after Induction of a Double-Strand Break Is an Active Process Prevented by the RMX Repair Complex. Current Biology *14*, 2107–2112.

Loeb, L.A. (2016). Human Cancers Express a Mutator Phenotype: Hypothesis, Origin, and Consequences. Cancer Res. *76*, 2057–2059.

Lopes, M., Cotta-Ramusino, C., Pellicioli, A., Liberi, G., Plevani, P., Muzi-Falconi, M., Newlon, C.S., and Foiani, M. (2001). The DNA replication checkpoint response stabilizes stalled replication forks. Nature *412*, 557–561.

Lou, Z., Minter-Dykhouse, K., Franco, S., Gostissa, M., Rivera, M.A., Celeste, A., Manis, J.P., van Deursen, J., Nussenzweig, A., Paull, T.T., et al. (2006). MDC1 maintains genomic stability by participating in the amplification of ATM-dependent DNA damage signals. Mol. Cell *21*, 187–200.

Lu, H., Shamanna, R.A., Keijzers, G., Anand, R., Rasmussen, L.J., Cejka, P., Croteau, D.L., and Bohr, V.A. (2016). RECQL4 Promotes DNA End Resection in Repair of DNA Double-Strand Breaks. Cell Rep *16*, 161–173.

Ludes-Meyers, J.H., Bednarek, A.K., Popescu, N.C., Bedford, M., and Aldaz, C.M. (2003). WWOX, the common chromosomal fragile site, FRA16D, cancer gene. Cytogenet. Genome Res. *100*, 101–110.

Lukas, C., Savic, V., Bekker-Jensen, S., Doil, C., Neumann, B., Pedersen, R.S., Grøfte, M., Chan, K.L., Hickson, I.D., Bartek, J., et al. (2011). 53BP1 nuclear bodies form around DNA lesions generated by mitotic transmission of chromosomes under replication stress. Nat. Cell Biol. *13*, 243–253.

Lupardus, P.J., Byun, T., Yee, M., Hekmat-Nejad, M., and Cimprich, K.A. (2002). A requirement for replication in activation of the ATR-dependent DNA damage checkpoint. Genes Dev. *16*, 2327–2332.

MacGregor, J.T., Schlegel, R., Wehr, C.M., Alperin, P., and Ames, B.N. (1990). Cytogenetic damage induced by folate deficiency in mice is enhanced by caffeine. Proc. Natl. Acad. Sci. U.S.A. *87*, 9962–9965.

Mackay, D.R., and Ullman, K.S. (2015). ATR and a Chk1-Aurora B pathway coordinate postmitotic genome surveillance with cytokinetic abscission. Mol Biol Cell *26*, 2217–2226.

Mancini, F., and Moretti, F. (2009). Mitochondrial MDM4 (MDMX): an unpredicted role in the p53-mediated intrinsic apoptotic pathway. Cell Cycle *8*, 3854–3859.

Mannironi, C., Bonner, W.M., and Hatch, C.L. (1989). H2A.X. a histone isoprotein with a conserved C-terminal sequence, is encoded by a novel mRNA with both DNA replication type and polyA 3' processing signals. Nucleic Acids Res. *17*, 9113–9126.

Mariotti, L.G., Pirovano, G., Savage, K.I., Ghita, M., Ottolenghi, A., Prise, K.M., and Schettino, G. (2013). Use of the γ-H2AX Assay to Investigate DNA Repair Dynamics Following Multiple Radiation Exposures. PLoS ONE *8*, e79541.

Marnett, L.J. (1999). Lipid peroxidation-DNA damage by malondialdehyde. Mutat. Res. *424*, 83–95.

Martin, S.A., Lord, C.J., and Ashworth, A. (2008). DNA repair deficiency as a therapeutic target in cancer. Curr. Opin. Genet. Dev. *18*, 80–86.

Martínez, R., and Chacón-García, L. (2005). The search of DNA-intercalators as antitumoral drugs: what it worked and what did not work. Curr. Med. Chem. *12*, 127–151.

Martínez, P., Flores, J.M., and Blasco, M.A. (2012). 53BP1 deficiency combined with telomere dysfunction activates ATR-dependent DNA damage response. The Journal of Cell Biology *197*, 283–300.

Massey, A.J. (2016). Inhibition of ATR-dependent feedback activation of Chk1 sensitises cancer cells to Chk1 inhibitor monotherapy. Cancer Lett. *383*, 41–52.

McKay, B.C., Becerril, C., Spronck, J.C., and Ljungman, M. (2002). Ultraviolet light-induced apoptosis is associated with S-phase in primary human fibroblasts. DNA Repair (Amst.) *1*, 811–820.

McKinnon, P.J. (2004). ATM and ataxia telangiectasia. EMBO Rep. *5*, 772–776.

McManus, K.J., and Hendzel, M.J. (2005). ATM-dependent DNA damage-independent mitotic phosphorylation of H2AX in normally growing mammalian cells. Mol. Biol. Cell *16*, 5013–5025.

Meerang, M., Ritz, D., Paliwal, S., Garajova, Z., Bosshard, M., Mailand, N., Janscak, P., Hübscher, U., Meyer, H., and Ramadan, K. (2011). The ubiquitin-selective segregase VCP/p97 orchestrates the response to DNA double-strand breaks. Nat. Cell Biol. *13*, 1376–1382.

Migliorini, D., Denchi, E.L., Danovi, D., Jochemsen, A., Capillo, M., Gobbi, A., Helin, K., Pelicci, P.G., and Marine, J.-C. (2002). Mdm4 (Mdmx) Regulates p53-Induced Growth Arrest and Neuronal Cell Death during Early Embryonic Mouse Development. Molecular and Cellular Biology *22*, 5527–5538.

Minca, E.C., and Kowalski, D. (2011). Replication fork stalling by bulky DNA damage: localization at active origins and checkpoint modulation. Nucleic Acids Res *39*, 2610–2623.

Mini, E., Nobili, S., Caciagli, B., Landini, I., and Mazzei, T. (2006). Cellular pharmacology of gemcitabine. Ann. Oncol. *17 Suppl 5*, v7-12.

Mirkin, E.V., and Mirkin, S.M. (2007). Replication Fork Stalling at Natural Impediments. Microbiology and Molecular Biology Reviews *71*, 13–35.

Mišković, K., Bujak, M., Baus Lončar, M., and Glavaš-Obrovac, L. (2013). Antineoplastic DNA-binding compounds: intercalating and minor groove binding drugs. Arh Hig Rada Toksikol *64*, 593–602.

Mistrik, M., Oplustilova, L., Lukas, J., and Bartek, J. (2009). Low-dose DNA damage and replication stress responses quantified by optimized automated single-cell image analysis. Cell Cycle *8*, 2592–2599.

Mistrik, M., Vesela, E., Furst, T., Hanzlikova, H., Frydrych, I., Gursky, J., Majera, D., and Bartek, J. (2016). Cells and Stripes: A novel quantitative photo-manipulation technique. Sci Rep *6*, 19567.

Mladenov, E., Magin, S., Soni, A., and Iliakis, G. (2016). DNA double-strand-break repair in higher eukaryotes and its role in genomic instability and cancer: Cell cycle and proliferation-dependent regulation. Semin. Cancer Biol. *37–38*, 51–64.

Mochan, T.A., Venere, M., DiTullio, R.A., and Halazonetis, T.D. (2003). 53BP1 and NFBD1/MDC1-Nbs1 function in parallel interacting pathways activating ataxia-telangiectasia mutated (ATM) in response to DNA damage. Cancer Res. *63*, 8586–8591.

Mochan, T.A., Venere, M., DiTullio, R.A., and Halazonetis, T.D. (2004). 53BP1, an activator of ATM in response to DNA damage. DNA Repair (Amst.) *3*, 945–952.

Moles, R., Bai, X.T., Chaib-Mezrag, H., and Nicot, C. (2016). WRN-targeted therapy using inhibitors NSC 19630 and NSC 617145 induce apoptosis in HTLV-1-transformed adult T-cell leukemia cells. J Hematol Oncol *9*, 121.

Mortusewicz, O., Ame, J.-C., Schreiber, V., and Leonhardt, H. (2007). Feedback-regulated poly(ADP-ribosyl)ation by PARP-1 is required for rapid response to DNA damage in living cells. Nucleic Acids Research *35*, 7665–7675.

Moynahan, M.E., Chiu, J.W., Koller, B.H., and Jasin, M. (1999). Brca1 controls homology-directed DNA repair. Mol. Cell *4*, 511–518.

Muñoz, D.P., Kawahara, M., and Yannone, S.M. (2013). An autonomous chromatin/DNA-PK mechanism for localized DNA damage signaling in mammalian cells. Nucleic Acids Res. *41*, 2894–2906.

Murga, M., Campaner, S., Lopez-Contreras, A.J., Toledo, L.I., Soria, R., Montaña, M.F., Artista, L.D., Schleker, T., Guerra, C., Garcia, E., et al. (2011). Exploiting oncogene-induced replicative stress for the selective killing of Myc-driven tumors. Nat Struct Mol Biol *18*, 1331–1335.

Naim, V., and Rosselli, F. (2009). The FANC pathway and BLM collaborate during mitosis to prevent micro-nucleation and chromosome abnormalities. Nature Cell Biology *11*, 761–768.

Nakanishi, K., Yang, Y.-G., Pierce, A.J., Taniguchi, T., Digweed, M., D'Andrea, A.D., Wang, Z.-Q., and Jasin, M. (2005). Human Fanconi anemia monoubiquitination pathway promotes homologous DNA repair. Proceedings of the National Academy of Sciences *102*, 1110–1115.

Nijman, S.M.B., Huang, T.T., Dirac, A.M.G., Brummelkamp, T.R., Kerkhoven, R.M., D'Andrea, A.D., and Bernards, R. (2005). The Deubiquitinating Enzyme USP1 Regulates the Fanconi Anemia Pathway. Molecular Cell *17*, 331–339.

Niu, H., Erdjument-Bromage, H., Pan, Z.Q., Lee, S.H., Tempst, P., and Hurwitz, J. (1997). Mapping of amino acid residues in the p34 subunit of human single-stranded DNA-binding protein phosphorylated by DNA-dependent protein kinase and Cdc2 kinase in vitro. J. Biol. Chem. *272*, 12634–12641.

Noll, D.M., Mason, T.M., and Miller, P.S. (2006). Formation and Repair of Interstrand Cross-Links in DNA. Chem Rev *106*, 277–301.

O'Driscoll, M., and Jeggo, P.A. (2003). Clinical impact of ATR checkpoint signalling failure in humans. Cell Cycle *2*, 194–195.

O'Driscoll, M., Ruiz-Perez, V.L., Woods, C.G., Jeggo, P.A., and Goodship, J.A. (2003). A splicing mutation affecting expression of ataxia-telangiectasia and Rad3-related protein (ATR) results in Seckel syndrome. Nat. Genet. *33*, 497–501.

Olson, E., Nievera, C.J., Klimovich, V., Fanning, E., and Wu, X. (2006). RPA2 is a direct downstream target for ATR to regulate the S-phase checkpoint. J. Biol. Chem. *281*, 39517–39533.

Ozeri-Galai, E., Lebofsky, R., Rahat, A., Bester, A.C., Bensimon, A., and Kerem, B. (2011). Failure of origin activation in response to fork stalling leads to chromosomal instability at fragile sites. Mol. Cell *43*, 122–131.

Pace, P., Mosedale, G., Hodskinson, M.R., Rosado, I.V., Sivasubramaniam, M., and Patel, K.J. (2010). Ku70 corrupts DNA repair in the absence of the Fanconi anemia pathway. Science *329*, 219–223.

Pagano, M., Pepperkok, R., Verde, F., Ansorge, W., and Draetta, G. (1992). Cyclin A is required at two points in the human cell cycle. EMBO J *11*, 961–971.

Palakodeti, A., Lucas, I., Jiang, Y., Young, D.J., Fernald, A.A., Karrison, T., and Le Beau, M.M. (2010). Impaired replication dynamics at the FRA3B common fragile site. Hum. Mol. Genet. *19*, 99–110.

Palchaudhuri, R., and Hergenrother, P.J. (2007). DNA as a target for anticancer compounds: methods to determine the mode of binding and the mechanism of action. Curr. Opin. Biotechnol. *18*, 497–503.

Palumbo, E., Matricardi, L., Tosoni, E., Bensimon, A., and Russo, A. (2010). Replication dynamics at common fragile site FRA6E. Chromosoma *119*, 575–587.

Paull, T.T., and Gellert, M. (1999). Nbs1 potentiates ATP-driven DNA unwinding and endonuclease cleavage by the Mre11/Rad50 complex. Genes Dev. *13*, 1276–1288.

Paull, T.T., Rogakou, E.P., Yamazaki, V., Kirchgessner, C.U., Gellert, M., and Bonner, W.M. (2000). A critical role for histone H2AX in recruitment of repair factors to nuclear foci after DNA damage. Curr. Biol. *10*, 886–895.

Paulsen, R.D., and Cimprich, K.A. (2007). The ATR pathway: fine-tuning the fork. DNA Repair (Amst.) *6*, 953–966.

Perdiz, D., Grof, P., Mezzina, M., Nikaido, O., Moustacchi, E., and Sage, E. (2000). Distribution and repair of bipyrimidine photoproducts in solar UV-irradiated mammalian cells. Possible role of Dewar photoproducts in solar mutagenesis. J. Biol. Chem. *275*, 26732–26742.

Periasamy, N., and Verkman, A.S. (1998). Analysis of fluorophore diffusion by continuous distributions of diffusion coefficients: application to photobleaching measurements of multicomponent and anomalous diffusion. Biophys. J. *75*, 557–567.

Pikor, L., Thu, K., Vucic, E., and Lam, W. (2013). The detection and implication of genome instability in cancer. Cancer Metastasis Rev. *32*, 341–352.

Pirzio, L.M., Pichierri, P., Bignami, M., and Franchitto, A. (2008). Werner syndrome helicase activity is essential in maintaining fragile site stability. J. Cell Biol. *180*, 305–314.

Polo, S.E., and Jackson, S.P. (2011). Dynamics of DNA damage response proteins at DNA breaks: a focus on protein modifications. Genes Dev. *25*, 409–433.

Povirk, L.F. (1996). DNA damage and mutagenesis by radiomimetic DNA-cleaving agents: bleomycin, neocarzinostatin and other enediynes. Mutat. Res. *355*, 71–89.

Purschke, M., Rubio, N., Held, K.D., and Redmond, R.W. (2010). Phototoxicity of Hoechst 33342 in time-lapse fluorescence microscopy. Photochem. Photobiol. Sci. *9*, 1634–1639.

Rai, R., Phadnis, A., Haralkar, S., Badwe, R.A., Dai, H., Li, K., and Lin, S.-Y. (2008). Differential regulation of centrosome integrity by DNA damage response proteins. Cell Cycle *7*, 2225–2233.

Raj, A.S., and Heddle, J.A. (1980). Simultaneous detection of chromosomal aberrations and sister-chromatid exchanges: experience with DNA intercalating agents. Mutat. Res. *78*, 253–260.

Rau, K.R., Quinto-Su, P.A., Hellman, A.N., and Venugopalan, V. (2006). Pulsed laser microbeam-induced cell lysis: time-resolved imaging and analysis of hydrodynamic effects. Biophys. J. *91*, 317–329.

Ravanat, J.L., Douki, T., and Cadet, J. (2001). Direct and indirect effects of UV radiation on DNA and its components. J. Photochem. Photobiol. B, Biol. *63*, 88–102.

Reynolds, J.J., Bicknell, L.S., Carroll, P., Higgs, M.R., Shaheen, R., Murray, J.E., Papadopoulos, D.K., Leitch, A., Murina, O., Tarnauskaitė, Ž., et al. (2017). Mutations in DONSON disrupt replication fork stability and cause microcephalic dwarfism. Nat. Genet.

Reynolds, P., Botchway, S.W., Parker, A.W., and O'Neill, P. (2013). Spatiotemporal dynamics of DNA repair proteins following laser microbeam induced DNA damage – When is a DSB not a DSB? Mutation Research/Genetic Toxicology and Environmental Mutagenesis *756*, 14–20.

Roberts, S.A., Strande, N., Burkhalter, M.D., Strom, C., Havener, J.M., Hasty, P., and Ramsden, D.A. (2010). Ku is a 5'-dRP/AP lyase that excises nucleotide damage near broken ends. Nature *464*, 1214–1217.

Rodier, F., Coppé, J.-P., Patil, C.K., Hoeijmakers, W.A.M., Muñoz, D.P., Raza, S.R., Freund, A., Campeau, E., Davalos, A.R., and Campisi, J. (2009). Persistent DNA damage signalling triggers senescence-associated inflammatory cytokine secretion. Nat. Cell Biol. *11*, 973–979.

Rogakou, E.P., Pilch, D.R., Orr, A.H., Ivanova, V.S., and Bonner, W.M. (1998). DNA double-stranded breaks induce histone H2AX phosphorylation on serine 139. J. Biol. Chem. *273*, 5858–5868.

Rogakou, E.P., Boon, C., Redon, C., and Bonner, W.M. (1999). Megabase chromatin domains involved in DNA double-strand breaks in vivo. J. Cell Biol. *146*, 905–916.

Rothkamm, K., and Löbrich, M. (2003). Evidence for a lack of DNA double-strand break repair in human cells exposed to very low x-ray doses. Proc. Natl. Acad. Sci. U.S.A. *100*, 5057–5062.

Rybak, P., Hoang, A., Bujnowicz, L., Bernas, T., Berniak, K., Zarębski, M., Darzynkiewicz, Z., and Dobrucki, J. (2016). Low level phosphorylation of histone H2AX on serine 139 (γH2AX) is not associated with DNA double-strand breaks. Oncotarget *7*, 49574–49587.

Saquilabon Cruz, G.M., Kong, X., Silva, B.A., Khatibzadeh, N., Thai, R., Berns, M.W., and Yokomori, K. (2016). Femtosecond near-infrared laser microirradiation reveals a crucial role for PARP signaling on factor assemblies at DNA damage sites. Nucleic Acids Res *44*, e27.

Searle, M.S., and Embrey, K.J. (1990). Sequence-specific interaction of Hoechst 33258 with the minor groove of an adenine-tract DNA duplex studied in solution by 1H NMR spectroscopy. Nucleic Acids Res. *18*, 3753–3762.

Seiler, D.M., Rouquette, J., Schmid, V.J., Strickfaden, H., Ottmann, C., Drexler, G.A., Mazurek, B., Greubel, C., Hable, V., Dollinger, G., et al. (2011). Double-strand break-induced transcriptional silencing is associated with loss of tri-methylation at H3K4. Chromosome Res. *19*, 883–899.

Shahin, S., Cullinane, C., and Gray, P.J. (2001). Mitochondrial and nuclear DNA damage induced by sulphur mustard in keratinocytes. Chem. Biol. Interact. *138*, 231–245.

Shen, Z. (2011). Genomic instability and cancer: an introduction. J Mol Cell Biol *3*, 1–3.

Shibata, A., Moiani, D., Arvai, A.S., Perry, J., Harding, S.M., Genois, M.-M., Maity, R., van Rossum-Fikkert, S., Kertokalio, A., Romoli, F., et al. (2014). DNA Double-Strand Break Repair Pathway Choice Is Directed by Distinct MRE11 Nuclease Activities. Molecular Cell *53*, 7–18.

Shih, W., and Yamada, S. (2011). Live-cell imaging of migrating cells expressing fluorescently-tagged proteins in a three-dimensional matrix. J Vis Exp.

Shiloh, Y. (2003). ATM and related protein kinases: safeguarding genome integrity. Nat. Rev. Cancer *3*, 155–168.

Shiloh, Y., and Ziv, Y. (2013). The ATM protein kinase: regulating the cellular response to genotoxic stress, and more. Nat. Rev. Mol. Cell Biol. *14*, 197–210.

Shimada, M., Niida, H., Zineldeen, D.H., Tagami, H., Tanaka, M., Saito, H., and Nakanishi, M. (2008). Chk1 is a histone H3 threonine 11 kinase that regulates DNA damage-induced transcriptional repression. Cell *132*, 221–232.

Sibanda, B.L., Chirgadze, D.Y., and Blundell, T.L. (2010). Crystal structure of DNA-PKcs reveals a large open-ring cradle comprised of HEAT repeats. Nature *463*, 118–121.

Siemann, D.W., and Keng, P.C. (1986). Cell cycle specific toxicity of the Hoechst 33342 stain in untreated or irradiated murine tumor cells. Cancer Res. *46*, 3556–3559.

Sims, A.E., Spiteri, E., Sims, R.J., Arita, A.G., Lach, F.P., Landers, T., Wurm, M., Freund, M., Neveling, K., Hanenberg, H., et al. (2007). FANCI is a second monoubiquitinated member of the Fanconi anemia pathway. Nat. Struct. Mol. Biol. *14*, 564–567.

Smith, K.D., Fu, M.A., and Brown, E.J. (2009). Tim-Tipin dysfunction creates an indispensible reliance on the ATR-Chk1 pathway for continued DNA synthesis. J. Cell Biol. *187*, 15–23.

Solly, K., Wang, X., Xu, X., Strulovici, B., and Zheng, W. (2004). Application of real-time cell electronic sensing (RT-CES) technology to cell-based assays. Assay Drug Dev Technol *2*, 363–372.

Song, I.Y., Palle, K., Gurkar, A., Tateishi, S., Kupfer, G.M., and Vaziri, C. (2010). Rad18-mediated Translesion Synthesis of Bulky DNA Adducts Is Coupled to Activation of the Fanconi Anemia DNA Repair Pathway. Journal of Biological Chemistry *285*, 31525–31536.

Splinter, J., Jakob, B., Lang, M., Yano, K., Engelhardt, J., Hell, S.W., Chen, D.J., Durante, M., and Taucher-Scholz, G. (2010). Biological dose estimation of UVA laser microirradiation utilizing charged particle-induced protein foci. Mutagenesis *25*, 289–297.

Stevens, C., Smith, L., and La Thangue, N.B. (2003). Chk2 activates E2F-1 in response to DNA damage. Nat. Cell Biol. *5*, 401–409.

Stewart, G.S., Wang, B., Bignell, C.R., Taylor, A.M.R., and Elledge, S.J. (2003). MDC1 is a mediator of the mammalian DNA damage checkpoint. Nature *421*, 961–966.

Stixová, L., Hrušková, T., Sehnalová, P., Legartová, S., Svidenská, S., Kozubek, S., and Bártová, E. (2014). Advanced microscopy techniques used for comparison of UVA- and γ-irradiation-induced DNA damage in the cell nucleus and nucleolus. Folia Biol. (Praha) *60 Suppl 1*, 76–84.

Stordal, B., Timms, K., Farrelly, A., Gallagher, D., Busschots, S., Renaud, M., Thery, J., Williams, D., Potter, J., Tran, T., et al. (2013). BRCA1/2 mutation analysis in 41 ovarian cell lines reveals only one functionally deleterious BRCA1 mutation. Mol Oncol *7*, 567–579.

Stucki, M., Clapperton, J.A., Mohammad, D., Yaffe, M.B., Smerdon, S.J., and Jackson, S.P. (2005). MDC1 directly binds phosphorylated histone H2AX to regulate cellular responses to DNA double-strand breaks. Cell *123*, 1213–1226.

Subramanian, K., and Meyer, T. (1997). Calcium-induced restructuring of nuclear envelope and endoplasmic reticulum calcium stores. Cell *89*, 963–971.

Sutherland, G.R. (1991). Chromosomal fragile sites. Genet. Anal. Tech. Appl. *8*, 161–166.

Sy, S.M.H., Chen, J., and Huen, M.S.Y. (2010). The 53BP1-EXPAND1 connection in chromatin structure regulation. Nucleus *1*, 472–474.

Taniguchi, T., Garcia-Higuera, I., Xu, B., Andreassen, P.R., Gregory, R.C., Kim, S.-T., Lane, W.S., Kastan, M.B., and D'Andrea, A.D. (2002). Convergence of the fanconi anemia and ataxia telangiectasia signaling pathways. Cell *109*, 459–472.

Tashiro, S., Walter, J., Shinohara, A., Kamada, N., and Cremer, T. (2000). Rad51 Accumulation at Sites of DNA Damage and in Postreplicative Chromatin. J Cell Biol *150*, 283–292.

Tsantoulis, P.K., Kotsinas, A., Sfikakis, P.P., Evangelou, K., Sideridou, M., Levy, B., Mo, L., Kittas, C., Wu, X.-R., Papavassiliou, A.G., et al. (2008). Oncogene-induced replication stress preferentially targets common fragile sites in preneoplastic lesions. A genome-wide study. Oncogene *27*, 3256–3264.

Turinetto, V., and Giachino, C. (2015). Multiple facets of histone variant H2AX: a DNA double-strand-break marker with several biological functions. Nucleic Acids Research *43*, 2489–2498.

Unsal-Kaçmaz, K., and Sancar, A. (2004). Quaternary structure of ATR and effects of ATRIP and replication protein A on its DNA binding and kinase activities. Mol. Cell. Biol. *24*, 1292–1300.

Unsal-Kaçmaz, K., Chastain, P.D., Qu, P.-P., Minoo, P., Cordeiro-Stone, M., Sancar, A., and Kaufmann, W.K. (2007). The human Tim/Tipin complex coordinates an Intra-S checkpoint response to UV that slows replication fork displacement. Mol. Cell. Biol. *27*, 3131–3142.

Uto, K., Inoue, D., Shimuta, K., Nakajo, N., and Sagata, N. (2004). Chk1, but not Chk2, inhibits Cdc25 phosphatases by a novel common mechanism. EMBO J *23*, 3386–3396.

Vassin, V.M., Wold, M.S., and Borowiec, J.A. (2004). Replication protein A (RPA) phosphorylation prevents RPA association with replication centers. Mol. Cell. Biol. *24*, 1930–1943.

Vassin, V.M., Anantha, R.W., Sokolova, E., Kanner, S., and Borowiec, J.A. (2009). Human RPA phosphorylation by ATR stimulates DNA synthesis and prevents ssDNA accumulation during DNA-replication stress. J. Cell. Sci. *122*, 4070–4080.

Walter, J., Cremer, T., Miyagawa, K., and Tashiro, S. (2003). A new system for laser-UVA-microirradiation of living cells. J Microsc *209*, 71–75.

Wang, J., Aroumougame, A., Lobrich, M., Li, Y., Chen, D., Chen, J., and Gong, Z. (2014). PTIP associates with Artemis to dictate DNA repair pathway choice. Genes Dev. *28*, 2693–2698.

Wang, X., Kennedy, R.D., Ray, K., Stuckert, P., Ellenberger, T., and D'Andrea, A.D. (2007). Chk1-Mediated Phosphorylation of FANCE Is Required for the Fanconi Anemia/BRCA Pathway. Molecular and Cellular Biology *27*, 3098–3108.

Ward, I.M., Minn, K., van Deursen, J., and Chen, J. (2003). p53 Binding protein 53BP1 is required for DNA damage responses and tumor suppression in mice. Mol. Cell. Biol. *23*, 2556–2563.

Ward, I.M., Reina-San-Martin, B., Olaru, A., Minn, K., Tamada, K., Lau, J.S., Cascalho, M., Chen, L., Nussenzweig, A., Livak, F., et al. (2004). 53BP1 is required for class switch recombination. The Journal of Cell Biology *165*, 459–464.

Weber, A.M., and Ryan, A.J. (2015). ATM and ATR as therapeutic targets in cancer. Pharmacol. Ther. *149*, 124–138.

Weston, R., Peeters, H., and Ahel, D. (2012). ZRANB3 is a structure-specific ATP-dependent endonuclease involved in replication stress response. Genes Dev. *26*, 1558–1572.

Wilson, W.R., Harris, N.M., and Ferguson, L.R. (1984). Comparison of the mutagenic and clastogenic activity of amsacrine and other DNA-intercalating drugs in cultured V79 Chinese hamster cells. Cancer Res. *44*, 4420–4431.

Wouters, B.G., Denko, N.C., Giaccia, A.J., and Brown, J.M. (1999). A p53 and apoptotic independent role for p21waf1 in tumour response to radiation therapy. Oncogene *18*, 6540–6545.

Yamagata, K., Iwamoto, D., Terashita, Y., Li, C., Wakayama, S., Hayashi-Takanaka, Y., Kimura, H., Saeki, K., and Wakayama, T. (2012). Fluorescence cell imaging and manipulation using conventional halogen lamp microscopy. PLoS ONE *7*, e31638.

Yamori, T., Matsunaga, A., Sato, S., Yamazaki, K., Komi, A., Ishizu, K., Mita, I., Edatsugi, H., Matsuba, Y., Takezawa, K., et al. (1999). Potent antitumor activity of MS-247, a novel DNA minor groove binder, evaluated by an in vitro and in vivo human cancer cell line panel. Cancer Res. *59*, 4042–4049.

Yang, S., Kuo, C., Bisi, J.E., and Kim, M.K. (2002). PML-dependent apoptosis after DNA damage is regulated by the checkpoint kinase hCds1/Chk2. Nat. Cell Biol. *4*, 865–870.

Yang, X.H., Shiotani, B., Classon, M., and Zou, L. (2008). Chk1 and Claspin potentiate PCNA ubiquitination. Genes & Development *22*, 1147–1152.

Yano, T., Hatogai, K., Morimoto, H., Yoda, Y., and Kaneko, K. (2014). Photodynamic therapy for esophageal cancer. Ann Transl Med *2*, 29.

Yin, B., Savic, V., Juntilla, M.M., Bredemeyer, A.L., Yang-Iott, K.S., Helmink, B.A., Koretzky, G.A., Sleckman, B.P., and Bassing, C.H. (2009). Histone H2AX stabilizes broken DNA strands to suppress chromosome breaks and translocations during V(D)J recombination. J. Exp. Med. *206*, 2625–2639.

Yin, Y., Seifert, A., Chua, J.S., Maure, J.-F., Golebiowski, F., and Hay, R.T. (2012). SUMO-targeted ubiquitin E3 ligase RNF4 is required for the response of human cells to DNA damage. Genes Dev. *26*, 1196–1208.

You, Z., Bailis, J.M., Johnson, S.A., Dilworth, S.M., and Hunter, T. (2007). Rapid activation of ATM on DNA flanking double-strand breaks. Nat. Cell Biol. *9*, 1311–1318.

Zellweger, R., Dalcher, D., Mutreja, K., Berti, M., Schmid, J.A., Herrador, R., Vindigni, A., and Lopes, M. (2015). Rad51-mediated replication fork reversal is a global response to genotoxic treatments in human cells. J. Cell Biol. *208*, 563–579.

Zeman, M.K., and Cimprich, K.A. (2014). Causes and consequences of replication stress. Nat. Cell Biol. *16*, 2–9.

Zernik-Kobak, M., Vasunia, K., Connelly, M., Anderson, C.W., and Dixon, K. (1997). Sites of UV-induced phosphorylation of the p34 subunit of replication protein A from HeLa cells. J. Biol. Chem. *272*, 23896–23904.

Zhang, H., and Freudenreich, C.H. (2007). An AT-rich sequence in human common fragile site FRA16D causes fork stalling and chromosome breakage in S. cerevisiae. Mol. Cell *27*, 367–379.

Zhang, J., Dai, Q., Park, D., and Deng, X. (2016). Targeting DNA Replication Stress for Cancer Therapy. Genes (Basel) *7*.

Zhang, X., Zhang, S.C., Sun, D., Hu, J., Wali, A., Pass, H., Fernandez-Madrid, F., Harbut, M.R., and Tang, N. (2011). New insight into the molecular mechanisms of the biological effects of DNA minor groove binders. PLoS ONE *6*, e25822.

Zhou, B.B., and Elledge, S.J. (2000). The DNA damage response: putting checkpoints in perspective. Nature *408*, 433–439.

Zimonjic, D.B., Druck, T., Ohta, M., Kastury, K., Croce, C.M., Popescu, N.C., and Huebner, K. (1997). Positions of chromosome 3p14.2 fragile sites (FRA3B) within the FHIT gene. Cancer Res. *57*, 1166–1170.

Zlotorynski, E., Rahat, A., Skaug, J., Ben-Porat, N., Ozeri, E., Hershberg, R., Levi, A., Scherer, S.W., Margalit, H., and Kerem, B. (2003). Molecular Basis for Expression of Common and Rare Fragile Sites. Mol Cell Biol *23*, 7143–7151.

Zou, L., and Elledge, S.J. (2003). Sensing DNA damage through ATRIP recognition of RPA-ssDNA complexes. Science *300*, 1542–1548.

Zou, L., Cortez, D., and Elledge, S.J. (2002). Regulation of ATR substrate selection by Rad17-dependent loading of Rad9 complexes onto chromatin. Genes Dev. *16*, 198–208.